M.3 Structural Evaluation

M.3.1 Structural Design

M.3.1.1 Discussion

This section describes the structural evaluation of the NUHOMS®-32PT system. The NUHOMS®-32PT system consists of the NUHOMS® HSM, the OS197 and OS197H TCs, and the 32PT DSC basket and shell assemblies. No changes have been made to the HSM or the OS197 or OS197H TCs to accommodate the 32PT DSC. Where the new components have an effect on the structural evaluations presented in the FSAR, the changes are included in this section. Sections that do not effect the evaluations presented in the FSAR include a statement that there is no change to the FSAR. In addition, a complete evaluation of the 32PT DSC shell and basket components has been performed and is summarized in this section.

The 32PT DSC shell assembly is shown on drawings NUH-32PT-1001 and NUH-32PT-1002. These drawings are provided in Section M.1.5. The NUHOMS®-32PT DSC shell assembly is the same as the NUHOMS®-24P DSC with the following exceptions:

- The nominal DSC shell thickness has been reduced to 0.5 inch thick from 0.625 inch thick.
- The nominal thickness of the outer top cover plate has been increased from 1.25 inches to 1.50 inches.
- The nominal thickness of the inner top cover plate has been increased from 0.75 inches to 1.25 inches.
- The nominal thickness of the inner bottom cover plate has been increased from 0.75 inches to 1.75 inches and has been designed for the internal pressure loads without credit taken for the structural support of the bottom shield plug and outer bottom cover plate.
- The nominal thickness of the top shield plug has been reduced from 8.25 inches to 6.25 inches for the 32PT-S100 and 32PT-L100 and to 7.5 inches for the 32PT-S125 and 32PT-L125.
- The nominal thickness of the bottom shield plug has been reduced from 6.25 inches to 4.00 inches for the 32PT-S100 and 32PT-L100 and to 5.25 inches for the 32PT-S125 and 32PT-L125.
- An optional configuration has been added for the inner bottom cover plate that allows the use of a forging to provide the same structural function as the plate design.
- A test port has been added to the top cover plate to allow testing of the inner top cover plate welds and vent and siphon port cover plate welds to a leak tight criteria.

The NUHOMS®-32PT basket is a welded assembly of stainless steel plates or tubes that make up a fuel support assembly grid designed to accommodate up to 32 PWR fuel assemblies. The basket structure consists of the fuel support structure, the transition rails, aluminum heat transfer material, and neutron absorbing material.

The 32PT basket assembly is shown on drawings NUH-32PT-1003 through NUH-32PT-1006. These drawings are provided in Section M.1.5.

- The fuel support structure is fabricated from high strength (Type XM-19) stainless steel and contains 32 square fuel compartments in a box arrangement.

- The transition rails provide the transition between the "rectangular" fuel support grid and the cylindrical internal diameter of the DSC shell. There are two sizes of transition rails. The large rails are referred to as the R90 transition rails. The smaller transition rails are referred to as the R45 transition rails. Two material/fabrication options are provided for the transition rails:

    - Solid Aluminum Rails: The transition rails are solid sections of 6061 aluminum alloy. The large (R90) rails include an XM-19 "cover plate" between the fuel support grid and the aluminum body. The structural evaluation of the rails uses properties for annealed aluminum (no credit is taken for enhanced properties obtained by heat treatment).

    - Welded Steel Transition Rails: The steel transition rails are welded steel structures fabricated with 3/8" thick Type 304 stainless steel. To enhance heat transfer through the rails, aluminum plates are connected to the transition rail structure. No credit is taken for these aluminum plates in the structural evaluation of the steel transition rails.

- The fuel support grid structure contains aluminum alloy 1100 plates as heat transfer material and borated aluminum or Boralyn® neutron absorbing plates. No credit is taken for the structural capacity of the aluminum heat transfer plates or neutron absorbing materials in the structural evaluation of the support grid structure.

- The connections between the transition rails and fuel support structure are not required to maintain structural capacity of the basket assembly. These connections are primarily to simplify fabrication and are designed to allow free thermal expansion of the connected parts.

The basket structure is open at each end such that longitudinal fuel assembly loads are applied directly to the DSC/cask body and not to the basket structure. The fuel assemblies are laterally supported by the XM-19 fuel support structure. The basket is laterally supported by the basket transition rails and the DSC inner shell.

Inside the TC, the DSC rests on two 3" wide rails ("cask rails"), attached to the inside of the TC at +/-18.5° from the bottom centerline of the DSC. In the HSM, the DSC is supported by rails located at +/-30° from the bottom centerline of the DSC.

The nominal open dimension of each fuel compartment cell is 8.70 in. x 8.70 in. which provides clearance around the fuel assemblies. The overall basket length is less than the DSC cavity length to allow for thermal expansion and tolerances.

M.3.1.2 Design Criteria

Design criteria for the DSC shell and basket are provided in Section M.2.2.

M.3.1.2.1 DSC Shell Assembly Confinement Boundary

The primary confinement boundary consists of the DSC shell, the inner top cover plate, the inner bottom cover plate, the siphon vent block, the siphon/vent port cover plates, and the associated welds. Figure M.3-1 provides a graphic representation of the 32PT-DSC confinement boundary.

The welds made during fabrication of the 32PT-DSC that affect the confinement boundary of the DSC include the inner bottom cover plate to shell weld and the circumferential and longitudinal seam welds applied to the shell. These welds are inspected (radiographic or ultrasonic inspection, and liquid penetrant inspection) according to the requirements of Subsection NB of the ASME Code. The vent and siphon block weld is also made during fabrication and is liquid penetrant inspected in accordance with Subsection NB of the ASME Code.

The welds applied to the vent and siphon port covers and the inner top cover plate during closure operations define the confinement boundary at the top end of the 32PT-DSC. These welds are applied using a multiple-layer technique with multi-level PT in accordance with ASME Code Case N-595-2 [3.1].

The basis for the allowable stresses for the confinement boundary is ASME Code Section III, Division I, Subsection NB Article NB-3200 [3.1] for normal (Level A) condition loads , off-normal (Level B) condition loads and off-normal/accident (Level C) condition loads, and Appendix F for accident (Level D) condition loads. See Section M.2.2 for additional design criteria.

M.3.1.2.2 DSC Basket

The basket is designed to meet heat transfer, nuclear criticality, and structural requirements. The basket structure provides sufficient rigidity to maintain a subcritical configuration under the applied loads. The Type XM-19 stainless steel members in the NUHOMS®-32PT basket are the primary structural components. The aluminum heat transfer plates and neutron poison plates are the primary heat conductors, and provide the necessary criticality control. The transition rails provide support to the fuel compartment grid for mechanical loads and also transfer heat from the fuel compartments to the DSC shell.

The stress analyses of the basket do not take credit for the neutron absorbing/heat transfer plate material.

The basket structural design criteria is provided in Section M.2.2. The basis for the allowable stresses for the stainless steel components in the basket assembly is Section III, Division I, Subsection NG of the ASME Code [3.1]:

- Normal conditions are evaluated using criteria from NG-3200.
- Accident conditions are classified as Level D events and are evaluated using stress and stability criteria from Section III, Appendix F of the ASME Code [3.1].

M.3.1.2.3 ASME Code Exceptions for the 32PT DSC

The primary confinement boundary of the NUHOMS®-32PT DSC consists of the DSC shell, the inner top cover plate, the inner bottom cover plate, the siphon vent block, and the siphon/vent port cover plate. Even though the ASME B&PV code is not strictly applicable to the DSC, it is TNW's intent to follow Section III, Subsection NB of the Code as closely as possible for design and construction of the confinement vessel. The DSC may, however, be fabricated by other than N-stamp holders and materials may be supplied by other than ASME Certificate Holders. Thus the requirements of NCA are not imposed. TNW's quality assurance requirements, which are based on 10CFR72 Subpart G and NQA-1 are imposed in lieu of the requirements of NCA-3800. The SAR is prepared in place of the ASME design and stress reports. Surveillances are performed by TNW and utility personnel rather than by an Authorized Nuclear Inspector (ANI).

The basket is designed, fabricated and inspected in accordance with the ASME Code Subsection NG, to the maximum practical extent. The following exceptions are taken:

The poison rod assemblies, poison plates, and aluminum heat transfer plates are not considered for structural integrity. Therefore, these materials are not required to be Code materials. The quality assurance requirements of NQA-1 is imposed in lieu of NCA-3800. The basket is not Code stamped. Therefore, the requirements of NCA are not imposed. Fabrication and inspection surveillances are performed by TNW and utility personnel rather than by an ANI.

A complete list of the ASME Code exceptions and justification for the confinement boundary of the NUHOMS®-32PT DSC and basket is provided in Table M.3.1-1 and Table M.3.1-2.

Table M.3.1-1
ASME Code Exceptions for the NUHOMS®-32PT DSC Confinement Boundary

Reference ASME Code Section/Article	Code Requirement	Exception, Justification & Compensatory Measures
NCA	All	Not compliant with NCA
NB-1100	Requirements for Code Stamping of Components	The NUHOMS®-32PT DSC shell is designed & fabricated in accordance with the ASME Code, Section III, Subsection NB to the maximum extent practical. However, Code Stamping is not required. As Code Stamping is not required, the fabricator is not required to hold an ASME "N" or "NPT" stamp, or to be ASME Certified.
NB-2130	Material must be supplied by ASME approved material suppliers	All materials designated as ASME on the SAR drawings are obtained from ASME approved MM or MS supplier(s) with ASME CMTR's. Material is certified to meet all ASME Code criteria but is not eligible for certification or Code Stamping if a non-ASME fabricator is used. As the fabricator is not required to be ASME certified, material certification to NB-2130 is not possible. Material traceability & certification are maintained in accordance with TNW's NRC approved QA program
NB-4121	Material Certification by Certificate Holder	
NB-4243 and NB-5230	Category C weld joints in vessels and similar weld joints in other components shall be full penetration joints. These welds shall be examined by UT or RT and either PT or MT	The joints between the top outer and inner cover plates and containment shell are designed and fabricated per ASME Code Case N-595-2. The welds are partial penetration welds and the root and final layer are PT examined.
NB-6100 and 6200	All completed pressure retaining systems shall be pressure tested	The vent and siphon block is not pressure tested due to the manufacturing sequence. The siphon block weld is helium leak tested when fuel is loaded and then covered with the outer top closure plate.
NB-7000	Overpressure Protection	No overpressure protection is provided for the NUHOMS®-32PT DSC . The function of the NUHOMS®-32PT DSC is to contain radioactive materials under normal, off-normal and hypothetical accident conditions postulated to occur during transportation and storage. The NUHOMS®-32PT DSC is designed to withstand the maximum possible internal pressure considering 100% fuel rod failure at maximum accident temperature. The NUHOMS®-32PT DSC is pressure tested in accordance with ASME Code Case N-595-2.
NB-8000	Requirements for nameplates, stamping & reports per NCA-8000	The NUHOMS®-32PT DSC nameplate provides the information required by 10CFR71, 49CFR173 and 10CFR72 as appropriate. Code stamping is not required for the NUHOMS®-32PT DSC. QA Data packages are prepared in accordance with the requirements of 10CFR71, 10CFR72 and TNW's approved QA program.

Table M.3.1-2
ASME Code Exceptions for the NUHOMS®-32PT DSC Basket Assembly

Reference ASME Code Section/Article	Code Requirement	Exception, Justification & Compensatory Measures
NG-1100	Requirements for Code Stamping of Components	The NUHOMS®-32PT DSC baskets are designed & fabricated in accordance with the ASME Code, Section III, Subsection NG to the maximum extent practical as described in the SAR, but Code Stamping is not required. As Code Stamping is not required, the fabricator is not required to hold an ASME N or NPT stamp or be ASME Certified.
NG-2000	Use of ASME Material	The poison material and aluminum plates are not used for structural analysis, but to provide criticality control and heat transfer. They are not ASME Code Class I material. Material properties in the ASME Code for Type 6061 aluminum are limited to 400°F to preclude the potential for annealing out the hardening properties. Annealed properties (as published by the Aluminum Association and the American Society of Metals) are conservatively assumed for the solid aluminum rails for use above the Code temperature limits.
NCA	All	Not compliant with NCA as no Code stamp is used.

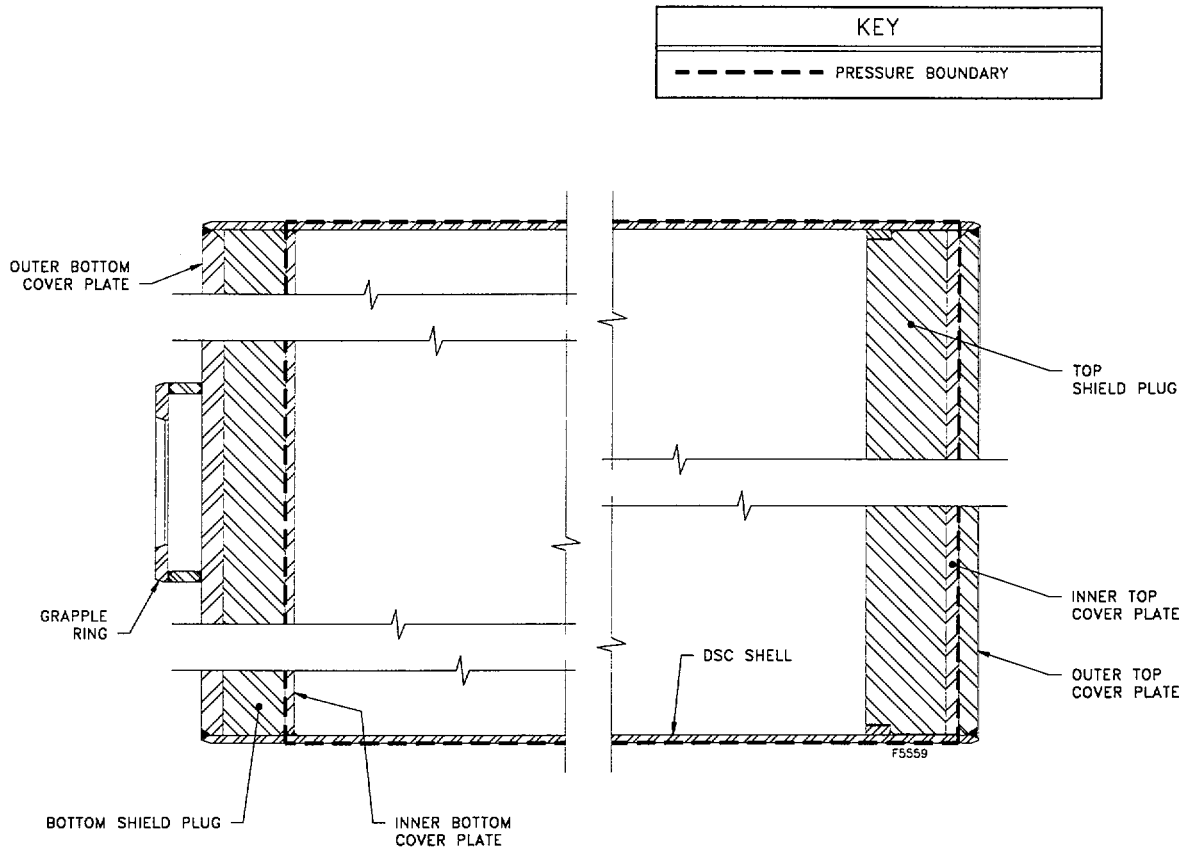

Figure M.3-1
32PT-DSC Confinement Boundary

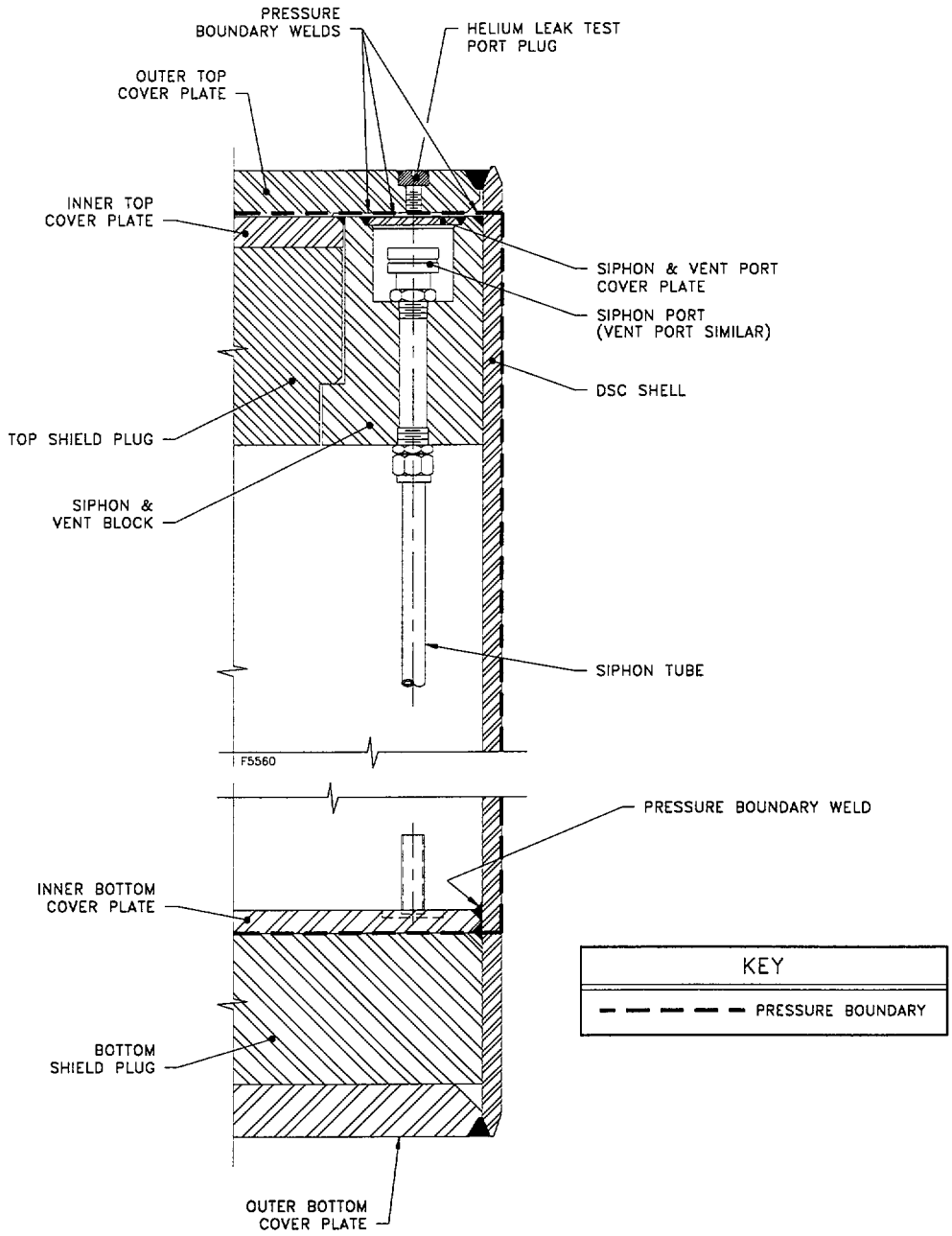

Figure M.3-1
32PT-DSC Confinement Boundary
(Concluded)

M.3.2 Weights and Centers of Gravity

Table M.3.2-1 shows the weights of the various components of the NUHOMS®-32PT system including basket, DSC, standard HSM and OS197 and OS197H TC. The dead weights of the components are determined based on nominal dimensions.

Table M.3.2-1
Summary of the NUHOMS®-32PT System Component Nominal Weights

Component Description	CALCULATED WEIGHT (kips)			
	32PT-S100	32PT-S125	32PT-L100	32PT-L125
DSC Shell Assembly[1]	13.06	14.28	13.24	14.46
DSC Top Shield Plug Assembly[2]	8.71	9.93	8.71	9.93
DSC Internal Basket Assembly	22.44	22.10	23.25	22.91
Total Empty Weight	**44.21**	**46.31**	**45.20**	**47.30**
32 PWR Spent Fuel Assemblies	≤ 43.68[3]	≤ 53.82[4]	≤ 43.68[3]	≤ 53.82[4]
Total Loaded DSC Weight (Dry)	**87.90**	**100.14**	**88.89**	**101.13**
Water in Loaded DSC	6.81[5]	10.75	6.40[6]	11.37
Total Loaded DSC Weight (Wet)	**94.7**	**110.9**	**95.3**	**112.5**
Cask Spacer	1.10	1.10	0.79	0.79
OS197 (OS197H) TC Empty Weight[7]	106.67	111.25	106.67	111.25
Total Loaded TC Weight	**195.7**	**212.5**	**196.4**	**213.2**
HSM Single Module Weight (Empty)	**248.0**	**248.0**	**248.0**	**248.0**
HSM Single Module Weight (Loaded)	**335.9**	**348.1**	**336.9**	**349.1**

Notes:

1. Excludes top cover plates and shield plug.
2. Includes top cover plates and shield plug.
3. Based on a fuel weight of 1,365 lbs per assembly. This is a limit for the 32PT-S100 and 32PT-L100 DSCs to ensure that the maximum lift weight of the loaded TC is under 100 tons.
4. Based on B&W 15x15 fuel (with control components) weight of 1,682 lbs per assembly.
5. Based on water volume reduced to 50% of capacity to ensure that the maximum lift weight of the loaded TC is under 100 tons for the 32PT-S100 DSC.
6. Based on water volume reduced to 45% of capacity to ensure that the maximum lift weight of the loaded TC is under 100 tons for the 32PT-L100 DSCs.
7. Includes cask top cover plate. The neutron shield is filled with demineralized water for the 32PT-S125 and 32PT-L125 DSCs. For the 32PT-S100 and 32PT-L100 DSCs, the neutron shield is not filled with demineralized water to ensure that the maximum lift weight of the loaded cask is under 100 tons .

M.3.3 Mechanical Properties of Materials

M.3.3.1 Material Properties

The DSC shell and inner and outer top and bottom cover plates are fabricated from Type 304 stainless steel. The properties for the material are from ASME Code Section II Part D [3.2] and are listed in Table M.3.3-1.

The top and bottom shield plugs are fabricated from A36 carbon steel. The properties from ASME Code Section II Part D [3.2], as listed in Table M.3.3-2, are applied to this material.

The fuel support grid in the 32PT basket is fabricated with Type XM-19 high strength stainless steel. The properties of this material are from ASME Code Section II, Part D [3.2] and are listed in Table M.3.3-3.

The welded steel transition rails in the 32PT basket are fabricated with Type 304 stainless steel. The properties of this material are from ASME Code Section II, Part D [3.2] and are listed in Table M.3.3-1.

The aluminum transition rails use solid sections (e.g., machined plates) of Type 6061 aluminum. The large (R90) rails include a 1/4" thick XM-19 plate (same material and thickness as the fuel support structure) while the small (R45) transition rails are solid aluminum parts with no cover plates. Analysis properties are taken from [3.3] for annealed aluminum. Use of properties for annealed material ensures that no credit is taken for enhanced properties obtained by heat treatment. The selection of properties for annealed material is based on the possibility that the maximum temperature in the rails may exceed the temperatures for which strength properties are provided (for aluminum) in the ASME Code (see Table M.3.3-4). This is acceptable for the following reasons:

1. The transition rails are not pressure boundary parts. Loading on the rails is primarily bearing and the transition rails are "captured" between the fuel support structure and the DSC shell. Deformation of the transition rails (to conform to the inside diameter of the DSC shell) will distribute the applied loads and will not adversely impact the basket structure.

2. For applications where the aluminum properties result from heat treatment, it is necessary to limit the maximum temperature to values below which the effects of the heat treatment are maintained. Heat treatment provides significant differences in strength properties at low temperatures. However, as temperature increases, the effect(s) of heat treatment on strength properties decreases. The strength properties used in the design of the 32PT are based on annealed aluminum. Thus, changes in strength which may occur under exposure to temperatures exceeding 400°F have no adverse impact on the properties used in the design.

For the stress analyses of the 32PT basket with aluminum rails, properties for the rails are taken directly from Table M.3.3-5. For elastic-plastic analyses, the plastic slope of the aluminum is

taken as 0.01E. This approximates elastic-perfectly plastic properties while providing a small stiffness to enhance analytical stability.

Table M.3.3-6 provides additional material properties.

M.3.3.2 Materials Durability

The materials used in the fabrication of the NUHOMS®-32PT system are shown in Table M.3.3-1 through Table M.3.3-5. Essentially all of the materials meet the appropriate requirements of the ASME Code, ACI Code, and appropriate ASTM Standards. The durability of the shell assembly and basket assembly stainless steel components is well beyond the design life of the applicable components. The aluminum material used in the basket is only relied upon for its thermal conductivity and bearing strength properties. The poison material selected for criticality control of the NUHOMS®-32PT system has been tested and is currently in use for similar applications. Additionally, the NUHOMS®-32PT basket assembly resides in an inert helium gas environment for the majority of the design life. The materials used in the NUHOMS®-32PT system will maintain the required properties for the design life of the system.

Table M.3.3-1
ASME Code Materials Data For SA-240 Type 304 Stainless Steel

Materials Data, SA-240 Type 304 (18Cr-8Ni) Stainless Steel

Temp. (°F)	E (ksi)	S_m (ksi)	S_y (ksi)	S_u (ksi)	α_{AVG} (x 10^{-6}°F^{-1})
-100	29,100	--	--	--	--
-20	--	20.0	30.0	75.0	--
70	28,300	--	--	--	8.5
100	--	20.0	30.0	75.0	8.6
200	27,600	20.0	25.0	71.0	8.9
300	27,000	20.0	22.4	66.2	9.2
400	26,500	18.7	20.7	64.0	9.5
500	25,800	17.5	19.4	63.4	9.7
600	25,300	16.4	18.4	63.4	9.8
650	--	16.2	18.0	63.4	9.9
700	24,800	16.0	17.6	63.4	10.0
750	--	15.6	17.2	63.3	10.0
800	24,100	15.2	16.9	62.8	10.1
Reference Section II-D	Table TM-1 Group G	Table 2A	Table Y-1	Table U	18Cr-8Ni TE-1, Group 3

Table M.3.3-2
Materials Data For ASTM A36 Steel

(Properties are taken from ASME Code Section II for SA-36 Steel. The ASME material specification is identical to the ASTM A36 Steel specification.)

Temp. (°F)	E (ksi)	S_m (ksi)	S_y (ksi)	S_u (ksi)	α_{AVG} (x 10^{-6} $°F^{-1}$)
-100	30,200	--	--	--	--
-20	--	19.3	36.0	58.0	--
70	29,500	19.3	36.0	58.0	--
100	--	19.3	36.0	58.0	6.5
200	28,800	19.3	33.0	58.0	6.7
300	28,300	19.3	31.8	58.0	6.9
400	27,700	19.3	30.8	58.0	7.1
500	27,300	19.3	29.3	58.0	7.3
600	26,700	17.7	27.6	58.0	7.4
650	--	17.4	26.7	58.0	7.5
700	25,500	17.3	25.8	58.0	7.6
750	--	--	--	--	7.7
800	24,200	--	--	--	7.8

Table M.3.3-3
ASME Code Materials Data For SA-240 Type XM-19 Stainless Steel

Materials Data, SA-240 Type XM-19 (22Cr-13Ni-5Mn)

Temp. (^{o}F)	E (ksi)	S_m (ksi)	S_y (ksi)	S_u (ksi)	α_{AVG} (x $10^{-6}{}^{o}F^{-1}$)
-100	29,100	--	--	--	--
-20	--	33.3	55.0	100.0	--
70	28,300	--	--	--	8.2
100	--	33.3	55.0	100.0	8.2
200	27,600	33.2	47.1	99.4	8.5
300	27,000	31.4	43.3	94.2	8.8
400	26,500	30.2	40.7	91.1	8.9
500	25,800	29.7	38.8	89.1	9.1
600	25,300	29.2	37.4	87.7	9.2
650	--	29.0	36.8	87.0	9.2
700	24,800	28.8	36.3	86.4	9.3
750	--	28.5	35.8	85.6	9.3
800	24,100	28.2	35.3	84.8	9.4
Reference Section II-D	Table TM-1 Group G	Table 2A	Table Y-1	Table U	22Cr-13Ni-5Mn TE-1, Group 4

Table M.3.3-4
ASME Code Properties for 6061 Aluminum

ASME Code Properties for 6061 Aluminum (Plate)

Temperature	Yield Strength (ksi)		E	α
(°F)	A96061-T451	A96061-T651	(ksi)	(x 10^{-6} °F^{-1})
75	16.0	35.0	10,000	12.1
100	16.0	35.0	--	12.4
150	15.7	34.6	--	12.7
200	15.5	33.7	9,600	13.0
250	15.3	32.4	--	13.1
300	15.3	27.4	9,200	13.3
350	15.3	20.0	--	13.4
400	11.6	13.3	8,700	13.6
450	--	--	--	13.8
500	--	--	8,100	13.9
550	--	--	--	14.1
600	--	--	--	14.2
Reference	Table Y-1 .250" - 3.00"	Table Y-1 .250" - 6.00"	Table TM-2 A96061	Table TE-2

Table M.3.3-5
Analysis Properties for Aluminum Transition Rails

6061-O Aluminum (Annealed)

Temperature (°F)	S_u, 6061-O (ksi)	S_y, 6061-O (ksi)	E (ksi)
75	18.0	8.0	9,900
212	18.0	8.0	9,500
300	15.0	8.0	9,100
350	12.0	8.0	8,900
400	10.0	7.5	8,600
450	8.5	6.0	8,300
500	7.0	5.5	7,900
600	5.0	4.2	6,800
700	3.6	3.0	5,500
800	2.8	2.2	--
900	2.2	1.6	--
1000	1.6	1.2	--

Note: Data from "Properties of Aluminum Alloys", ASM International/The Aluminum Association, 1999

Table M.3.3-6
Additional Material Properties

Material Property	Value	Reference
Aluminum Density (1100 and 6061)	0.098 lb/in^3	Section II, Part D, Table NF-2
Aluminum Melting Point (Alloy 1100)	1190°F - 1215°F	Section II, Part D, Table NF-2
Aluminum Melting Point (Alloy 6061)	1080°F - 1205°F	Section II, Part D, Table NF-2
Neutron Absorber Density	0.098 lb/in^3	Taken as equal to the density of pure aluminum
Steel Density	$\frac{493\ lb}{1728\ in^3} = .285\ lb/in^3$	

M.3.4 General Standards for Casks

M.3.4.1 Chemical and Galvanic Reactions

The materials of the 32PT DSC and basket have been reviewed to determine whether chemical, galvanic or other reactions among the materials, contents and environment might occur during any phase of loading, unloading, handling or storage. This review is summarized below:

The 32PT DSC is exposed to the following environments:

- During loading and unloading, the DSC is placed inside of the OS197 or OS197H TC. The annulus between the cask and DSC is filled with demineralized water and an inflatable seal is used to cover the annulus between the DSC and cask. The exterior of the DSC will not be exposed to pool water.

- The space between the top of the DSC and inside of the TC is sealed to prevent contamination. For PWR plants the pool water is borated. This affects the interior surfaces of the DSC, the shield plug, and the basket. The TC and DSC are kept in the spent fuel pool for a short period of time, typically about 6 hours to load or unload fuel, and 2 hours to lift the loaded TC/DSC out of the spent fuel pool.

- During storage, the interior of the DSC is exposed to an inert helium environment. The helium environment does not support the occurrence of chemical or galvanic reactions because both moisture and oxygen must be present for a reaction to occur. The DSC is thoroughly dried before storage by a vacuum drying process. It is then backfilled with helium, thus stopping corrosion. Since the DSC is vacuum dried, galvanic corrosion is also precluded as no water is present at the point of contact between dissimilar metals.

- During storage, the exterior of the DSC is protected by the concrete NUHOMS® HSM. The HSM is vented, so the exterior of the DSC is exposed to the atmosphere. The DSC shell and cover plates are fabricated from austenitic stainless steel and are resistant to corrosion.

The NUHOMS®-32PT DSC materials are shown in the Parts List on Drawings NUH-32PT-1001 through NUH-32PT-1006 provided in Section M.1.5. The DSC shell material is SA-240 Type 304 Stainless Steel. The top and bottom shield plug material is A36 carbon steel. The top shield plug is coated with a corrosion resistant electroless nickel coating.

The basket grid structure is composed of either plate or tube assemblies made from XM-19 stainless steel. Within the grid structure are plates of Type 1100 aluminum and neutron absorbing materials composed of either enriched borated aluminum alloy or Boralyn® plates. These plates are attached to the grid structure using corrosion resistant fasteners. Poison Rod Assemblies (PRAs) are also used with some fuel assembly loading options.

There are two transition rail designs that provide the transition between the fuel compartment grid structure and the DSC shell: Stainless steel and solid aluminum. The solid aluminum transition rails are made of solid pieces Type 6061 aluminum. The stainless steel rails consist of Type 304 stainless steel plate with sheets of Type 1100 aluminum attached to the stainless steel

plates using corrosion resistant fasteners. The transition rails may be bolted to the grid structure for ease of fabrication.

Potential sources of chemical or galvanic reactions are the interaction between the aluminum, aluminum-based neutron poison and stainless steel within the basket and the pool water. Additionally, an interaction exists with the stainless steel top and bottom plates and the top shield plug.

Typical water chemistry in a PWR Spent Fuel pool is as follows:

pH (77°F)	4.5 - 9.0
Chloride, max	0.15 ppm
Fluoride, max	0.1 ppm
Dissolved Air, max	Saturated
Lithium, max	2.5 ppm
Boric Acid	2100 - 2600 ppm
Pool Temperature Range	40 - 120°F

A. Behavior of Aluminum in Borated Water

Aluminum is used for many applications in spent fuel pools. In order to understand the corrosion resistance of aluminum within the normal operating conditions of spent fuel storage pools, a discussion of each of the types of corrosion is addressed separately. None of these corrosion mechanisms is expected to occur in the short time period that the cask is submerged in the spent fuel pool.

General Corrosion

General corrosion is a uniform attack of the metal over the entire surfaces exposed to the corrosive media. The severity of general corrosion of aluminum depends upon the chemical nature and temperature of the electrolyte and can range from superficial etching and staining to dissolution of the metal. Figure M.3.4-1 shows a potential-pH diagram for aluminum in high purity water at 77°F and 140°F. The potential for aluminum coupled with stainless steel and the limits of pH for PWR pools are shown in the diagram to be well within the passivation domain at both temperatures. The passivated surface of aluminum (hydrated oxide of aluminum) affords protection against corrosion in the domain shown because the coating is insoluble, non-porous and adherent to the surface of the aluminum. The protective surface formed on the aluminum is known to be stable up to 275°F and in a pH range of 4.5 to 8.5.

The water aluminum reactions are self limiting because the surface of the aluminum becomes passive by the formation of a protective and impervious coating making further reaction impossible until the coating is removed by mechanical or chemical means.

The ability of aluminum to resist corrosion from boron ions is evident from the wide usage of aluminum in the handling of borax and in the manufacture of boric acid. Aluminum storage racks with Boral plates (aluminum 1100 exterior layer) in contact with 800 ppm borated water showed only small amounts of pitting after 17 years in the pool at the Yankee Rowe Power Plant. These racks maintained their structural integrity.

During immersion in the spent fuel pool, the 32PT-DSC basket temperatures are close to the water temperature, which is typically near 80°F, and the pH range is typically 4.0 to 6.5. Based on the above discussion, general corrosion is not expected on the aluminum after the protective coating has been formed.

Galvanic Corrosion

Galvanic corrosion is a type of corrosion which could cause degradation of dissimilar metals exposed to a corrosive environment for a long period of time.

Galvanic corrosion is associated with the current of a galvanic cell consisting of two dissimilar conductors in an electrolyte. The two dissimilar conductors of interest in this discussion are aluminum and stainless steel in borated water. There is little galvanic corrosion in borated water since the water conductivity is very low. There is also less galvanic current flow between the aluminum-stainless steel couple than the potential difference on stainless steel which is known as polarization. It is because of this polarization characteristic that stainless steel is compatible with aluminum in all but severe marine, or high chloride, environmental conditions [3.4].

Pitting Corrosion

Pitting corrosion is the forming of small sharp cavities in a metal surface. The first step in the development of corrosion pits is a local destruction of the protective oxide film. Pitting will not occur on commercially pure aluminum when the water is kept sufficiently pure, even when the aluminum is in electrical contact with stainless steel. Pitting and other forms of localized corrosion occur under conditions like those that cause stress corrosion, and are subject to an induction time which is similarly affected by temperature and the concentration of oxygen and chlorides. As with stress corrosion, at the low temperatures and low chloride concentrations of a spent fuel pool, the induction time for initiation of localized corrosion will be greater than the time that the DSC internal components are exposed to the aqueous environment.

Crevice Corrosion

Crevice corrosion is the corrosion of a metal that is caused by the concentration of dissolved salts, metal ions, oxygen or other gases in crevices or pockets remote from the principal fluid stream, with a resultant build-up of differential galvanic cells that ultimately cause pitting. Crevice corrosion could occur in the basket grid assembly plates around the stainless steel welds. However, due to the short time in the spent fuel pool, this type of corrosion is expected to be insignificant.

Intergranular Corrosion

Intergranular corrosion is corrosion occurring preferentially at grain boundaries or closely adjacent regions without appreciable attack of the grains or crystals of the metal itself. Intergranular corrosion does not occur with commercially pure aluminum and other common work hardened aluminum alloys.

Stress Corrosion

Stress corrosion is failure of the metal by cracking under the combined action of corrosion and stresses approaching the yield stress of the metal. During spent fuel pool operations, the 32PT-DSC is upright and there is negligible load on the basket assembly. The stresses on the basket are small, well below the yield stress of the basket materials.

B. Behavior of Austenitic Stainless Steel in Borated Water

The fuel compartments are made from XM-19 stainless steel and the transition rails that support the fuel compartments are made from either Type 304 stainless steel with attached aluminum plates or of solid aluminum. Stainless steel does not exhibit general corrosion when immersed in borated water. Galvanic attack can occur between the aluminum in contact with the stainless steel in the water. However, the attack is mitigated by the passivity of the aluminum and the stainless steel in the short time the pool water is in the DSC. Also the low conductivity of the pool water tends to minimize galvanic reactions.

Stress corrosion cracking in the Type 304 and XM-19 stainless steel welds of the basket is also not expected to occur, since the baskets are not highly stressed during normal operations. There may be some residual fabrication stresses as a result of welding of the stainless steel plates together.

Of the corrosive agents that could initiate stress corrosion cracking in the stainless steel basket welds, only the combination of chloride ions with dissolved oxygen occurs in spent fuel pool water. Although stress corrosion cracking can take place at very low chloride concentrations and at low temperatures such as those in spent fuel pools (less than 10 ppb and 160°F, respectively), the effect of low chloride concentration and low temperature greatly increases the induction time. That is, the time period during which the corrodent is breaking down the passive oxide film on the stainless steel surface is increased. Below 60°C (140°F), stress corrosion cracking of austenitic stainless steel does not occur at all. At 100°C (212 °F), chloride concentration on the order of 15% is required to initiate stress corrosion cracking [3.5]. At 288 °C (550 °F), with tensile stress at 100% of yield in PWR water that contains 100 ppm O_2, time to crack is about 40 days in sensitized 304 stainless steel [3.6]. Thus, the combination of low chlorides, low temperature and short time of exposure to the corrosive environment eliminates the possibility of stress corrosion cracking in the basket and DSC welds.

The chloride content of all expendable materials which come in contact with the basket materials are restricted and water used for cleaning the baskets is restricted to 1.0 ppm chloride.

C. Behavior of Aluminum Based Neutron Poison in Borated Water

To investigate the use of borated aluminum in a spent fuel pool, tests were performed by Eagle Picher to evaluate its dimensional stability, corrosion resistance and neutron capture ability. These studies showed that borated aluminum performed well in a spent fuel pool environment.

The 1100 series aluminum component is a ductile metal having a high resistance to corrosion. Its corrosion resistance is provided by the buildup of a protective oxide film on the metal surface when exposed to a water or moisture environment. As stated above, for aluminum, once a stable film develops, the corrosion process is arrested at the surface of the metal. The film remains stable over a pH range of 4.5 to 8.5.

Tests were performed by Eagle Picher which concluded that borated aluminum exhibits a strong corrosion resistance at room temperature in either reactor grade deionized water or in 2000 ppm borated water. The behavior is only slightly different than 1100 series aluminum, hence, satisfactory long-term usage in these environments is expected. Neutron irradiation up to 10^{17} n/cm^2 level did not cause any measurable dimensional changes or any other damage to the material.

At high temperature, the borated aluminum still exhibits high corrosion resistance in the pure water environment. However, at temperatures of 80°C, in 2000 ppm borated water, local pitting corrosion has been observed. At 100°C and room temperature, the pitting attack was less than at 80°C. In all cases, passivation occurs limiting the pit depth.

From tests on pure aluminum, it was found that borated aluminum was more resistant to uniform corrosion attack than pure aluminum. Local pitting corrosion, can occur over time, causing localized damage to the borated aluminum.

There are no chemical, galvanic or other reactions that could reduce the areal density of boron in the 32PT-DSC neutron poison plates.

D. Electroless Nickel Plated Carbon Steel

The carbon steel top shield plug of the DSC is plated with electroless nickel. This coating is identical to the coating used on the NUHOMS®-52B DSC. It has been evaluated for potential galvanic reactions in Transnuclear West's response to NRC Bulletin 96-04 [3.7]. In PWR pools, the reported corrosion rates are insignificant and are expected to result in a negligible rate of reaction for the NUHOMS® PWR systems.

Lubricants and Cleaning Agents

Lubricants and cleaning agents used on the NUHOMS®-32PT DSC are limited to those with chlorine contents of less than 1 ppm chloride. Never-seez or Neolube (or equivalent) is used to coat the threads and bolt shoulders of the closure bolts. The lubricant should be selected for compatibility with the spent fuel pool water and the DSC materials, and for its ability to maintain lubricity under long term storage conditions.

The DSC is cleaned in accordance with approved procedures to remove cleaning residues prior to shipment to the storage site. The basket is also cleaned prior to installation in the DSC. The cleaning agents and lubricants have no significant affect on the DSC materials and their safety related functions.

Hydrogen Generation

During the initial passivation state, small amounts of hydrogen gas may be generated in the 32PT DSC. The passivation stage may occur prior to submersion of the TC into the spent fuel pool. Any amounts of hydrogen generated in the DSC will be insignificant and will not result in a flammable gas mixture within the DSC.

The small amount of hydrogen which may be generated during DSC operations does not result in a safety hazard. In order for concentrations of hydrogen in the cask to reach flammability levels, most of the DSC would have to be filled with water for the hydrogen generation to occur, and the lid would have to be in place with both the vent and drain ports closed. This does not occur during DSC loading or unloading operations.

An estimate of the maximum hydrogen concentration can be made, ignoring the effects of radiolysis, recombination, and solution of hydrogen in water. Testing was conducted by Transnuclear [3.9] to determine the rate of hydrogen generation for aluminum metal matrix composite in intermittent contact with 304 stainless steel. The samples represent the neutron poison plates paired with the basket compartment tubes. The test specimens were submerged in deionized water for 12 hours at 70 °F to represent the period of initial submersion and fuel loading, followed by 12 hours at 150 °F to represent the period after the fuel is loaded, until the water is drained. The hydrogen generated during each period was removed from the water and the test vessel and measured. Since the test was performed in deionized water, and the 32PT DSC will be used in borated water, the test results over-predict the hydrogen generation rates.

The test results were:

	12 hours @ 70°F		**12 hours @ 150°F**	
Aluminum MMC/SS304	$cm^3hr^{-1}dm^{-2}$	$ft^3hr^{-1}ft^{-2}$	$cm^3hr^{-1}dm^{-2}$	$ft^3hr^{-1}ft^{-2}$
	0.517	1.696E-4	0.489	1.604E-4

During the welding cycle, the most limiting case for hydrogen concentration is the 32PT-L100 DSC with stainless steel rails because it has the most aluminum surfaces. The total surface area of all aluminum components including the neutron absorber plates is 3495 ft^2. After 750 gallons of water has been drained, 1868 ft^2 of aluminum remains submerged. This surface area, combined with the test data at 150°F above result in a hydrogen generation rate of

$$(1.60 \times 10^{-4}\ ft^3/ft^2hr)(1868\ ft^2) = 0.30\ ft^3/hr$$

The minimum free volume of the DSC is 99.6 ft^3, which is equivalent to the 750 gallons of water drained from the DSC cavity. The following assumptions are made to arrive at a conservative estimate of hydrogen concentration:

- All generated hydrogen is released instantly to the plenum between the water and the shield plug, that is, no dissolved hydrogen is pumped out with the water, and no released hydrogen escapes through the open vent port, and

- The welding and backfilling process takes 8 hours to complete.

Under these assumptions, the hydrogen concentration in the space between the water and the shield plug is a function of the time water is in the DSC prior to backfilling with helium. The hydrogen concentration is (0.30 ft^3 H_2/hr)*(8 hr) / (99.6 ft^3) = 2.39%. Monitoring of the hydrogen concentration before and during welding operations is performed to ensure that the hydrogen concentration does not exceed 2.4%, which is well below the ignitable limit of 4%. If the hydrogen concentration exceeds 2.4%, welding operations are suspended and the DSC is purged with an inert gas. In an inert atmosphere, hydrogen will not be generated.

Effect of Galvanic Reactions on the Performance of the System

There are no significant reactions that could reduce the overall integrity of the DSC or its contents during storage. The DSC and fuel cladding thermal properties are provided in Section M.4. The emissivity of the fuel compartment is 0.46, which is typical for non-polished stainless steel surfaces. If the stainless steel is oxidized, this value would increase, improving heat transfer. The fuel rod emissivity value used is 0.80, which is a typical value for oxidized Zircaloy. Therefore, the passivation reactions would not reduce the thermal properties of the component cask materials or the fuel cladding.

There are no reactions that would cause binding of the mechanical surfaces or the fuel to basket compartment boxes due to galvanic or chemical reactions.

There is no significant degradation of any safety components caused directly by the effects of the reactions or by the effects of the reactions combined with the effects of long term exposure of the materials to neutron or gamma radiation, high temperatures, or other possible conditions.

M.3.4.2 Positive Closure

Positive closure is provided by the OS197 and OS197H TCs. No change.

M.3.4.3 Lifting Devices

The evaluations for the OS197 and OS197H TC trunnions are based on critical lift weights (with water in the DSC) of 208,500 lbs and 250,000 lbs, respectively. The maximum critical lift weight with a NUHOMS®-32PT DSC is approximately 224,000 lbs. Therefore, the OS197H cask is acceptable with any NUHOMS®-32PT DSC and the OS197 cask is acceptable with a NUHOMS®-32PT DSC where the total critical lift weight is not more than 208,500 lbs (32PT-S100 and 32PT-L100 with water drained from the DSC cavity to meet the weight limit).

M.3.4.4 Heat and Cold

M.3.4.4.1 Summary of Pressures and Temperatures

Temperatures and pressures for the 32PT DSC and basket are calculated in Section M.4. Section M.4.4 provides the thermal evaluation of normal conditions. Section M.4.5 provides the thermal evaluation for off-normal conditions. Section M.4.6 provides the thermal evaluation of accident conditions. Section M.4.7 provides the thermal evaluation during vacuum drying operations. Section M.4 provides the calculated temperatures for the various components during storage, transfer and vacuum drying operations respectively.

Section M.4.4.4 also provides the maximum pressures during normal, off-normal and accident conditions which are used in the evaluations presented later in this Appendix.

M.3.4.4.2 Differential Thermal Expansion

To minimize thermal stress, clearance is provided between the poison plates and inside of the fuel cells, between the basket outer diameter and DSC cavity inside diameter, and in the axial direction between the DSC cavity and all basket parts. Additionally, the connections between the transition rails and the fuel support grid and between the aluminum heat transfer plate material and the fuel support grid are made to permit relative axial growth.

- In the axial direction, required clearances are determined using hand calculations.
- In the "radial" direction, clearance between the fuel cells and the neutron absorbing and heat transfer plate materials, is evaluated using hand calculations.
- In the "radial" direction, clearance between the basket assembly (fuel support grid and transition rails) was included in the ANSYS thermal stress analyses described in Section M.3.4.4.3. The normal condition stress analyses are described in M.3.6 and the accident condition analyses are described in M.3.7. Thus, stresses due to any thermal interferences are included in the stress results.

As noted above, hand calculations are used to evaluate thermal expansion in the axial direction and between the fuel cells and the poison/heat transfer material. Sample calculations and results for the hand calculations are described below. Results from the ANSYS thermal stress evaluations are described in Section M.3.4.4.3.

Basket assembly temperatures for normal conditions are listed in Tables M.4-3 to M.4-5; off-normal temperatures are listed in Tables M.4-9 through M.4-11.

The thermal analyses of the basket for the handling/transfer conditions are described in Section M.4. As described there, thermal analyses are performed to determine the temperature distributions in the 32PT DSC for the following cases:

- Vacuum Drying
- Blocked Vent Storage
- On-Site Transfer at -40°F ambient

- On-Site Transfer at 0°F ambient
- On-Site Transfer at 100°F ambient
- On-Site Transfer at 117°F ambient
- HSM Storage at -40°F ambient
- HSM Storage at 0°F ambient
- HSM Storage at 70°F ambient
- HSM Storage at 100°F ambient
- HSM Storage at 117°F ambient

Based on the temperature distributions for the cases listed above, hand calculations are used to evaluate the effects of differential thermal expansion for the vacuum drying and -40°F storage cases. These cases are selected since they maximize the temperature differentials, and differential expansion, in the DSC and basket assembly.

The following calculations show the evaluation of relative radial growth between the fuel support grid and the heat transfer/neutron absorbing material. For these parts, the relative growth is evaluated between parts that are immediately adjacent to each other (i.e., between the heat transfer/neutron absorbing material at the center of the basket and the XM-19 at the center of the basket), Thus the temperatures of the two materials are equal.

Radial Expansion

In the radial direction, the thermal expansion values for the fuel support grid and the heat transfer materials are evaluated at the maximum allowable material temperature of 800°F. This maximizes the relative expansion between the parts:

$$\begin{aligned}\Delta L_{GRID} &= \alpha_{XM19} L_{GRID} \Delta T \\ &= (9.40 \times 10^{-6} °F^{-1})(8.825\ in)(800°F - 70°F) \\ &= .061\ in \\ \Delta L_{AL\_N} &= \alpha_{1100} L_{GRID} \Delta T \\ &= (14.8 \times 10^{-6} °F^{-1})(8.56\ in)(800°F - 70°F) \\ &= .092\ in\end{aligned}$$

Comparing the relative expansion of the heat transfer/neutron absorbing material and the Type XM-19 fuel grid to the design clearance:

$$\begin{aligned}\text{Design Clearance} &= (8.825\ in) - (8.56\ in) \\ &= 0.265\ in \\ \text{Relative Growth} &= \Delta L_{AL\_N} - \Delta L_{GRID} \\ &= .092\ in - .061\ in \\ &= .031\ in\end{aligned}$$

The clearance is much larger than the differential growth. Thus there is no stress due to differential "radial" expansion between the heat transfer/neutron absorbing material(s) and the Type XM-19 fuel grid.

Axial Expansion

For the vacuum drying condition, axial thermal expansion of the basket components is calculated below.

Component	T_{max} (°F)	T_{min} (°F)	α_{avg} ($°F^{-1}$)	L	ΔL
Fuel Grid	800	--	9.4E-06	174.7 in	1.199 in
"	--	534	9.1E-06	174.7 in	0.738 in
Heat Transfer Material / Neutron Absorber	800	--	1.48E-05	174.7 in	1.887 in
Type 304 T. Rails	600	--	9.8E-06	174.7 in	0.907 in
"	--	525	9.7E-06	174.7 in	0.771 in
6061 (Al.) T. Rails	600	--	1.42E-05	174.7 in	1.315 in
"	--	525	14.0E-06	174.7 in	1.113 in
DSC Cavity	--	215	9.0E-06	174.7 in	0.228 in

Relative expansion is determined by comparing values calculated above. For example, the "worst case" required clearances between the end of the DSC cavity and the structural parts of the basket assembly can be determined by comparing the cavity expansion to the expansion of the basket assembly calculated using the maximum component temperatures:

Relative Axial Thermal Growth (Vacuum Drying)	Component Growth	Cavity Growth	Required Clearance[1]
Fuel Grid to Cavity	1.12 in	0.228 in	0.90 in
Steel Transition Rails to Cavity	.91 in	0.228 in	0.68 in
6061 Transition Rails to Cavity	1.32 in	0.228 in	1.10 in

Notes: 1. Required Clearance is the room temperature clearance between the top of the listed component and the bottom of the top shield plug and is determined by subtracting the cavity expansion from the component expansion.

The differential axial growth between the Aluminum Alloy 1100 heat transfer material (and neutron absorbing material) and the fuel support grid is determined using similar methods. An average value of axial expansion is used since the overall growth of the fuel support grid will be related to the average grid temperature. A maximum value of aluminum expansion is used.

Relative Axial Thermal Growth (Vacuum Drying)	Fuel Support Grid Axial Growth	1100 Alloy Growth	Required Clearance[1]
Fuel Grid to Aluminum Heat Transfer Material (Alloy 1100)	$\Delta L = \frac{1.12\text{ in} + .74\text{ in}}{2} = 0.93\text{ in}$	1.89 in	0.96 in

Notes: 1. Required Clearance is the room temperature clearance between the neutron absorbing sheets and Alloy 1100 aluminum heat transfer material and the stop plates attached to the fuel grid.

M.3.4.4.3 Thermal Stress Calculations

The thermal stress calculations for the various system components other than the basket are provided in Sections 3.6 and 3.7 for normal, off-normal and accident conditions. The thermal stress calculations for the 32PT basket are presented below.

Thermal stresses are considered separately and in combination with other loads on the basket assembly. Only the separate thermal stresses are presented here. Thermal stresses in combination with other loads are addressed in the appropriate sections.

As noted in M.3.4.4.2, clearances are provided such that there is free thermal expansion in the axial direction.

Thermal stresses in the basket assembly are evaluated using the ANSYS [3.11] finite element model described in M.3.6.1.3. As described in M.3.6.1.3.1, the ANSYS model includes the fuel support grid, R90 transition rails, R45 transition rails, the DSC shell, and the cask ID and cask rails. For the evaluation of thermal stresses only (i.e., thermal stresses without deadweight or other loads), the cask ID and cask rails are removed from the solution by eliminating the contact elements between the shell OD and the cask ID with cask rails. For the evaluation of thermal loads combined with other loads (e.g., thermal plus deadweight), all contact elements are active and the effects of the cask and cask rails are included.

As listed below, a total of 30 thermal stress analyses were performed for each of the two basket transition rail configuration options (stainless steel and solid aluminum).

Condition / Ambient Temperature		**Heat Load Zoning Configurations (see Figures M.1-1, M.1-2 and M.1-3)**		
		1	**2**	**3**
Vacuum Drying		X	X	
Blocked Vent Storage		X		
On-Site Transfer	-40°F ambient	X	X	X
	0°F ambient	X	X	X
	100°F ambient	X	X	X
	117°F ambient	X	X	X
HSM Storage	-40°F ambient	X	X	X
	0°F ambient	X	X	X
	70°F ambient	X	X	X
	100°F ambient	X	X	X
	117°F ambient	X	X	X

Maximum thermal stresses (ANSYS nodal stress intensities) are summarized in Table M.3.4-1 for the steel transition rails and Table M.3.4-2 for the solid aluminum transition rails. As shown by the tables, thermal stresses in the 32PT basket are low. Based on these results, the temperature distribution corresponding to 117°F ambient temperature, DSC in the TC, with heat load zoning configuration 1 was selected for combination with other loads. Selection of a high

temperature case ensures the application of lower allowable stresses (since allowable stresses decrease with temperature), and reduced structural stiffness (since stability is directly related to E and S_y).

Results of the thermal stress analysis are shown in Figures M.3.4-2 through M.3.4-5. These figures show the applied temperature distribution and resulting thermal stresses for cold)-40°F in cask) and hot (117°F in cask) conditions. Separate figures are included for the 32PT basket assembly with Type 304 transition rails and with 6061 Alloy transition rails.

Table M.3.4-1
Summary of Thermal Stress Results - 32PT Basket with Steel Transition Rails

Operating Condition	Maximum Stress Intensities (ksi)		
	Fuel Grid	R90 Transition Rails	R45 Transition Rails
Vacuum Drying	6.50	11.4	3.50
Blocked Vent Storage	4.00	.50	.80
On-Site Transfer & Storage[1]	4.50	1.0	1.0

Note: 1. Includes all cases except for vacuum drying and blocked vent storage.

Table M.3.4-2
Summary of Thermal Stress Results - 32PT Basket with Aluminum Transition Rails

Operating Condition	Maximum Stress Intensities (ksi)			
	Fuel Grid	R90 Transition Rail (XM-19 Cover Plate)	R90 Transition Rail (Aluminum)	R45 Transition Rail (Aluminum)
Vacuum Drying	4.33	2.55	.55	1.40
Blocked Vent Storage	4.25	2.75	.60	1.40
On-Site Transfer & Storage[1]	4.95	2.50	.60	1.50

Note: 1. Includes all cases except for vacuum drying and blocked vent storage.

POTENTIAL VERSUS pH DIAGRAM FOR ALUMINUM-WATER SYSTEM

At 25°C (77°F):

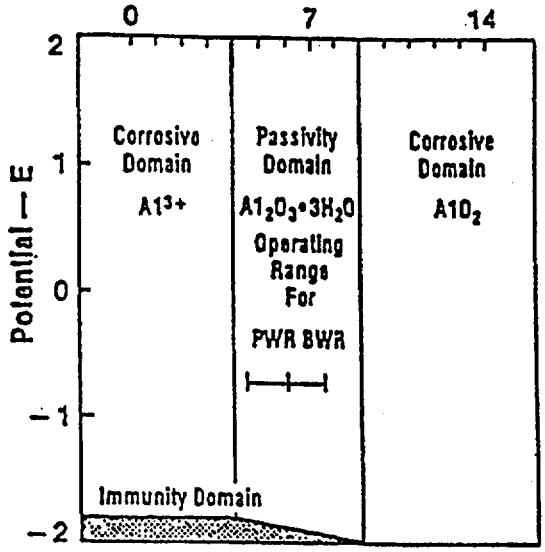

At 60°C (140°F):

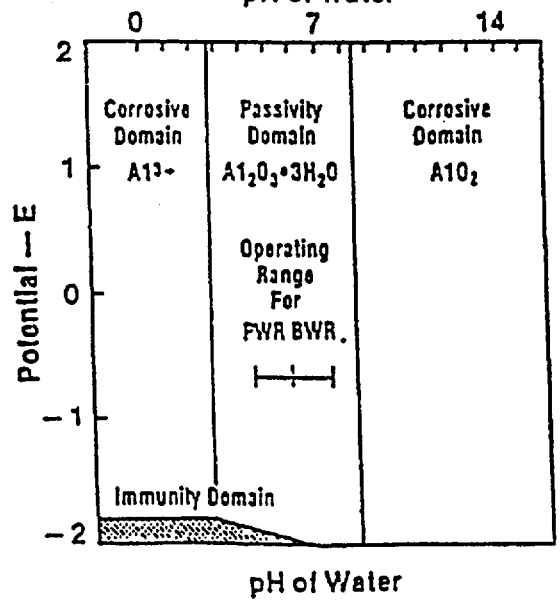

Figure M.3.4-1
Potential Versus pH Diagram for Aluminum-Water System

M.3.5 Fuel Rods

No change to the evaluation presented in the FSAR.

M.3.6 Structural Analysis (Normal and Off-Normal Operations)

In accordance with NRC Regulatory Guide 3.48 [3.12], the design events identified by ANSI/ANS 57.9-1984, [3.14] form the basis for the accident analyses performed for the standardized NUHOMS® System. Four categories of design events are defined. Design event Types I and II cover normal and off-normal events and are addressed in Section 8.1. Design event Types III and IV cover a range of postulated accident events and are addressed in Section 8.2. The purpose of this section of the Appendix is to present the structural analyses for normal and off-normal operating conditions for the NUHOMS®-32PT system using a format similar to the one used in Section 8.1 for analyzing the NUHOMS®-24P systems.

M.3.6.1 Normal Operation Structural Analysis

Table M.3.6-1 shows the normal operating loads for which the NUHOMS® safety-related components are designed. The table also lists the individual NUHOMS® components which are affected by each loading. The magnitude and characteristics of each load are described in Section M.3.6.1.1.

The method of analysis and the analytical results for each load are described in Sections M.3.6.1.2 through M.3.6.1.9.

M.3.6.1.1 Normal Operating Loads

The normal operating loads for the NUHOMS® System components are:

- Dead Weight Loads
- Design Basis Internal and External Pressure Loads
- Design Basis Thermal Loads
- Operational Handling Loads
- Design Basis Live Loads

These loads are described in detail in the following paragraphs.

(A) Dead Weight Loads

Table M.3.2-1 shows the weights of various components of the NUHOMS®-32PT system. The dead weight of the component materials is determined based on nominal component dimensions.

(B) Design Basis Internal and External Pressure

The maximum internal pressures of the NUHOMS®-32PT DSC for the storage and transfer mode are presented in Section M.4.

(C) Design Basis Thermal Loads

The normal condition temperature distributions for the 32PT-DSC are presented in Section M.4. Stress analysis for normal thermal loads for the DSC shell assembly are provided in Section M.3.6.1.2(C) and in Section M.3.4.4 for the basket assembly.

(D) Operational Handling Loads

There are two categories of handling loads: (1) inertial loads associated with on-site handling and transporting the DSC between the fuel handling/loading area and the HSM, and (2) loads associated with loading the DSC into, and unloading the DSC from, the HSM. These handling loads are described in Section 8.1.1.1C.

Based on the surface finish and the contact angle of the DSC support rails inside the HSM (described in Chapter 4), a bounding coefficient of friction is conservatively assumed to be 0.25. Therefore, the nominal ram load required to slide the DSC under normal operating conditions is approximately 29,300 lbs., calculated as follows:

$$P = \frac{0.25\ W}{\text{Cos}\,\theta} = 0.29\ W = 0.29(101{,}100\ \text{lbs}) \approx 29{,}300\ \text{lbs.}$$

Where:

P = Push/Pull Load,

W = Loaded DSC Weight ≈ 101,100 lbs. (See Table M.3.2-1), and

θ = 30 degrees, Angle of the Canister Support Rail.

However, the DSC bottom cover plate and grapple ring assembly are designed to withstand a normal operating insertion force equal to 80,000 pounds and a normal operating extraction force equal to 60,000 pounds. To insure retrievability for a postulated jammed DSC condition, the ram is sized with a capacity for a load of 80,000 pounds, as described in Section 8.1.2. These loads bound the friction force postulated to be developed between the sliding surfaces of the DSC and TC during worst case off-normal conditions.

(E) Design Basis Live Loads

As discussed in Section 3.2.4, a live load of 200 pounds per square foot is conservatively selected to envelope all postulated live loads acting on the HSM, including the effects of snow and ice. Live loads which may act on the TC are negligible, as discussed in Section 3.2.4.

M.3.6.1.2 Dry Shielded Canister Analysis

The standardized NUHOMS®-32PT DSC shell assembly is analyzed for the normal, off-normal and postulated accident load conditions using two basic ANSYS [3.11] finite element models: a top-end half-length model of the DSC shell assembly and a bottom-end half-length model of the

DSC shell assembly. Typical models of the top and bottom halves of the DSC shell assembly are shown in Figures 8.1-14a and 8.1-14b.

These models are used to evaluate stresses in the NUHOMS®-32PT DSC due to:

- Dead Weight
- Design Basis Normal Operating Internal and External Pressure Loads
- Normal Operating Thermal Loads
- Normal Operation Handling Loads

The methodology used to evaluate the effects of these normal loads is addressed in the following paragraphs. Table M.3.6-2 summarizes the resulting stresses for normal operating loads.

Dead load analyses of the DSC are performed for both vertical and horizontal positions of the DSC. In the vertical position, the DSC shell supports its own empty weight and the entire weight of the top end components. When inside the TC, the weight of the fuel and the bottom end components is transferred to the TC by bearing through the inner bottom cover plate, shield plug and outer bottom cover plate. When in the horizontal position, the DSC is in the TC or in the HSM. In this position, the DSC shell assembly end components and the internal basket assembly bear against the DSC shell. The DSC shell assembly is supported by two rails located at ± 18.5° when in the TC and at ± 30° when in the HSM. This is shown schematically in Figure 8.1-13.

(A) DSC Dead Load Analysis

Dead load stresses are obtained from static analyses performed using the ANSYS finite element models described above. Both, the top-end half and bottom-end half models are analyzed for a 1g load, using the appropriate finite element model and boundary conditions, for horizontal and vertical configurations. For the horizontal dead load analyses, the DSC is conservatively assumed to be supported on one rail. In addition, the fuel-loaded portions of the basket assembly bear on the inner surface of the DSC shell. DSC shell stresses in the region of the basket assembly resulting from the bearing load and from local deformations at the cask rails are evaluated using the ANSYS model described in Section M.3.6.1.3. The DSC shell assembly components are evaluated for primary membrane and membrane plus bending stress and for primary plus secondary stress range. Enveloping maximum stress intensities are summarized in Table M.3.6-2 for the NUHOMS®-32PT DSC.

(B) DSC Normal Operating Design Basis Pressure Analysis

The NUHOMS®-32PT DSC shell assembly analytical models shown in Figure 8.1-14a and Figure 8.1-14b are used for the normal operating design pressure analyses. The calculated maximum internal pressures for the NUHOMS®-32PT DSC are shown in Section M.4. The design internal pressure of 20 psig is used. The resulting maximum stress intensities are reported in Table M.3.6-2.

(C) DSC Normal Operating Thermal Stress Analysis

The thermal analysis of the DSC for the various conditions, as presented in Section M.4.0, provide temperature distributions for the DSC shell, along with maximum and minimum DSC component temperatures. These temperature distributions are imposed onto the DSC shell assembly ANSYS stress analysis models shown in Figure 8.1-14a and Figure 8.1-14b for thermal stress evaluation. Corresponding component temperatures are used to determine material properties and allowable stress values used in the stress analyses. DSC shell assembly materials are all Type 304 stainless steel with the exception of the shield plugs, which are made of A36 carbon steel. However, because these dissimilar materials are not mechanically fastened, allowing free differential thermal growth, the thermal stresses in the DSC shell components are due entirely to thermal gradients. The results of the thermal analysis show that for the range of normal operating ambient temperature conditions, the thermal gradients are primarily along the axial and tangential directions of the DSC and that no significant thermal gradients exist through the wall of the DSC. Stresses resulting from thermal gradients are classified as secondary stresses and are evaluated for Service Level A and B conditions. Maximum stress intensities resulting from the thermal stress analyses are summarized in Table M.3.6-2 for the NUHOMS®-32PT DSC.

(D) DSC Operational Handling Load Analysis

To load the DSC into the HSM, the DSC is pushed out of the TC using a hydraulic ram. The applied force from the hydraulic ram, specified in Section M.3.6.1.1(D), is applied to the center of the DSC outer bottom cover plate at the center of the grapple ring assembly. The ANSYS finite element model shown in Figure 8.1-14b is used to calculate the stresses in the DSC shell assembly. In the analysis, the ram load is applied to the cover plate in the form of two arcs, assuming that the load is concentrated at the barrel diameter of the ram, excluding the cutouts for extension of the grapple arms.

To unload the HSM, the DSC is pulled using grapples which fit into the grapple ring. For analysis of grapple pull loading, the 180° ANSYS finite element model of the bottom half DSC assembly is refined in the area of the grapple assembly and outer cover plate, as shown in Figure 8.1-15.

The controlling stresses from these analyses are tabulated in Table M.3.6-2.

(E) Evaluation of the Results

The maximum calculated DSC shell stresses induced by normal operating load conditions are shown in Table M.3.6-2. The calculated stresses for each load case are combined in accordance with the load combinations presented in Table M.2-15. The resulting stresses for the controlling load combinations are reported in Section M.3.7.10 along with the ASME Code allowable stresses.

M.3.6.1.3 NUHOMS®-32PT Basket Structural Analysis

Stresses in the basket assembly are determined using a combination of hand calculations and a two dimensional (planar) ANSYS finite element model. The following loads are addressed:

- Dead Weight
- Thermal Stresses
- Handling/Transfer Loads
- Side Drops
- Seismic Loads

Thermal loads for the basket are addressed in Section M.3.4.4. The side drop loads are Level D loads and are addressed in Section M.3.7. The seismic loads are Level C loads, but are enveloped by the on-site handling loads as described in Section M.3.6.1.3.2.

M.3.6.1.3.1 ANSYS Finite Element Model Analysis

(A) ANSYS Finite Element Model Description

The ANSYS models of the 32PT basket assembly use Plane42 (2-D Structural Solid) elements to represent a unit length of the 32PT basket. A minimum of three (3) elements are used through the thickness of all parts except the cask shell and cask rails. The cask shell and cask rails, which are extremely rigid relative to the other parts of the structure, are included as "ground" and are fixed around their entire circumference. Therefore, the cask shell is modeled with only one through thickness element. Table M.3.6-3 lists the structural parts included in the model.

The geometry of the basket model is shown in Figures M.3.6-1 and M.3.6-2 for the 32PT DSC with steel transition rails and Figures M.3.6-3 and M.3.6-4 for the 32PT DSC with aluminum transition rails.

ANSYS contact elements, Contac48, 2-D Point-to-Surface Contact, are used between the separate parts of the structure. Since the components are modeled with actual thicknesses, the initial gap dimensions are determined by the geometry of the contacting surfaces. Contact elements are included between the following interfacing components:

- Fuel support grid to transition rails,
- Transition Rails to DSC Shell ID, and
- DSC Shell OD to Cask ID and Cask Rail.

Springs elements are provided between the fuel support grid and the transition rails. These springs, which act in parallel to the contact elements, are defined with non-linear stiffnesses such that low stiffness is active for motion of the rails away from the grid, allowing the transition rails

to separate from the grid and a higher stiffness which is active for compression between the two structures.

Inertial loads are applied to the structure by including the appropriate weight density of the materials and applying accelerations. Fuel loads are applied using pressure loads on the fuel grid elements. Thermal effects are included by applying temperatures corresponding to the 117°F in cask temperature distribution, to each node in the model (see M.3.4.4.3).

For all stress analyses, 1g (deadweight) loads are applied and stresses determined. These deadweight stresses are classified as primary membrane and membrane plus bending stresses. Additional load steps are then used to apply temperatures corresponding to the 117°F ambient temperature condition. The thermal plus deadweight stresses are classified as primary plus secondary. Tables of the temperature-dependent material properties (e.g., S_y versus temperature) are included in the ANSYS model, such that the appropriate properties are applied at each point in the structure.

For each cell of the fuel support structure, stresses were linearized at the 12 locations shown in Figure M.3.6-5 using the ANSYS LPATH, PRSEC commands. Maximum values are reported in this Appendix.

(B) Material Properties

The material properties used in the ANSYS stress analyses for normal conditions are summarized in Table M.3.6-4. As listed in this table, linear elastic properties are used for the normal condition analyses. With the exception of the solid aluminum transition rails, properties for all materials are directly from the ASME Code. Properties for the aluminum rails are described in Section M.3.3.

M.3.6.1.3.2 Normal Condition Loading

Postulated loads on the 32PT basket structure for non-accident conditions are described in the following sections. The loads and load combinations for the 32PT basket structure are simplified by consideration that the basket is unaffected by either pressure loads or HSM insertion/retrieval loads.

(A) Thermal

The analysis of the 32PT basket for thermal loads is described in Section M.3.4.4. As shown in Section M.3.4.4, thermal stresses are small.

(B) Vertical Deadweight

Deadweight load conditions include: (1) vertical deadweight during fuel loading operations, (2) horizontal deadweight in the TC with support through the cask rails at ±18.5°, and (3) horizontal deadweight in the HSM with support through the HSM rails at ±30°.

Under axial loads, the fuel assemblies and fuel compartment are supported by the bottom of the cask. Thus, the fuel assemblies react directly against the bottom of the canister/cask and do not load the basket structure. Stresses under axial loading are from self weight of the basket structure. Maximum axial compressive stresses occur at the supported end of the basket.

Vertical deadweight was evaluated using hand calculations and by comparing the calculated axial compression stresses to stability allowables developed considering both stability criteria and the general membrane criteria (P_m) from Subsection NG (see M.2.2.5.1.2). Calculated stresses for the vertical deadweight condition also applied to the vacuum drying case.

Calculated stresses are listed in Table M.3.6-5 along with the appropriate compressive allowables. As shown by the table, stresses for this load condition are small.

(C) Horizontal Deadweight

Horizontal deadweight cases were evaluated using the ANSYS model described in M.3.6.1.3.1. As appropriate the elements representing the support rails were located at either ±18.5° or ±30° from bottom center for support by the TC or HSM, respectively. Separate analyses were performed for the 32PT fuel grid supported by the steel transition rails and by the aluminum transition rails. Thus, the following four (4) analysis cases were evaluated:

1. 32PT DSC with steel transition rails supported at ±18.5° (Figure M.3.6-6)

2. 32PT DSC with solid alloy 6061 aluminum rails supported at ±18.5° (Figure M.3.6-10)

3. 32PT DSC with steel transition rails supported at ±30° (Figure M.3.6-8)

4. 32PT DSC with solid alloy 6061 aluminum rails supported at ± 30° (Figure M.3.6-12)

Primary plus secondary stresses were evaluated by combining deadweight stresses with the thermal stresses resulting from the 117°F in cask temperature distribution. Maximum stresses are summarized in Table M.3.6-5 along with a comparison to Level A allowables from Subsection NG.

(D) Vacuum Drying

As described above, the axial compression stresses under the vacuum drying condition are equal to the axial compression stresses under vertical deadweight.

As described in M.3.4.4.3, maximum stresses from the vacuum drying temperature distribution are listed in Tables M.3.4-1 and M.3.4-2. These thermal stresses are classified as secondary by the Code and, as shown by the tables, these stresses are small.

(E) Handling/On-Site Transfer Loads

These cases include the loads associated with loading (and unloading) the 32PT DSC into an HSM and the inertial loads associated with on-site handling. The insertion/retrieval loads do not

directly impact the 32PT basket assembly and do not require additional consideration. The inertia loads to be considered are:

- DW + 1g Axial
- DW + 1g Transverse.
- DW + 1g Vertical
- DW + 0.5g Axial + 0.5 Transverse + 0.5 Vertical

These loads are enveloped by a 2g resultant acceleration applied in the most critical orientation.

The 2.0g resultant axial load is evaluated using hand calculations and the same methodology used for the vertical deadweight analyses. Maximum compressive stresses resulting from this load case are listed in Table M.3.6-6 along with a comparison to the axial stability criteria described in M.2.2.5.1.2.

Loads transverse to the axis of the DSC are evaluated using the ANSYS models described in M.3.6.1.3.1. Loads are enveloped by selection of maximum stresses from the analysis load cases listed in Table M.3.6-7. Table M.3.6-7 lists the on-site handling analyses performed for the 32PT basket considering the basket transition rail configuration and DSC support conditions in the OS197, OS197H and HSM. Enveloping 32PT basket stresses are summarized in Table M.3.6-6 along with a comparison to Service Level A allowables.

(F) Evaluation of Results

ANSYS plots showing typical analysis results for the 32PT basket are provided in Figure M.3.6-6 through Figure M.3.6-9 for the basket configuration with steel transition rails and in Figure M.3.6-10 through Figure M.3.6-13 for basket with solid aluminum transition rails. These figures and summary tables in the previous sections show that the basket stress criteria is met.

Welds in the fuel support structure are sized to maintain full moment capacity of the plates across all welded connections.

Within the basket grid structure are plates of Type 1100 aluminum and neutron absorbing materials composed of either enriched borated aluminum alloy or Boralyn® plates which perform heat transfer and criticality functions. As shown in Section M.4, the maximum short term basket temperature is 791°F, which is well below the melting point of the aluminum plates (approximately 1200°F). As discussed in Section M.3.4, adequate clearance is provided for thermal expansion so that thermal stresses in the aluminum plates are negligible. The bounding normal or off-normal axial stress in the plates is 0.04 ksi, due to the 2g handling load, which is well below the yield stress value of 1.3 ksi (Type 1100 aluminum at 791°F). This ensures that the plates remain in position to perform their heat transfer and criticality functions. Under inertia loading in the transverse direction, the aluminum plates are supported along their length by either the grid structure or the fuel assemblies. Deflection of the aluminum plates in the transverse direction is limited by the gap between the grid structure and the fuel assembly and does not significantly affect the heat transfer function of the plates. The effect of this gap is bounded by the criticality evaluation.

M.3.6.1.4 DSC Support Structure Analysis

The DSC support structure is shown in Figures 4.2-6 and 4.2-7.

As presented in Section 8.1.1.4, the various components of the DSC support structure are subjected to normal operating loads including dead weight, thermal, and operational handling loads which are greater than or equal to the corresponding loads for the 32PT DSC. Therefore, the limiting DSC support structure components are acceptable.

M.3.6.1.5 HSM Design Analysis

The HSM loads evaluated in Section 8.1.1.5 bound the corresponding loads for the 32PT system. Therefore, there is no change to the structural evaluation of the HSM.

M.3.6.1.6 HSM Door Analyses

As discussed in Section M.3.6.1.5 there is no change to the structural evaluation of the HSM.

M.3.6.1.7 HSM Heat Shield Analysis

As discussed in Section M.3.6.1.5 there is no change to the structural evaluation of the HSM.

M.3.6.1.8 HSM Axial Retainer for DSC

As discussed in Section M.3.6.1.5 there is no change to the structural evaluation of the HSM.

M.3.6.1.9 On-Site TC Analysis

The on-site TC is evaluated for normal operating condition loads including:

- Dead Weight Load
- Thermal Loads
- Handling Loads
- Live Loads.

Section 8.1.1.9 provides the evaluation of the TCs for the normal operating loads. Thermal loads and live loads for the OS197 and OS197H TCs with the 32PT DSC are equivalent to or less than those evaluated in Section 8.1.1.9. The evaluations for the OS197 and OS197H casks are based on payloads of 90,000 lbs. and 116,000 lbs., respectively. The maximum total cask payload with a dry-loaded NUHOMS®-32PT DSC is approximately 102,000 lbs. Therefore, the OS197H cask is acceptable with any NUHOMS®-32PT DSC and the OS197 cask is acceptable with a NUHOMS®-32PT DSC where the total cask payload is not more than 90,000 lbs.

M.3.6.2 Off-Normal Load Structural Analysis

Table M.3.6-8 shows the off-normal operating loads for which the NUHOMS® safety-related components are designed. This section describes the design basis off-normal events for the NUHOMS® System and presents analyses which demonstrate the adequacy of the design safety features of a NUHOMS® System with the 32PT DSC.

For an operating NUHOMS® System, off-normal events could occur during fuel loading, cask handling, trailer towing, canister transfer and other operational events. Two off-normal events are defined which bound the range of off-normal conditions. The limiting off-normal events are defined as a jammed DSC during loading or unloading from the HSM and the extreme ambient temperatures of -40°F (winter) and +117°F (summer). These events envelope the range of expected off-normal structural loads and temperatures acting on the DSC, TC, and HSM. These off-normal events are described in Section 8.1.2.

M.3.6.2.1 Jammed DSC During Transfer

The interfacing dimensions of the top end of the TC and the HSM access opening sleeve are specified so that docking of the TC with the HSM is not possible should gross misalignments between the TC and HSM exist. Furthermore, beveled lead-ins are provided on the ends of the TC, DSC, and DSC support rails to minimize the possibility of a jammed DSC during transfer. Nevertheless, it is postulated that if the TC is not accurately aligned with respect to the HSM, the DSC binds or becomes jammed during transfer operations.

The interfacing dimensions and design features of the HSM access opening, DSC Support Structure and the OS197 and OS197H TCs, as described in Section 8.1.2, remain unchanged. The insertion and extraction forces applied on the NUHOMS®-32PT during loading and unloading operations are the same as those specified for the NUHOMS®-24P system. The discussion in Section 8.1.2B applies to the 32PT DSC. However, the NUHOMS®-32PT DSC shell thickness is 0.5 inches (compared to 0.625 inches for the NUHOMS®-24P DSC shell) and the outside radius is 33.595 inches. Hence, the NUHOMS®-32PT DSC shell stresses, based on a force of 80 kips and a moment arm of 33.595 inches are calculated below.

Axial Sticking of the DSC

$$S_{mx} = \frac{M}{S}$$ (From Equation 8.1-9, Section 8.1.2.1)

Where:

M = 80 x 33.595 = 2690 in.-kip, Bending moment

S = 1734 $in.^3$, DSC section modulus

Therefore:

S_{mx} = 1.55 ksi

This magnitude of stress is negligible when compared to the allowable membrane stress of 17.5 ksi and is bounded by stresses for other handling loads as shown Table M.3.6-2.

There is no change to the structural evaluation of the HSM.

Binding of the DSC

As discussed in Section 8.1.2C, if axial alignment within system operating specifications is not achieved, it may be possible to pinch the DSC shell as shown in Figure 8.1-32. From Section 8.1.2C, the pinching force is taken as the product of the maximum ram loading of 80,000 pounds and the sine of a 1 degree angle, or 1,400 pounds.

The 1,400 pound load is conservatively assumed to be applied as a point load at a location away from the ends of the cask or DSC. The resulting maximum stresses are given by Table 31, Case 9a of Roark [3.10] as:

Membrane stress:

$$\sigma = \frac{0.4P}{t^2}$$

Bending stress:

$$\sigma' = \frac{2.4P}{t^2}$$

Therefore, the maximum membrane plus bending stress is:

$$\sigma + \sigma' = \frac{2.8P}{t^2}$$

For the DSC shell, t = 0.500 inch. Substituting for t and using a value of P equal to 1,400 pounds, the maximum extreme fiber stresses in the DSC shell are 15.7 ksi. This local stress is conservative in that small deformations create a larger contact area, i.e., not a point load, and the stress is actually lower than calculated. In addition, the deformations are limited by the gap between the shell and basket. As such, this stress is considered a secondary stress and is enveloped by the handling stresses shown in Table M.3.6-2.

The tangential component of ram loading under the assumed condition is less than the 80,000 lbs force of the jammed condition, axial sticking, calculated above and as such is not considered further.

In both scenarios for a jammed DSC, the stress in the DSC shell is demonstrated to be much less than the ASME Code allowable stress and below the yield value of the material. Therefore, permanent deformation of the DSC shell does not occur. There is no potential for breach of the DSC containment pressure boundary and, therefore, no potential for release of radioactive material.

There is no change to the structural evaluation of the OS197 and OS197H TC as shown in the FSAR.

There is no change to the required corrective actions, as described in the FSAR, for the jammed DSC conditions.

M.3.6.2.2 Off-Normal Thermal Loads Analysis

As described in Section 8.1.2, the NUHOMS® System is designed for use at all reactor sites within the continental United States. Therefore, off-normal ambient temperatures of -40°F (extreme winter) and 117°F (extreme summer) are conservatively chosen. In addition, even though these extreme temperatures would likely occur for a short period of time, it is conservatively assumed that these temperatures occur for a sufficient duration to produce steady state temperature distributions in each of the affected NUHOMS® components. Each licensee should verify that this range of ambient temperatures envelopes the design basis ambient temperatures for the ISFSI site. The NUHOMS® System components affected by the postulated extreme ambient temperatures are the TC and DSC during transfer from the plant's fuel/reactor building to the ISFSI site, and the HSM during storage of a DSC.

Section M.4 provides the off-normal thermal analyses for storage and transfer mode for the NUHOMS®-32PT DSC. Maximum DSC shell assembly thermal stress analysis results for the normal and off-normal conditions are summarized in Table M.3.6-2. Basket assembly thermal results are summarized in Section M.3.4.4. The resulting stress intensities for the NUHOMS®-32PT are acceptable.

Table M.3.6-1
NUHOMS® Normal Operating Loading Identification

Load Type	AFFECTED COMPONENT				
	DSC Shell Assembly	DSC Basket	DSC Support Structure	Reinforced Concrete HSM	On-site TC
Dead Weight	X	X	X	X	X
Internal/External Pressure	X				
Normal Thermal	X	X	X	X	X
Normal Handling	X	X	X	X	X
Live Loads				X	X

Table M.3.6-2
Maximum NUHOMS®-32PT DSC Shell Assembly Stresses for Normal and Off-Normal Loads

DSC Components	Stress Type	Maximum Stress Intensity (ksi)[1]			
		Dead Weight	Internal Pressure[6]	Thermal[2]	Handling[4]
DSC Shell	Primary Membrane	2.65	8.90	N/A	4.10
	Membrane + Bending	6.00	9.18	N/A	6.00
	Primary + Secondary	7.00	16.29	37.55	51.43[7]
Inner Top Cover Plate	Primary Membrane	0.58	0.74	N/A	1.68
	Membrane + Bending	1.67	16.76	N/A	1.84
	Primary + Secondary[5]	1.63	16.76	24.52	1.85
Outer Top Cover Plate	Primary Membrane	1.11	2.65	N/A	1.11
	Membrane + Bending	1.63	7.43	N/A	1.63
	Primary + Secondary[5]	1.17	7.22	23.69	1.17

See end of table for notes.

Table M.3.6-2
Maximum NUHOMS®-32PT DSC Shell Assembly Stresses for Normal and Off-Normal Loads
(concluded)

DSC Components	Stress Type	Maximum Stress Intensity (ksi)[1]			
		Dead Weight	Internal Pressure[6]	Thermal[2]	Handling[4]
Inner Bottom Cover Plate	Primary Membrane	0.71	0.56	N/A	3.22
	Membrane + Bending	0.84	1.48	N/A	4.80
	Primary + Secondary[5]	0.83	1.51	30.21	43.06[8]
Outer Bottom Cover Plate	Primary Membrane	0.74	0.83	N/A	5.27
	Membrane + Bending	1.31	1.47	N/A	22.72
	Primary + Secondary[5]	1.18	1.15	30.81	39.97[8]

(1) Values shown are maximum irrespective of location.
(2) Envelope of Normal and Off-Normal ambient temperature conditions.
(3) Not used.
(4) Maximum of deadweight, 1g axial, 60 kips pull or 80 kips push (except as noted).
(5) Per Note 2 of Table NB3217-1, the stress at the intersection between a shell and a flat head may be classified as secondary (Q) if the bending moment at the edge is not required to maintain the bending stresses in the middle of the head within acceptable limits. Thus, the primary plus secondary stresses were computed in a finite element model that assumed moment transferring connections, whereas the primary membrane plus bending stresses were computed assuming pinned connections. All thermal stresses are classified as secondary.
(6) Due to the off-normal 20 psig internal pressure condition.
(7) Results are for the combination of deadweight, 15 psi internal pressure, the 1g vertical transfer load and thermal.
(8) Results are for the combination of deadweight, 20 psi internal pressure, the 80 kip ram push load and thermal.

Table M.3.6-3
NUHOMS®-32PT Basket Model Components, Element Types and Materials

Structural Component	ANSYS Element Type	Material
Fuel Support Structure	Plane42	Type XM-19 Stainless Steel
DSC Shell	Plane42	Type 304 Stainless Steel
R45 Transition Rails	Plane42	Type 304 Stainless Steel or 6061 Aluminum
R90 Transition Rails	Plane42	Type 304 or 6061 Aluminum w/XM-19 Cover Plate
Cask Shell & Cask Rails	Plane42	Type 304 (Elastic)
DSC/Cask Shell Springs	Combin39	N/A

Table M.3.6-4
Material Properties Used in Normal Condition 32PT Basket Analyses

Component	Material	Normal Condition Stress Analysis Material Properties[2]	Evaluation Temperature[1]
Fuel Support Grid	1/4" Thick, Type XM-19 Stainless Steel	Elastic (Code Properties)	800°F (All conditions)
Welded Steel Transition Rails	3/8" Thick Type 304 Stainless Steel	Elastic (Code Properties)	610°F/610°F (Vacuum Drying/Other)
Solid Aluminum Transition Rails, R90 Cover Plates	1/4" Thick, Type XM-19 Stainless Steel	Elastic (Code Properties)	610°F/600°F (Vacuum Drying/Other)
Solid Aluminum Transition Rails, Aluminum Bodies	6061 Aluminum Alloy	Elastic[3]	500°F/450°F (Blocked Vent / Other)

Notes:
1. For the steel components, stress checks were performed at the enveloping temperatures listed. For the aluminum transition rails, stress checks were performed at temperatures corresponding to the maximum stress point. Temperatures listed are for the maximum stress points of the most highly loaded rail (the large R90 transition rail at the "bottom" of the basket).
2. ASME Code properties for Type XM-19 and Type 304 Stainless Steels from Tables M.3.3-3 and M.3.3-2, respectively.
3. Properties for 6061 Aluminum from Table M.3.3-5.

Table M.3.6-5
Summary of Results for 32PT Basket Assembly Deadweight Analyses

Vertical Deadweight

Component	Stress (Axial Compression)			Notes[1]
	Calculated	Allowable	Ratio	
Fuel Support Grid	.06 ksi	23.7 ksi	< .01	XM-19, 800°F
Steel Transition Rails	.06 ksi	12.3 ksi	< .01	Type 304, 600°F
Aluminum Transition Rails	.02 ksi	4.2 ksi	< .01	6061 Al., ≈600°F

Notes: 1. For vacuum drying, the maximum transition rail temperature is less than 610°F. It occurs in the R90 rails and is localized at the point closest to the basket center, the average temperature is less than 600°F.

Horizontal Deadweight

Component	Stress Category	Stress Intensity		Stress Ratio	Notes
		Calculated	Allowable		
Fuel Support Grid	P_m	.57 ksi	28.2 ksi	.02	XM-19, 800°F
	$P_m + P_b$	2.72 ksi	42.3 ksi	.06	
	$P_m + P_b + Q$	7.41 ksi	84.6 ksi	.09	
Type 304 Transition Rails	P_m	.94 ksi	16.4 ksi	.06	Type 304, 600°F
	$P_m + P_b$	4.40 ksi	24.6 ksi	.18	
	$P_m + P_b + Q$	4.70 ksi	49.2 ksi	.10	
Transition Rail Cover Plates	P_m	.30 ksi	28.2 ksi	.01	XM-19, 800°F
	$P_m + P_b$	2.50 ksi	42.3 ksi	.06	
	$P_m + P_b + Q$	2.50 ksi	84.6 ksi	.03	
6061 Aluminum Transition Rails	Maximum Stress	1.32 ksi	6.0 ksi	.22	Al. 6061, 450°F

Table M.3.6-6
Summary of Results for 32PT Basket Assembly On-Site Handling (2.0g Loads)

Vertical Handling/Seismic

Component	Stress (Axial Compression)			Notes
	Calculated	Allowable	Ratio	
Fuel Support Grid	.11 ksi	23.7 ksi	< .01	XM-19, 800°F
Steel Transition Rails	.11 ksi	12.3 ksi	.01	Type 304, 600°F
Aluminum Transition Rails	.04 ksi	4.2 ksi	.01	6061 Al., 600°F

Horizontal/45° Handling/Seismic

Component	Stress	Stress Intensity		Stress	Notes
	Category	Calculated	Allowable	Ratio	
Fuel Support Grid	P_m	2.68 ksi	28.2 ksi	.10	XM-19, 800°F
	$P_m + P_b$	18.3 ksi	42.3 ksi	.43	
	$P_m + P_b + Q$	18.3 ksi	84.6 ksi	.22	
Type 304 Transition Rails	P_m	3.55 ksi	16.4 ksi	.22	Type 304, 600°F
	$P_m + P_b$	13.5 ksi	24.6 ksi	.55	
	$P_m + P_b + Q$	13.5 ksi	49.2 ksi	.27	
Transition Rail Cover Plates	P_m	2.19 ksi	28.2 ksi	.08	XM-19, 800°F
	$P_m + P_b$	11.1 ksi	42.3 ksi	.26	
	$P_m + P_b + Q$	11.1 ksi	84.6 ksi	.13	
6061 Aluminum Transition Rails	Maximum Stress	4.64 ksi	6.0 ksi	0.77	Al. 6061, 450°F

Note: 1. For the steel components, stress checks were performed at the enveloping temperatures listed. For the aluminum transition rails, stress checks were performed at temperatures corresponding to the maximum stress point. Temperatures listed are for the maximum stress points of the most highly loaded rail (the large R90 transition rail at the "bottom" of the basket).

Table M.3.6-7
32PT Basket Analyses Used to Determine On-Site Handling Loads

Case	Resultant Load	Basket Assembly Configuration	Support Conditions
1	2g resultant load in the "vertical" orientation	32PT Basket Assembly with steel transition rails	HSM (Support Rails at ± 30)
2	2g resultant load in the "vertical" orientation	32PT Basket Assembly with steel transition rails	OS197 (Support Rails at ± 18.5°)
3	2g resultant load oriented 45° from bottom center	32PT Basket Assembly with steel transition rails	OS197 (Support Rails at ± 18.5°)
4	2g resultant load in the "vertical" orientation	32PT Basket Assembly with aluminum transition rails	HSM (Support Rails at ± 30
5	2g resultant load in the "vertical" orientation	32PT Basket Assembly with aluminum transition rails	OS197 (Support Rails at ± 18.5°)
6	2g resultant load oriented 45° from bottom center	32PT Basket Assembly with aluminum transition rails	OS197 (Support Rails at ± 18.5°)

Table M.3.6-8
NUHOMS® Off-Normal Operating Loading Identification

Load Type	AFFECTED COMPONENT				
	DSC Shell Assembly	DSC Basket	DSC Support Structure	Reinforced Concrete HSM	On-site TC
Dead Weight	X	X	X	X	X
Internal/External Pressure	X				
Off-Normal Thermal	X	X	X	X	X
Off-Normal Handling	X	X	X	X	X

Figure M.3.6-1
32PT Basket Model with Steel Transition Rails

Figure M.3.6-2
32PT Basket Model with Steel Transition Rails

Figure M.3.6-3
32PT Basket Model with Aluminum Transition Rails

Figure M.3.6-4
32PT Basket Model with Aluminum Transition Rails

Figure M.3.6-5
Location and Numbering of Stress Cuts for 32PT Basket Analyses

M.3.7 Structural Analysis (Accidents)

The design basis accident events specified by ANSI/ANS 57.9-1984, and other credible accidents postulated to affect the normal safe operation of the standardized NUHOMS® System are addressed in this section. Analyses are provided for a range of hypothetical accidents, including those with the potential to result in an annual dose greater than 25 mrem outside the owner controlled area in accordance with 10CFR72. The postulated accidents considered in the analysis of the 32PT DSC and the associated NUHOMS® components affected by each accident condition are the same as those shown in Table 8.2-1.

In the following sections, each accident condition is analyzed to demonstrate that the requirements of 10CFR72.122 are met and that adequate safety margins exist for the standardized NUHOMS® System design. The resulting accident condition stresses in the NUHOMS® System components are evaluated and compared with the applicable code limits set forth in Section 3.2. Where appropriate, these accident condition stresses are combined with those of normal operating loads in accordance with the load combination definitions in Tables 3.2-5, 3.2-6, and 3.2-7. Load combination results for the HSM, DSC, and TC and the evaluation for fatigue effects are presented in Section M.3.7.10.

The postulated accident conditions addressed in this section include:

- Reduced HSM air inlet and outlet shielding (M.3.7.1),
- Tornado winds and tornado generated missiles (M.3.7.2),
- Design basis earthquake (M.3.7.3),
- Design basis flood (M.3.7.4),
- Accidental TC drop with loss of neutron shield (M.3.7.5),
- Lightning effects (M.3.7.6),
- Debris blockage of HSM air inlet and outlet opening (M.3.7.7),
- Postulated DSC leakage (M.3.7.8), and
- Pressurization due to fuel cladding failure within the DSC (M.3.7.9).

M.3.7.1 Reduced HSM Air Inlet and Outlet Shielding

This postulated accident is the partial loss of shielding for the HSM air inlet and outlet vents provided by the adjacent HSM. All other components of the NUHOMS® System are assumed to be functioning normally.

There are no structural consequences that affect the safe operation of the NUHOMS® System resulting from the separation of the HSMs. The thermal effects of this accident results from the

blockage of HSM air inlet and outlet openings on the HSM side walls in contact with each other. This would block the ventilation air flow provided to the HSMs in contact from these inlet and outlet openings. The increase in spacing between the HSM on the opposite side from 6 inches to 12 inches will reduce the ventilation air flow resistance through the air inlet and outlet openings on these side walls, which will partially compensate the ventilation reduction from the blocked side. However, the effect on the DSC, HSM and fuel temperatures is bounded by the complete blockage of air inlet and outlet openings described in Section M.3.7.7.

M.3.7.2 Tornado Winds/Tornado Missile

The applicable design parameters for the design basis tornado (DBT) are specified in Section 3.2.1. The determination of the tornado wind and tornado missile loads acting on the HSM are detailed in Section 3.2.2. The end modules of an array utilize shield walls to resist tornado wind and missile loads. For this conservative generic analysis, the tornado loads are assumed to act on a single free-standing HSM (with two end shield walls and a rear shield wall). This case conservatively envelopes the effects of wind on an HSM array. The TC is also designed for the tornado wind and tornado missile loads defined in Section 3.2.2. Thus, the requirements of 10CFR72.122 are met.

For DBT wind and missile effects, the HSM is more stable when loaded with a heavier DSC since the overturning moment is not a function of the DSC weight while the resisting moment increases with the increased payload. The DSC weight does not have any effect on HSM sliding stability, since the weight terms on either side of the sliding equation presented in Section 8.2.2 cancel out. Since the weight of the NUHOMS®-32PT DSC is bounded by the DSC weights used in Section 8.2.2, there is no change to the structural evaluation of the HSM for DBT winds and missile effects.

M.3.7.3 Earthquake

As discussed in Section 3.2.3 and as shown in Figure 8.2-2, the peak horizontal ground acceleration of 0.25g and the peak vertical ground acceleration of 0.17g are utilized for the design basis seismic analysis of the NUHOMS® components. Based on NRC Reg. Guide 1.61 [3.15], a damping value of three percent is used for the DSC seismic analysis. Similarly, a damping value of seven percent for DSC support steel and concrete is utilized for the HSM. An evaluation of the frequency content of the loaded HSM is performed to determine the dynamic amplification factors associated with the design basis seismic response spectra for the NUHOMS® HSM and DSC. Since the weight of the NUHOMS®-32PT DSC is bounded by the DSC weights used in Section 8, there is no change to the seismic response of the HSM.

M.3.7.3.1 DSC Seismic Evaluation

The maximum calculated seismic accelerations for the DSC inside the HSM are 0.40g horizontally and 0.17g vertically. An analysis using these seismic loads shows that the DSC will not lift off the support rails inside the HSM. The resulting stresses in the DSC shell due to vertical and horizontal seismic loads are also determined and included in the appropriate load combinations. The seismic evaluation of the DSC is described in the paragraphs that follow.

The DSC basket and support structure are also subjected to the calculated DSC seismic reaction loads as discussed in Sections M.3.7.3.2 and M.3.7.3.4, respectively.

M.3.7.3.1.1 DSC Natural Frequency Calculation

Two natural frequencies, each associated with a distinct mode of vibration of the DSC are evaluated. These two modes are the DSC shell cross-sectional ovalling mode and the mode with the DSC shell bending as a beam.

M.3.7.3.1.1.1 DSC Shell Ovalling Mode

The natural frequency for the DSC shell ovalling mode is determined from the Blevins [3.16] correlation as follows.

$$f = \frac{\lambda_i}{2\pi R}\sqrt{\frac{E}{\mu(1-\nu^2)}} \quad \text{(Blevins, Table 12-1, Case 3)}$$

where: R = 33.34 in, DSC mean radius,

E = 26.5×10^6 psi, Young's Modulus,

ν = 0.3, Poisson's ratio,

λi = $\lambda_i = 0.289\frac{t}{R}\frac{i(i^2-1)}{\sqrt{1+i^2}}$,

t = 0.5 in., Thickness of DSC shell, and

μ = 0.288/g lb/in^3, Steel mass density.

The lowest natural frequency corresponds to the case when i = 2.

Hence: λ_2 = 0.0116 sec.

Substituting gives: f = 10.9 Hertz

The resulting spectral accelerations in the horizontal and vertical directions for this DSC ovalling frequency are less than 1.0g and 0.68g, respectively.

M.3.7.3.1.1.2 DSC Beam Bending Mode

The DSC shell is conservatively assumed to be simply supported at the two ends of the DSC. The beam bending mode natural frequency of the DSC was calculated from the Blevins correlation:

$$f_i = \frac{\lambda_i^2}{2\pi L^2}\sqrt{\frac{EI}{m}} \quad \text{(Blevins, Table 8.1, Case 5)}$$

where: E = 26.5E6 psi, Young's Modulus,

I = 58,400 in.4, DSC moment of inertia,

L = 192.55 in., Total length of DSC,

m = 101,130/192.55 = 525/g lb/in, and

λ = $i\pi$; for lowest natural frequency, i = 1.

Substituting yields: f_1 = 45.1 Hertz.

The DSC spectral accelerations at this frequency correspond to the zero period acceleration. These seismic accelerations are bounded by those of the ovalling mode frequency that are used in the subsequent stress analysis of the DSC shell.

M.3.7.3.1.2 DSC Seismic Stress Analysis

With the DSC conservatively assumed to be resting on a single support rail inside the HSM, the stresses induced in the DSC shell are calculated due to the 1.0g horizontal and 0.68g vertical seismic accelerations, and increased by a factor of 1.5 to account for the effects of possible multimode excitation. Thus, the DSC shell is qualified to seismic accelerations of 1.5g horizontal and 1.0g vertical. The DSC shell stresses obtained from the analyses of vertical and horizontal seismic loads are summed absolutely. See Table M.3.7-9 for the Level C seismic stress evaluation of the NUHOMS®-32PT DSC. The seismic load combination includes deadweight + pressure + 1.5g horizontal and 1g vertical (load combinations HSM-7 and HSM-8 as shown in Table M.2-15).

As stated, in Section 4.2.3.2, an axial retainer is included in the design of the DSC support system inside the HSM to prevent sliding of the DSC in the axial direction during a postulated seismic event. The stresses induced in the DSC shell and bottom cover plate due to the restraining action of this retainer for a horizontal seismic load, applied along the axis of the DSC, are included in the seismic response evaluation of the DSC shell assembly.

The stability of the DSC against lifting off one of the support rails during a seismic event is evaluated by performing a rigid body analysis, using the 0.40g horizontal and 0.17g vertical input accelerations. The factor of 1.5 used in the DSC analysis to account for multimode behavior need not be included in the seismic accelerations for this analysis, as the potential for lift off is due to rigid body motion, and no frequency content effects are associated with this action. The horizontal equivalent static acceleration of 0.40g is applied laterally to the center of gravity of the DSC. The point of rigid body rotation of the DSC is assumed to be the center of the support rail, as shown in Figure M.3.7-1. The applied moment acting on the DSC is calculated by summing the overturning moments. The stabilizing moment, acting to oppose the applied moment, is calculated by subtracting the effects of the upward vertical seismic acceleration of 0.17g from the total weight of the DSC and summing moments at the support rail. Since the stabilizing moment calculated below is greater than that of the applied moment, the DSC will not lift off the DSC support structure inside the HSM.

Referring to Figure M.3.7-1Figure M.3.7-1, the factor of safety associated with DSC lift-off is calculated as follows:

$M_{am} = yF_H$,

and $M_{sm} = (F_{v1} - F_{v2})x$.

where: M_{am} = the applied seismic moment, and

M_{sm} = the stabilizing moment

All other variables are defined in Figure M.3.7-1Figure M.3.7-1.

Substituting yields: M_{am} = 1177.1 K-in.

and M_{sm} = 1410.2 K-in.

Thus, the factor of safety (SF) against DSC lift off from the DSC support rails inside the HSM obtained from this bounding analysis is:

$$SF = \frac{M_{sm}}{M_{am}} = 1.20$$

M.3.7.3.2 Basket Seismic Evaluation

Seismic loads on the 32PT basket are enveloped by the 2.0g loads used for the on-site handling evaluation described in Section M.3.6. Therefore, based on the following considerations, specific qualification/evaluation for seismic loads is not required for the 32PT basket assembly:

- seismic loads are enveloped by the on-site handling loads evaluated in Section M.3.6.1.3.2(E).
- the handling load evaluation is performed using Service Level A allowables, while seismic loads are classified as Service Level C loads.

Therefore, the qualification for on-site handling in Section M.3.6.1.3.2(E) also demonstrates qualification for seismic loading and no additional evaluation is required.

M.3.7.3.3 HSM Seismic Evaluation

The weight of the NUHOMS®-32PT DSC is bounded by the DSC weight used in Section 8.2.3.2(B). Therefore, there is no change to the HSM seismic evaluation.

M.3.7.3.4 DSC Support Structure Seismic Evaluation

The weight of the NUHOMS®-32PT DSC is bounded by the DSC weight used in Section 8.2.3.2(C). Therefore, there is no change to the DSC support structure seismic evaluation.

M.3.7.3.5 DSC Axial Retainer Seismic Evaluation

The weight of the NUHOMS®-32PT DSC is bounded by the DSC weight used in Section 8.2.3.2(C). Therefore, there is no change to the DSC Axial Retainer seismic evaluation.

M.3.7.3.6 TC Seismic Evaluation

The effects of a seismic event occurring when a loaded NUHOMS®-24P DSC is resting inside the TC are described in Section 8.2.3.2(D). The stabilizing moment to prevent overturning of the cask/trailer assembly due to the 0.25g horizontal and 0.17g vertical seismic ground accelerations is calculated and compared to the dead weight stabilizing moment. The results of this analysis show that there is a factor of safety of at least 2.0 against overturning that ensures that the cask/trailer assembly has sufficient margin for the design basis seismic loading. Since the weight of the NUHOMS®-32PT DSC is bounded by the DSC weights used in Section 8.2.3, and the TC was evaluated using peak spectrum amplification factors (See Section 8.2.3.2D) this factor of safety against overturning due to seismic remains bounding for the NUHOMS®-32PT DSC.

M.3.7.4 Flood

Since the source of flooding is site specific, the exact source, or quantity of flood water, should be established by the licensee. However, for this generic evaluation of the 32PT DSC and HSM, bounding flooding conditions are specified that envelop those that are postulated for most plant sites. As described in Section 3.2, the design basis flooding load is specified as a 50 foot static head of water and a maximum flow velocity of 15 feet per second. Each licensee should confirm that this represents a bounding design basis for their specific ISFSI site.

M.3.7.4.1 HSM Flooding Analysis

For flooding effects, the HSM is more stable when loaded with a heavier DSC since the overturning moment is not a function of the DSC weight while the resisting moment increases with the increased payload. Since the weight of the NUHOMS®-32PT DSC is bounded by the DSC weights used in Section 8.2.4, there is no change to the HSM flooding analysis.

M.3.7.4.2 DSC Flooding Analyses

The DSC is evaluated for the design basis fifty foot hydrostatic head of water producing external pressure on the DSC shell and outer cover plates. To conservatively determine design margin which exists for this condition, the maximum allowable external pressure on the DSC shell is calculated for Service Level A stresses using the methodology presented in NB-3133.3 of the ASME Code [3.1]. The resulting allowable pressure of 39.7 psi is 1.8 times the maximum external pressure of 21.7 psi due to the postulated fifty foot flood height. This demonstrates stability of the DSC under the worst case external pressure due to flooding.

The DSC shell stresses for the postulated flood condition are determined using the ANSYS analytical model shown in Figure 8.1-14a and Figure 8.1-14b. The 21.7 psig external pressure is applied to the model as a uniform pressure on the outer surfaces of the top cover plate, DSC shell and bottom cover plate. The maximum DSC shell primary membrane plus bending stress

intensity for the 21.7 psi external pressure is 3.00 ksi which is considerably less than the Service Level C allowable primary membrane plus bending stress of 32.6 ksi. The maximum primary membrane plus bending stress in the flat heads of the DSC occurs in the inner bottom cover plate. The maximum primary membrane plus bending stress in the inner bottom cover plate is 1.54 ksi. This value is considerably less than the ASME Service Level C allowable of 32.6 ksi for primary membrane plus bending. These stresses are combined using the load combinations shown in Table M.2-15.

M.3.7.5 Accidental Cask Drop

This section addresses the structural integrity of the standardized NUHOMS® on-site TC, the DSC and its internal basket assembly when subjected to postulated cask drop accident conditions.

Cask drop evaluations include the following:

- DSC Shell Assembly (M.3.7.5.2),
- Basket Assembly (M.3.7.5.3),
- On-Site TC (M.3.7.5.4), and
- Loss of the TC Neutron Shield (M.3.7.5.5).

The DSC shell assembly, TC, and loss of TC neutron shield evaluations are based on the approaches and results presented in Section 8.2. The 32PT DSC basket assembly cask drop evaluation is presented in more detail since the 32PT basket assembly is a new design.

A short discussion of the effect of the NUHOMS®-32PT DSC on the transfer operation, accident scenario and load definition is presented in Section M.3.7.5.1.

M.3.7.5.1 General Discussion

Cask Handling and Transfer Operation

Various TC drop scenarios have been evaluated in Section 8.2.5. The NUHOMS®-32PT DSC is heavier than the NUHOMS®-24P DSC. Therefore, the expected g loads for the postulated drop accidents would be lower. However, for conservatism, the g loads used for the NUHOMS®-24P analyses in Section 8.2.5 are also used for the NUHOMS®-32PT DSC analyses.

Cask Drop Accident Scenarios

In spite of the incredible nature of any scenario that could lead to a drop accident for the TC, a conservative range of drop scenarios are developed and evaluated. These bounding scenarios assure that the integrity of the DSC and spent fuel cladding is not compromised. Analyses of these scenarios demonstrate that the TC will maintain the structural integrity of the DSC pressure containment boundary. Therefore, there is no potential for a release of radioactive materials to the environment due to a cask drop. The range of drop scenarios conservatively selected for design are:

1. A horizontal side drop from a height of 80 inches.

2. A vertical end drop from a height of 80 inches onto the top or bottom of the TC (two cases). Vertical end drops for the NUHOMS® DSC are non-mechanistic. However, 60g vertical end drop analyses are performed as a means of enveloping the 25g corner drop (in conjunction with the 75g horizontal drop).

3. An oblique corner drop from a height of 80 inches at an angle of 30° to the horizontal, onto the top or bottom corner of the TC. This case is not specifically evaluated. The side drop and end drop cases envelope the corner drop.

Cask Drop Accident Load Definitions

Same as Section 8.2.5.1(C).

Cask Drop Surface Conditions

Same as 8.2.5.1(D).

M.3.7.5.2 DSC Shell Assembly Drop Evaluation

The shell assembly consists of the DSC shell, the shield plugs, and the top and bottom inner and outer cover plates. The shell assembly drop evaluation is presented in three parts:

1. DSC shell assembly horizontal drop analysis,

2. DSC shell assembly vertical drop analysis, and

3. DSC shell stability analysis.

M.3.7.5.2.1 DSC Shell Assembly Horizontal Drop Analysis

The DSC shell assembly is analyzed for the postulated horizontal side drop using the ANSYS 3-D models of the DSC shell assembly discussed in Section M.3.6.1.2. Half-symmetry (180°) models of the top end and bottom end sections of the DSC shell assembly are developed based on the models for the end drops shown in Figure 8.1-14a and Figure 8.1-14b. Each model includes one-half of the height of the cylindrical shell. Each of the DSC shell assembly components is modeled using ANSYS solid 3-D elements. The full weight of the DSC is conservatively assumed to drop directly onto a single TC rail. Elastic-plastic analyses are performed and stresses are determined for each DSC shell assembly component. The NUHOMS®-32PT DSC shell stresses in the region of the basket assembly are also analyzed for the postulated horizontal side drop conditions. This analysis and results are presented in Section M.3.7.5.3.1.

M.3.7.5.2.2 DSC Shell Assembly Vertical Drop Analysis

For this drop accident case, the TC is assumed to be oriented vertically and dropped onto a uniform surface. The vertical cask drop evaluation conservatively assumes that the TC could be

dropped onto either the top or bottom surfaces. No credit is taken for the energy absorbing capacity of the cask top or bottom cover plate assemblies during the drop. Therefore, the DSC is analyzed as though it is dropped on to an unyielding surface. The principal components of the DSC and internals affected by the vertical drop are the DSC shell, the inner and outer top cover plates, the shield plugs, and the inner and outer bottom cover plates.

M.3.7.5.2.3 DSC Shell Assembly Stress Analysis

The ANSYS analytical models of the DSC shell assembly as described in Section M.3.6.1.2 and shown in Figure 8.1-14a and Figure 8.1-14b are used to determine the vertical end drop accident stresses in the DSC shell, the inner cover plates, the outer cover plates, and the shield plugs. The models consist of 90° quarter symmetry models and include one-half of the height of the cylindrical shell. To capture the maximum stress state in the DSC assembly components, each model was analyzed for end drop loading on the opposite end (i.e., the bottom end model was analyzed for top end drop, and the top end model was analyzed for bottom end drop). In these drop orientations, the end plates are supported at the perimeter by the shell. For the top and bottom end drops, the nodal locations on the impacted end are restrained in the vertical direction. An equivalent static linear elastic analysis is conservatively used for the vertical end drop analyses. Inertia loadings based on forces associated with the 75g deceleration are statically applied to the models. Analyses show that the stresses in the DSC cover plates and shield plugs are low. These low stresses occur because for the bottom end drop, the inner and outer top cover plates are supported by the top shield plug. During a top end drop, the outer top cover plate is assumed to be supported by the unyielding impacted surface and is subjected to a uniform bearing load imposed by the DSC internals. The same is true for the DSC bottom outer cover plate and shield plug for the bottom end drop. The highest stresses occur in the DSC shell and bottom inner cover plate. The maximum stresses in the inner bottom cover plate result from the top end vertical drop condition, in which the inner bottom cover plate is supported only at the edges. The maximum DSC shell membrane stresses, which occur near the top end of the DSC shell area, result from the accelerated weight of the DSC shell and the bottom end (for top end drop case) or top end (for the bottom end drop case) assemblies.

A summary of the calculated stresses for the main components of the DSC and associated welds is provided in Table M.3.7-1.

M.3.7.5.2.4 DSC Shell Stability Analysis

The stability of the DSC shell for a postulated vertical drop impact is also evaluated. For Level D conditions, the allowable axial stress in the DSC shell is based on Appendix F of the ASME Code. The maximum axial stress in the DSC shell obtained from the 75g end drop analyses is 11.08 ksi. The allowable axial stress is 11.14 ksi. Therefore, buckling of the DSC shell for a 75g vertical deceleration load does not occur.

M.3.7.5.3 Basket Assembly Drop Evaluation

As discussed in previous chapters, the structural components of the basket assembly include the fuel support grid and the transition rails.

The DSC resides in the TC for all drop conditions. Horizontally, the DSC is supported in the TC by two cask rails that are integral to the cask wall. The effect of these cask rails are included in the horizontal drop evaluations.

Vertical drops are non-mechanistic for the 32PT horizontal storage system, therefore, as noted in Section M.3.7.5.1, no end drops are postulated. However, to provide an enveloping load for the postulated 25g corner drop, a 60g end drop is evaluated. For this drop, the end of the DSC/basket assembly is supported by the ends of the TC.

The stress evaluation of the 32PT DSC basket assembly is presented in three parts:

1. Basket assembly horizontal drop stress analysis, which includes evaluation of the fuel support grid and transition rails using the ANSYS models described in Section M.3.6.1.3.

2. Basket assembly horizontal stability evaluation which uses the ANSYS models described in Section M.3.6.1.3 and the criteria of the ASME B&PV Code, Appendix F-1341.3. As noted, the ANSYS models include the fuel support grid and the transition rails.

3. Basket assembly vertical drop analysis which includes a stress evaluation of the fuel support grid and transition rails using hand calculations as described in Section M.3.6.1.3 for vertical deadweight. The stress criteria used for the vertical drop analysis also provide assurance of structural stability.

Within the basket grid structure are plates of Type 1100 aluminum and neutron absorbing materials composed of either enriched borated aluminum alloy or Boralyn® plates which perform heat transfer and criticality functions and are not included in the ANSYS models. The hand-calculated bounding accident condition axial stress in the plates is 1.0 ksi, due to the 60g end drop, which is below the yield stress value of 1.5 ksi (Type 1100 aluminum at 720°F). This ensures that the plates remain in position to perform their heat transfer and criticality functions. For the 75g side drop loading, the aluminum plates are supported in the transverse direction along their length by either the grid structure or the fuel assemblies. Deflection of the aluminum plates in the transverse direction is limited by the gap between the grid structure and the fuel assembly and does not significantly affect the heat transfer function of the plates. The effect of this gap is bounded by the criticality evaluation.

M.3.7.5.3.1 Basket Assembly Horizontal Drop Analysis

M.3.7.5.3.1.1 Basket and Basket Rail Stress Analysis

The ANSYS models described in Section M.3.6.1.3 are used to perform stress analyses of the 32PT basket assembly for horizontal drop loads. The ANSYS models include the fuel support grid, transition rails, DSC shell, and the effects of the TC rails. Contact elements between the parts of the structure are active for all the stress analyses.

Loads

Inertia loads corresponding to the drop accelerations are applied to the structure by including the appropriate weight density of the materials and applying accelerations. Fuel loads are applied

using pressure loads on the fuel grid elements. As previously described, thermal effects are included by applying temperatures (corresponding to the 117°F ambient temperature condition, DSC in the TC case) to each node in the model. This includes thermal effects in the model and applies the temperature dependent material properties at different model locations.

Side drop orientations were selected to maximize both axial compression and bending stresses in the basket structure. Zero degree (0°) drop orientations were selected to maximize axial compression while an orientation of 45° (from vertical) was selected to maximize bending loads. Drops onto the TC rails were selected to maximize load concentrations. Table M.3.7-2 lists the stress analyses configurations performed for the postulated side drop.

Material Properties

The material properties used in the accident condition stress analyses are listed in Table M.3.7-3 for the 32PT basket structural components. The evaluations were performed using bilinear elastic-plastic material properties. For the steel components, the plastic slope was taken as 5% of the elastic modulus (E_{tan} = 0.05E) and Code values of yield stresses were used. For the aluminum transition rails, yield stresses were taken from Table M.3.3-5, and a lower bound plastic slope of 0.01E was used.

Results

Enveloping stresses in each basket component are listed in Table M.3.7-4 for the postulated 75g side drop. Results are illustrated in Figure M.3.7-2 through Figure M.3.7-5. The stresses are the maximum values in each component from the four (4) analyses listed in Table M.3.7-2. Table M.3.7-4 includes a comparison of the calculated stresses to Service Level D stress allowables for elastic-plastic analyses based on the stress criteria from Table M.2-17 and materials data from Table M.3.3-1 and Table M.3.3-3. As shown, all stress ratios are less than 1.0.

M.3.7.5.3.2 Basket Assembly Part71 End Drop Analysis

As noted in Section M.3.7.5.1, end drops are non-mechanistic for the 32PT system. End drop results are included to demonstrate margin for the postulated 25g corner drop.

Under axial loading, the fuel assemblies and basket assembly are supported by the bottom of the DSC/cask. The fuel assemblies react directly against the bottom or top end of the DSC/cask and do not load the basket structure. Stresses under axial loading result only from the self weight/inertia of the basket structure. In addition, since any connections between the fuel support grid and transition rails are slotted (to allow for thermal expansion preventing thermal stresses), each part of the basket structure is loaded only by its own weight/inertia.

Compressive axial stresses are maximum at the "supported" end of the basket structure. Stresses are calculated using hand calculations and are summarized, and compared to the acceptance criteria, in Table M.3.7-5. As shown by the table, all stresses are well below the allowable values.

M.3.7.5.3.3 Basket Assembly Stability Analysis

Stability under axial loading is demonstrated by the results described in Section M.3.7.5.3.2 above. To demonstrate stability of the 32PT basket structure under side loading, a series of analyses were performed using the ANSYS models described in Section M.3.6.1.3. As listed in Table M.3.7-3, the stability evaluations were performed using the criteria of ASME B&PV Code, Appendix F-1341.3 which establishes the allowable load as 90% of the Limit Analysis Collapse Load where the Limit Analysis Collapse Load is the maximum load determined using elastic-perfectly plastic material properties with a yield stress equal to the lesser of $2.3S_m$ or $0.7S_u$.

The ANSYS stability analyses performed for the 32PT basket assembly are listed in Table M.3.7-6. The results of the ANSYS stability analyses are summarized in Table M.3.7-7. These analyses demonstrate stability of the structural components of the basket structure with ample margin for 75g loading.

LS-DYNA was used to perform confirmatory stability analyses. The LS-DYNA analyses used the same material properties and assumptions as the ANSYS analyses. Results of these analyses are listed in Table M.3.7-7 along with the ANSYS results. Displaced shape plots from the 0° and 180° analyses are included as Figure M.3.7-6 and Figure M.3.7-8, respectively. The plots show the geometry just past the stability load. Also included are displacement "time history" plots for the node locations indicated in the geometry plots (See Figure M.3.7-7 and Figure M.3.7-9). These "time history" plots clearly show the stability point of the structure.

M.3.7.5.3.3.1 Fuel Support Structure Stability Evaluation Using Hand Calculations

A confirmatory stability analyses for the fuel grid structure was performed using hand calculations, the column stability criteria of ASME B&PV Code, Appendix F-1334.3(b), and ASME Code yield stress values as listed in Table M.3-3. The criteria were developed for a material temperature of 600°F, which corresponds to the maximum temperature at the most highly loaded ligaments at the periphery of the fuel support grid.

The "bottom" span of the "center" ligament is selected as the critical location. The compressive load in this ligament is determined as follows:

- A load of 11.0 lb/in was applied to each fuel cell. This represents an enveloping load.
- The loads from the four (4) cells along the bottom edge of the basket are transferred directly into the transition rails without loading the "columns" of the fuel grid.
- The subject ligament is assumed to carry half the load in the central cells above the bottom row. Thus, there are 10 cells above the ligament, and 1/2 the load is carried by the subject ligament while the remaining load is carried by the adjacent columns. Therefore, the load from 5 fuel cells is applied to the subject ligament.

The self weight/inertia of the basket assembly was neglected.

The load on the subject ligament is:

$$P = (75g)(11.0\ {}^{lb}/_{in})(5\ \text{cells})(1.0\ \text{in})$$
$$= 4.13\ {}^{kip}/_{ligament}$$

The stress is:

$$f_a = \frac{(4.13\ {}^{kip}/_{ligament})}{0.25\ \text{in}} = 16.5\ \text{ksi}$$

The allowable under the side drop load is determined using the following equations from ASME B&PV Code, Appendix F-1334.3(b):

$$F_a = S_y\left(\frac{(1-\lambda^2/4)}{1.11+0.5\lambda+.17\lambda^2-0.28\lambda^3}\right)$$

where: $$\lambda = \left(\frac{Kl}{r}\right)\left(\frac{1}{\pi}\right)\left(\frac{S_y}{E}\right)^{1/2}$$

$$r = \frac{t}{(12)^{1/2}}$$

L = cell height of 8.825"

The allowable axial compression stress, F_a, is 19.0 ksi and the ratio of calculated to allowable stresses is:

$$\frac{16.5\ ksi}{19.0\ ksi} = 0.87$$

M.3.7.5.3.3.2 Results of Basket Stability Analysis

The results of the analyses indicate the structural capacity of the NUHOMS®-32PT basket assembly is higher than the postulated 75g side drop impact load. Thus, the 32PT basket assembly is stable under the postulated side drop loads.

M.3.7.5.4 On-site TC Horizontal and Vertical Drop Evaluation

An analysis has been performed in Section 8.2.5.2 to evaluate the OS197 and OS197H TCs for postulated horizontal and vertical drop accidents with a static equivalent deceleration of 75g's. The evaluations for the OS197 and OS197H casks are based on payload weights of 90,000 lbs and 116,000 lbs, respectively. The maximum total cask payload weight with a dry-loaded NUHOMS®-32PT DSC is approximately 102,000 lbs. Therefore, the OS197H cask is acceptable

with any NUHOMS®-32PT DSC and the OS197 cask is acceptable with a NUHOMS®-32PT DSC where the total cask payload weight is not more than 90,000 lbs.

M.3.7.5.5 Loss of Neutron Shield

No impact on the structural evaluation.

M.3.7.6 Lightning

No impact on the structural evaluation.

M.3.7.7 Blockage of Air Inlet and Outlet Openings

This accident conservatively postulates the complete blockage of the HSM ventilation air inlet and outlet openings on the HSM side walls.

Since the NUHOMS® HSMs are located outdoors, there is a remote probability that the ventilation air inlet and outlet vent openings could become blocked by debris. The NUHOMS® design features such as the perimeter security fence and the redundant protected location of the air inlet and outlet vent openings reduces the probability of occurrence of such an accident. Nevertheless, for this conservative generic analysis, such an accident is postulated to occur and is analyzed.

The structural consequences due to the weight of the debris blocking the air inlet and outlet vent openings are negligible and are bounded by the HSM loads induced for a postulated tornado (Section 8.2.2) or earthquake (Section 8.2.3).

The thermal effects of this accident for the NUHOMS®-32PT DSC are described in Section M.4.0.

M.3.7.8 DSC Leakage

There are no structural or thermal consequences resulting from the DSC leakage accident. The radiological consequences of this accident are described in Section M.11.2.8.

M.3.7.9 Accident Pressurization of DSC

The NUHOMS® 32PT DSC is evaluated and designed for the maximum accident pressures calculated in Section M.4.0. The pressure boundary stresses due to this pressure load are bounded by the results presented in Table M.3.7-10. Therefore, the 32PT-DSC is acceptable for this postulated accident condition.

M.3.7.10 Load Combinations

The load categories associated with normal operating conditions, off-normal conditions and postulated accident conditions are described and analyzed in previous sections. The load

combination results for the NUHOMS® components important to safety are presented in this section. Fatigue effects on the TC and the DSC are also addressed in this section.

M.3.7.10.1 DSC Load Combination Evaluation

As described in Section 3.2, the stress intensities in the DSC at various critical locations for the appropriate normal operating condition loads are combined with the stress intensities experienced by the DSC during postulated accident conditions. It is assumed that only one postulated accident event occurs at any one time. The DSC load combinations summarized in Table 3.2-6 are expanded in Table M.2-15 for the 32PT DSC. Since the postulated cask drop accidents are by far the most critical, the load combinations for these events envelope all other accident event combinations. Table M.3.7-8 through Table M.3.7-10 tabulate the maximum stress intensity for each component of the DSC calculated for the enveloping normal operating, off-normal, and accident load combinations. For comparison, the appropriate ASME Code allowables are also presented in these tables.

M.3.7.10.2 DSC Fatigue Evaluation

Although the normal and off-normal internal pressures for the NUHOMS®-32PT DSC are higher relative to the NUHOMS®-24P DSC, the range of pressure fluctuations due to seasonal temperature changes are essentially the same as those evaluated for the NUHOMS®-24P DSC. Similarly, the normal and off-normal temperature fluctuations for the NUHOMS®-32PT DSC due to seasonal fluctuations are essentially the same as those calculated for the NUHOMS®-24P DSC. Therefore, the fatigue evaluation presented in Section 8.2.10.2 for the 24P DSC remains applicable to the NUHOMS®-32PT DSC.

M.3.7.10.3 TC Load Combination Evaluation

There is no change to the TC load combination evaluations. The evaluations performed in Sections 8.1 and 8.2 for the OS197 and OS197H casks are based on payloads of 90,000 lbs and 116,000 lbs, respectively. The maximum total cask payload with a dry-loaded NUHOMS®-32PT DSC is approximately 102,000 lbs. Therefore, the OS197H cask is acceptable with any NUHOMS®-32PT DSC and the OS197 cask is acceptable with a NUHOMS®-32PT DSC where the total cask payload is not more than 90,000 lbs.

M.3.7.10.4 TC Fatigue Evaluation

No change.

M.3.7.10.5 HSM Load Combination Evaluation

Since the weight of the NUHOMS®-32PT DSC is bounded by the DSC weights used in Sections 8.1 and 8.2, there is no change to the HSM load combination evaluation.

M.3.7.10.6 Thermal Cycling of the HSM

No change.

M.3.7.10.7 DSC Support Structure Load Combination Evaluation

See Section M.3.7.10.5 above.

M.3.7.11 Evaluation of Poison Rod Assemblies

The Poison Rod Assemblies (PRA) consist of Type 304 stainless steel tubes filled with Boron carbide pellets or Boron powder that are inserted into the fuel assemblies through the guide tubes. They each contain up to 24 rods depending on the type of fuel assembly and are held together at the top end with a support plate as shown schematically in Figure M.1-2.

The PRAs are near the fuel rods, so their temperature is conservatively assumed to be the same temperature as the fuel cladding. Table M.4-13 reports that the maximum fuel cladding temperature during the postulated accidental blocked vent condition remains below 800°F. Table M.4-16 reports that the maximum fuel cladding temperature during vacuum drying is 810°F, which is acceptable because vacuum drying is a short term event.

In the vertical direction, the PRAs are supported by the support plate at the top end of the fuel assembly. The most limiting vertical load occurs during the postulated 60g end drop (See Section M.3.7.5.1) where the PRAs are supported by the support plate. All longitudinal loading is due solely to the inertia of each tube and contents. The PRAs are continuously supported by the guide tubes, thus elastic stability is not limiting. The PRAs are an open system and are thus not pressurized, so there is no hoop component of stress. Using the geometry of the PRA cladding shown in Figure M.1-2, the maximum fuel assembly length is 171.71 inches (see Table M.2-2). Assuming that the PRA contents have a density of 2.5 lb/in^3, the maximum longitudinal stress (and stress intensity) in the PRA cladding is approximately 5.9 ksi. This stress intensity is well below the Type 304 Service Level D membrane allowable stress of 36.5 ksi at 800° F (See Tables M.3-2 and M.2-16).

In the horizontal direction, the PRAs are supported by the guide tubes during all normal, off-normal and postulated accident conditions; therefore, there are no limiting stresses associated with horizontal deadweight, transfer handling (with a horizontal load component), and the postulated side drop.

Table M.3.7-1
Maximum NUHOMS®-32PT DSC Stresses for Drop Accident Loads

DSC Components	Stress Type	Calculated Stress (ksi)[1]	
		Vertical[3]	Horizontal
DSC Shell	Primary Membrane	13.43	36.47
	Membrane + Bending	36.60	55.83
Inner Top Cover Plate	Primary Membrane	2.41	25.08
	Membrane + Bending	5.87	39.19
Outer Top Cover Plate	Primary Membrane	2.22	34.46
	Membrane + Bending	5.12	55.25
Inner Bottom Cover Plate	Primary Membrane	7.61	21.84
	Membrane + Bending	25.27	55.17
Outer Bottom Cover Plate	Primary Membrane	1.69	31.91
	Membrane + Bending	3.67	49.85
Inner Top Cover Plate Weld[2]	Primary	2.18	22.81
Outer Top Cover Plate Weld[2]	Primary	0.68	11.53

Notes:

(1) Values shown are maximums irrespective of location.

(2) Stress values are the envelope of drop loads with and without 20psig internal pressure.

(3) The vertical end drops are non-mechanistic for the NUHOMS® 32PT DSC. They are performed as a means of demonstrating qualification of the 25g corner drop. The analyses reported here are conservatively based on 75g deceleration.

Table M.3.7-2
List of Drop Condition ANSYS Stress Analyses of the 32PT Basket Assembly

Case	Load	DSC Configuration	Support Conditions
1	75g Side Drop at 0°	32PT DSC with steel transition rails	OS197 (Support Rails at ± 18.5°)
2	75g Side Drop at 0°	32PT DSC with aluminum transition rails	OS197 (Support Rails at ± 18.5°)
3	75g Side Drop at 45°from bottom center	32PT DSC with steel transition rails	OS197 (Support Rails at ± 18.5°)
4	75g Side Drop at 45° from bottom center	32PT DSC with aluminum transition rails	OS197 (Support Rails at ± 18.5°)

Note: See Table M.3.7-6 for additional stability analyses performed for the 75g side drop load.

Table M.3.7-3
Summary of Material Properties for Drop Accident Analyses of the 32PT Basket Assembly

Component	Material	Drop Condition Analysis Material Properties		Evaluation Temperature
		Stress Analyses[1]	Stability Analyses[1,2]	
Fuel Support Grid	1/4" Thick, Type XM-19 Stainless Steel	Bilinear Elastic-Plastic S_y = Code S_y (Table M.3.3-3) E_{tan} =.05E_{Code} (Table M.3.3-3)	Bilinear Elastic-Perfectly Plastic (F-1341.3): S_y = min(2.3S_m,0.7S_u) E_{tan} = 0	800°F
Welded Steel Transition Rails	3/8" Thick Type 304 Stainless Steel	Bilinear Elastic-Plastic S_y = Code S_y (Table M.3.3-1) E_{tan} =.05E_{Code} (Table M.3.3-1)	Bilinear Elastic-Perfectly Plastic (F-1341.3): S_y = min(2.3S_m,0.7S_u) E_{tan} = 0	600°F
Solid Aluminum Transition Rails, R90 Cover Plates	1/4" Thick, Type XM-19 Stainless Steel	Bilinear Elastic-Plastic S_y = Code S_y (Table M.3.3-3) E_{tan} =.05E_{Code} (Table M.3.3-3)	Bilinear Elastic-Perfectly Plastic (F-1341.3): S_y = min(2.3S_m,0.7S_u) E_{tan} = 0	600°
Solid Aluminum Transition Rails, Aluminum Bodies	6061 Aluminum Alloy	Bilinear Elastic-Plastic S_y = (Table M.3.3-5) E_{tan} =.01E (Table 3.3-5)	Bilinear Elastic-Plastic S_y = (Table M.3.3-5) E_{tan} =.01E (Table M.3.3-5)	Note 3

Notes:

1. Prior to application of drop loads, the structure was initialized to the temperatures corresponding to the 117°F in cask case.

2. For the steel components, stress checks were performed at the enveloping temperatures listed. For the aluminum transition rails, stress checks were performed at temperatures corresponding to the maximum stress point. Temperatures listed are for the maximum stress points of the most highly loaded rail (the large 90° transition rail at the "bottom" of the basket).

3. For accident condition loading, the transition rails support the fuel support grid such that stresses and displacements in the fuel grid are acceptable. Since the transition rails are entrapped between the fuel grid and the DSC shell, no additional checks (of the aluminum) are required for accident/drop loading. Qualification of the fuel grid (and R90 cover plate) demonstrate that the rails perform their intended function.

Table M.3.7-4
32PT Basket, Enveloping Stress Results - 75g Side Drops

Component	Stress Category	Stress Intensity		Stress Ratio	Notes
		Calculated	Allowable		
Fuel Support Grid	P_m	26.2 ksi	59.4 ksi	.44	XM-19, 800°F
	$P_m + P_b$	73.9 ksi	76.3 ksi	.97	
Type 304 SS Transition Rails	P_m	21.6 ksi	44.4 ksi	.49	Type 304, 600°F
	$P_m + P_b$	44.0 ksi	57.1 ksi	.77	
Transition Rail Cover Plates	P_m	7.63 ksi	59.4 ksi	.13	XM-19, 800°F
	$P_m + P_b$	64.4 ksi	76.3 ksi	.84	

Note: 1. Although all the listed values include thermal effects, evaluation of secondary stress not required for Level D events.

Table M.3.7-5
32PT Basket, Enveloping Stress Results - 60g Part 71 End Drop

Component	Stress (Axial (Compression)			Notes
	Calculated	Allowable	Ratio	
Fuel Support Grid	3.30 ksi	31.8 ksi	.10	XM-19, 800°F
Steel Transition Rails	3.30 ksi	16.6 ksi	.20	Type 304, 600°F
Aluminum Transition Rails	1.03 ksi	4.20 ksi	.25	6061 Al., 600°F

Table M.3.7-6
Drop Condition ANSYS Stability Analyses for the 32PT Basket Assembly

Case	Load	DSC Configuration	Support Conditions
1	Side Drop at 0°	32PT DSC with steel transition rails	OS197 (Support Rails at ± 18.5°)
2	Side Drop at 0°	32PT DSC with aluminum transition rails	OS197 (Support Rails at ± 18.5°)
3	Side Drop at 45° from Bottom center	32PT DSC with steel transition rails	OS197 (Support Rails at ± 18.5°)
4	Side Drop at 45° from bottom center	32PT DSC with aluminum transition rails	OS197 (Support Rails at ± 18.5°)
5	Side Drop at 180° from Bottom center	32PT DSC with steel transition rails	n/a (cask rails not impacted)
6	Side Drop at 180° from Bottom center	32PT DSC with aluminum transition rails	n/a (cask rails not impacted)

Table M.3.7-7
Summary of 32PT Basket Stability Analysis -- Side Drops

Load / Drop Orientation[2]	ANSYS Stability Analyses		LS-DYNA Confirmatory Analyses[1]
	Type 304 SS Transition Rails	6061 Aluminum Transition Rails	Type 304 SS Transition Rails
0° (OS197)	98.0g	107.6g	98.6g
45° (OS197)	--	90.7g	105.3g
180°	99.9g	88.4g	110.4g

Notes: 1. These results included only to demonstrate the reasonableness of the ANSYS results.

2. The OS197 cask rails are at ± 18.5° from bottom center. The 180° drops do not impact cask rails.

Table M.3.7-8
NUHOMS®-32PT DSC Enveloping Load Combination Results for Normal and Off-Normal Loads

(ASME Service Levels A and B)

DSC Components	Stress Type	Controlling Load Combination[1]	Stress (ksi)	
			Calculated	Allowable[2]
DSC Shell	Primary Membrane	DD-1	9.08	17.5
	Membrane + Bending	TR-8	21.24	26.3
	Primary + Secondary	TR-3	51.43	54.3
Inner Bottom Cover Plate	Primary Membrane	LD-5	4.49	17.5
	Membrane + Bending	NO-1	23.07	40.5
	Primary + Secondary	LD-4	43.06	54.3
Outer Bottom Cover Plate	Primary Membrane	UL-5, UL-6	6.83	18.7
	Membrane + Bending	UL-5, UL-6	25.53	28.1
	Primary + Secondary	LD-4	39.97	54.3
Inner Top Cover Plate	Primary Membrane	TR-5	2.65	17.5
	Membrane + Bending	DD-1	16.83	26.3
	Primary + Secondary	DD-1	30.45	52.5
Outer Top Cover Plate	Primary Membrane	TR-7	4.21	17.5
	Membrane + Bending	TR-7	8.83	26.3
	Primary + Secondary	TR-7	27.38	52.5

See Table M.3.7-11 for notes.

Table M.3.7-9
NUHOMS®-32PT DSC Enveloping Load Combination Results for Accident Loads
(ASME Service Level C)

DSC Components	Stress Type	Controlling Load Combination[1]	Stress (ksi)	
			Calculated	Allowable[2]
DSC Shell	Primary Membrane	HSM-8	17.79	21.7
	Membrane + Bending	HSM-8	30.58	32.6
Inner Bottom Cover Plate	Primary Membrane	HSM-8	5.58	22.4
	Membrane + Bending	HSM-8	7.01	33.7
Outer Bottom Cover Plate	Primary Membrane	UL-7	8.59	22.4
	Membrane + Bending	UL-7	33.06	35.0
Inner Top Cover Plate	Primary Membrane	HSM-8	5.07	21.7
	Membrane + Bending	HSM-8	14.95	32.6
Outer Top Cover Plate	Primary Membrane	HSM-8	10.23	21.7
	Membrane + Bending	HSM-8	19.06	32.6

See Table M.3.7-11 for notes.

Table M.3.7-10
NUHOMS®-32PT DSC Enveloping Load Combination Results for Accident Loads
(ASME Service Level D) [3]

DSC Components	Stress Type	Controlling Load Combination[1]	Stress (ksi)	
			Calculated	Allowable[2]
DSC Shell	Primary Membrane	TR-10	36.47	44.4
	Membrane + Bending	TR-10	55.83	61.0[4]
Inner Bottom Cover Plate	Primary Membrane	TR-10	38.36	44.4
	Membrane + Bending	TR-10	56.65	59.6[5]
Outer Bottom Cover Plate	Primary Membrane	TR-10	32.74	44.4
	Membrane + Bending	TR-10	51.31	57.1
Inner Top Cover Plate	Primary Membrane	TR-10	25.08	44.4
	Membrane + Bending	TR-10	46.30	57.1
Outer Top Cover Plate	Primary Membrane	TR-10	36.85	44.4
	Membrane + Bending	TR-10	55.86	58.6[6]

See Table M.3.7-11 for notes.

Table M.3.7-11
DSC Enveloping Load Combination Table Notes

(1) See Table M.2-15 for load combination nomenclature.

(2) See Table M.2-16 and M.2-17 for allowable stress criteria. Material properties were obtained from Section M.3.3 at a design temperature of 500° F or as noted.

(3) In accordance with the ASME Code, thermal stresses need not be included in Service Level D load combinations.

(4) The maximum side drop membrane + bending stress is highly localized near the cask rail, at the outer bottom cover plate. The maximum temperature in this region is less than 266°F.

(5) The maximum side drop membrane + bending stress is highly localized over the cask rail. The maximum temperature in this region is less than 300°F.

(6) The maximum side drop membrane + bending stress is highly localized over the cask rail. The maximum temperature in this region is less than 350°F.

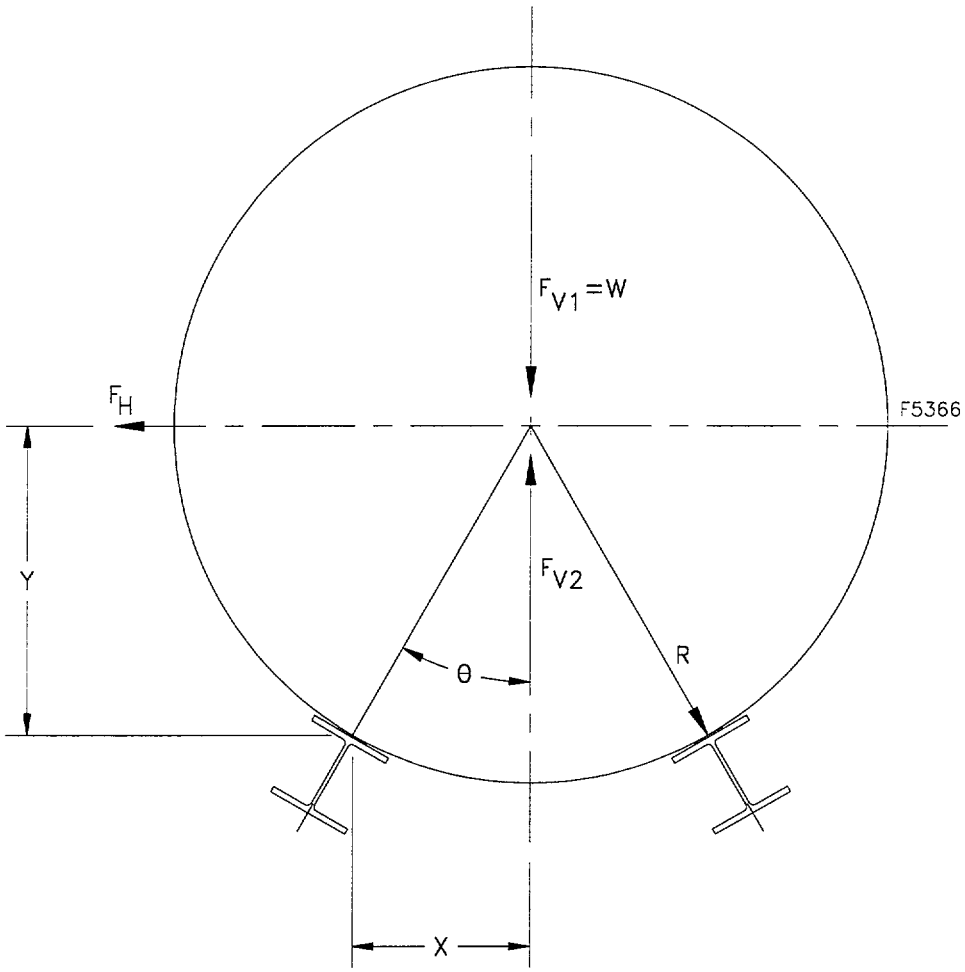

WHERE:

R = 33.595 in., DSC outer radius
θ = 30°
X = R Sin θ = 16.8 in.
Y = R Cos θ = 29.1 in.
F_{V1} = W = weight of DSC
F_{V2} = W(0.17g) = upward vertical seismic load
F_H = W(0.40g) = horizontal seismic load

Figure M.3.7-1
DSC Lift-Off Evaluation

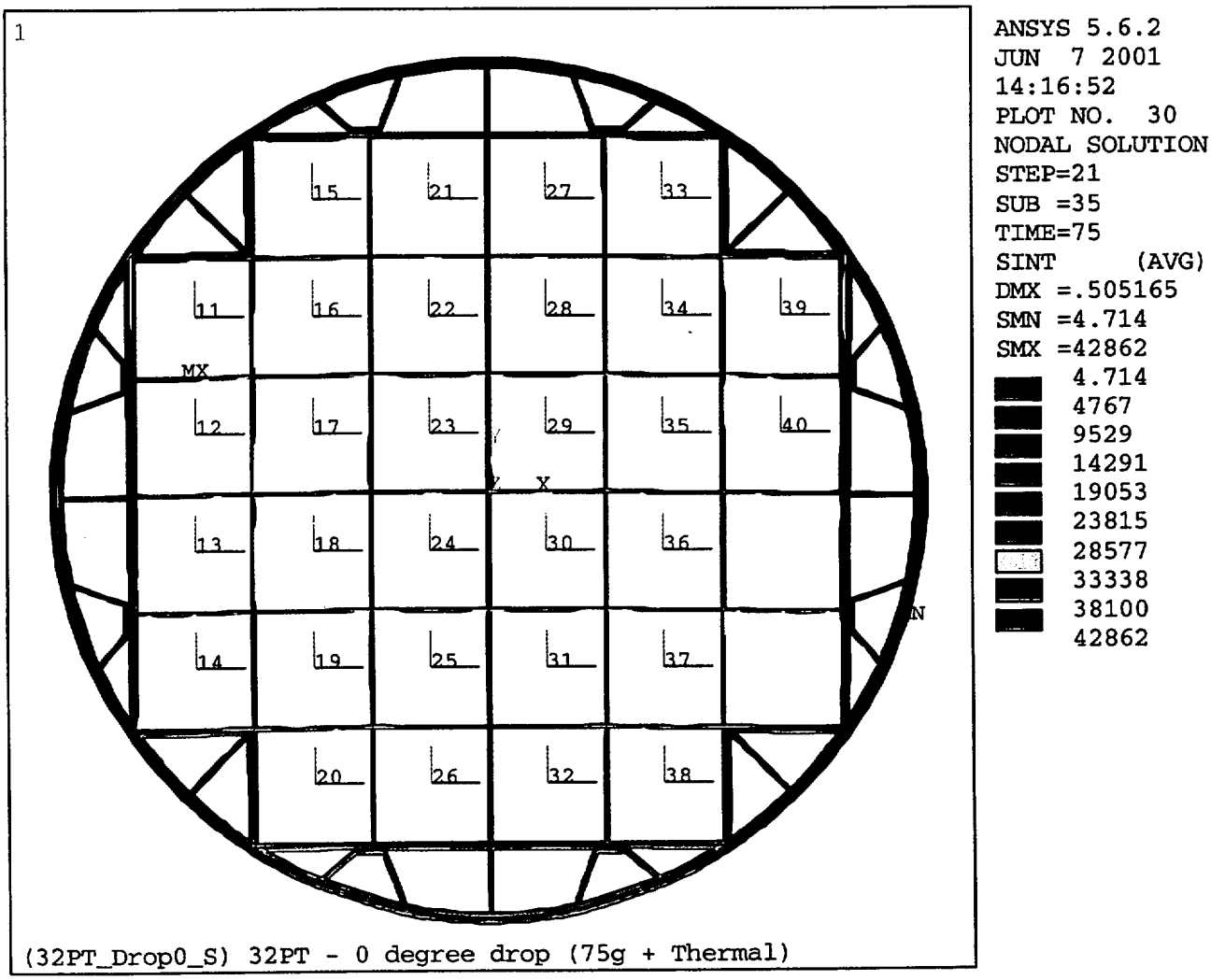

Figure M.3.7-2
0° Side Drop Stress Intensity, 32PT Basket with Steel Transition Rails
(Support Rails at ±18.5°)

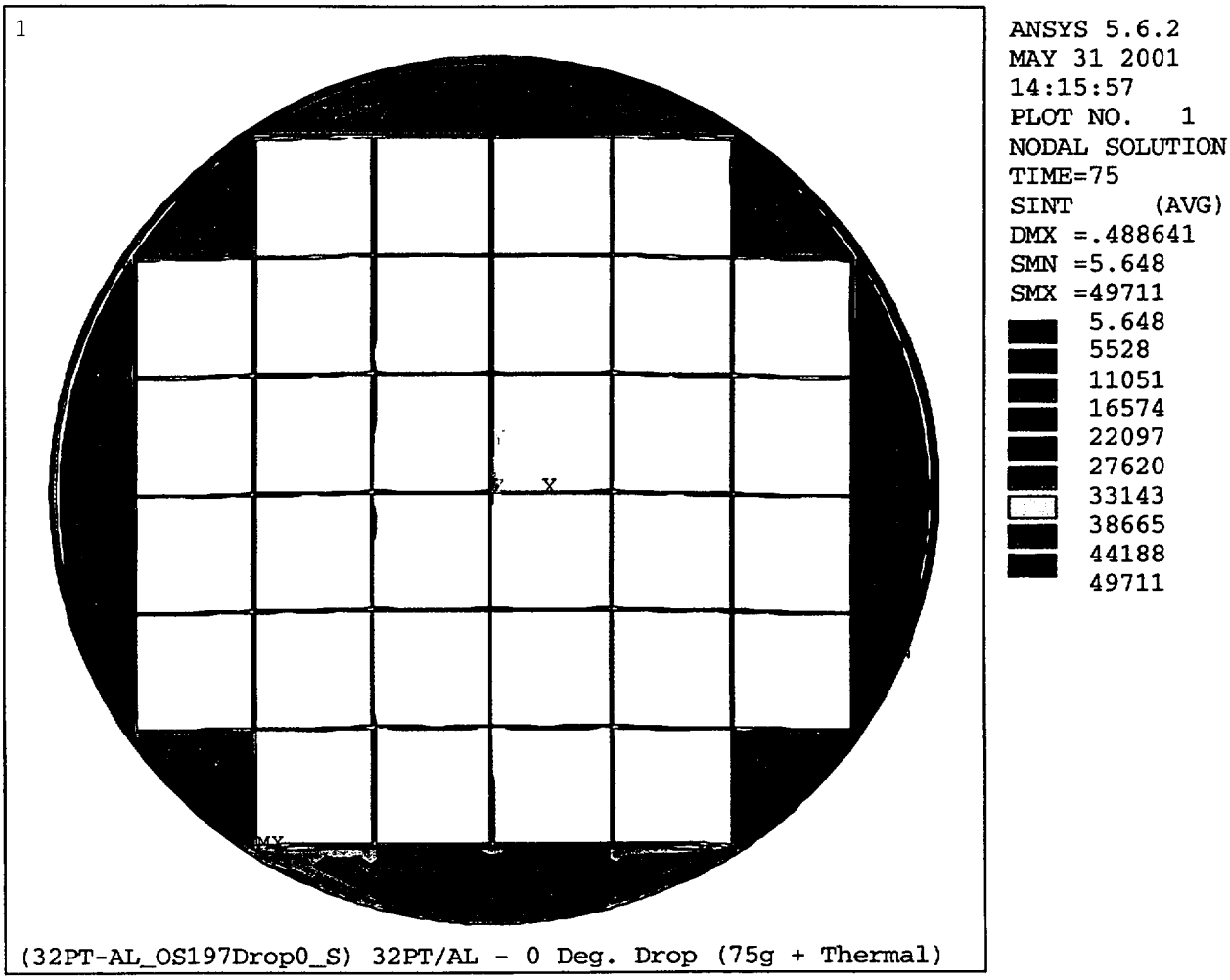

Figure M.3.7-3
0° Side Drop Stress Intensity, 32PT Basket with Aluminum Transition Rails (Support Rails at ±18.5°)

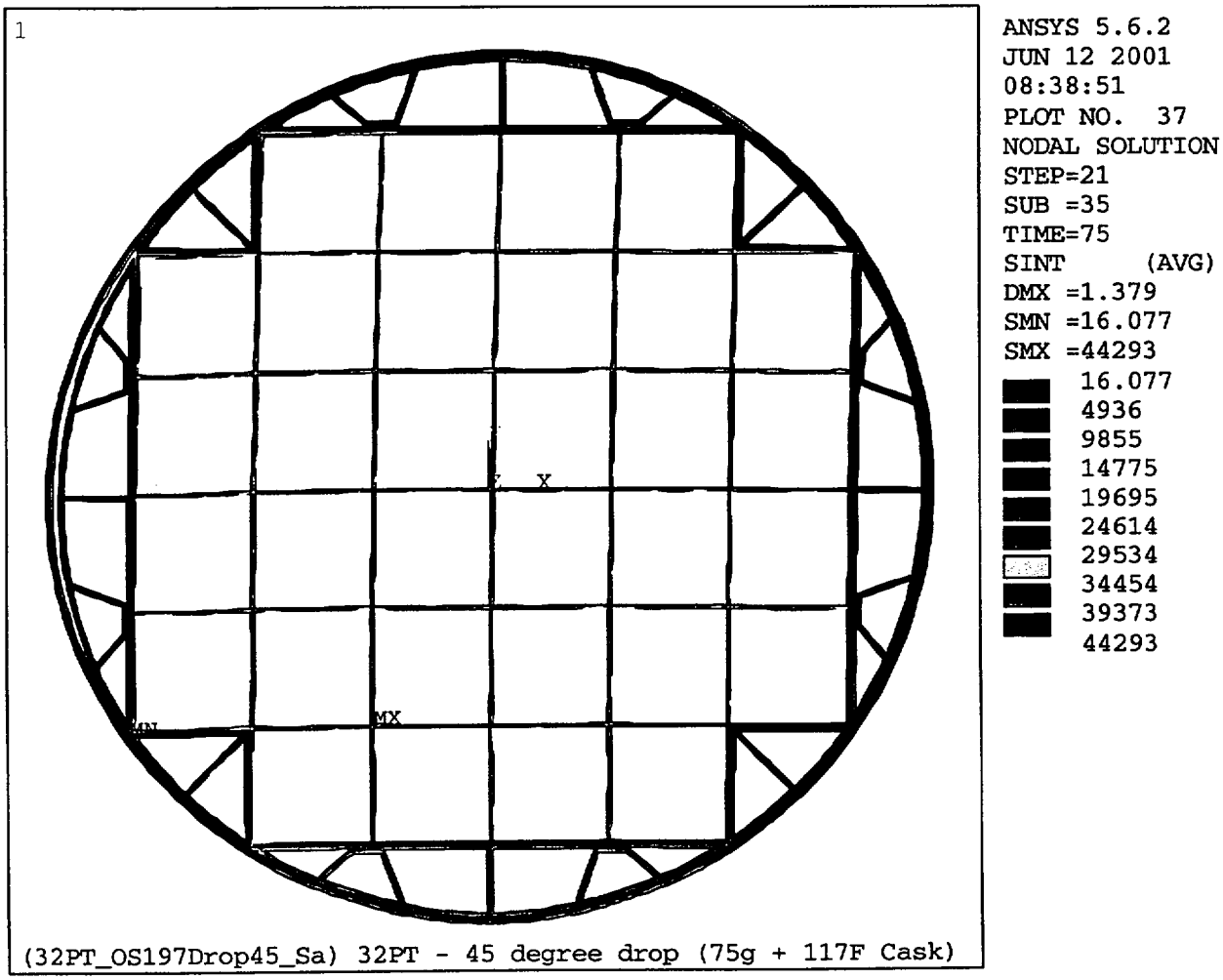

Figure M.3.7-4
45° Side Drop Stress Intensity, 32PT Basket with Steel Transition Rails
(Support Rails at ±18.5°)

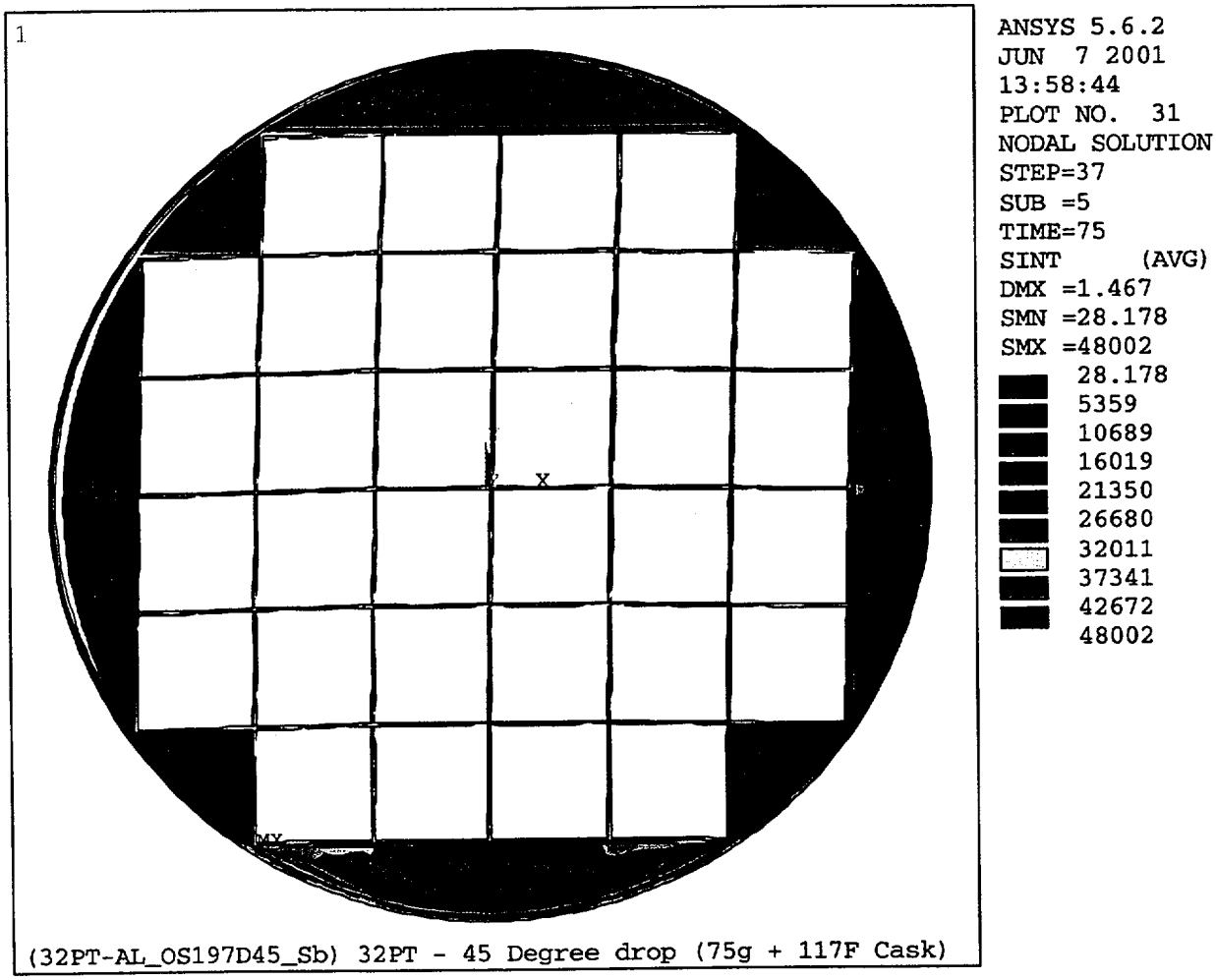

Figure M.3.7-5
45° Side Drop Stress Intensity, 32PT Basket with Aluminum Transition Rails (Support Rails at ±18.5°)

Figure M.3.7-6
Displaced Shape at 113g, LS-DYNA Confirmatory Stability Analysis for 0° Side Drop with Steel Transition Rails (Support Rails at ±18.5°))

(See displacement time history on following page)

Figure M.3.7-7
Displacement Time History, LS-DYNA Confirmatory Stability Analysis for 0° Side Drop with Steel Transition Rails

(See previous page for displaced shape and node locations)

Figure M.3.7-8
Displaced Shape at 124g, LS-DYNA Confirmatory Stability Analysis for 180° Side Drop with Steel Transition Rails
(No Cask Rails at 180°)

(See displacement time history on following page)

M.3.8 References

3.1 American Society of Mechanical Engineers, ASME Boiler and Pressure Vessel Code, Section III, Subsections NB, NF, NG, and Appendices 1998, with 2000 Addenda including Code Case N-595-2.

3.2 American Society of Mechanical Engineers, ASME Boiler and Pressure Vessel Code, Section II, Part D, 1998 with 2000 Addenda.

3.3 Kaufman, J.G., ed., "Properties of Aluminum Alloys: Tensile, Creep, and Fatigue Data and High and Low Temperatures", The Aluminum Association (Washington, D.C.) and ASM International (Metals Park, Ohio), 1999.

3.4 Pacific Northwest Laboratory Annual Report – FY 1979, "Spent Fuel and Fuel Pool Component Integrity," May 1980.

3.5 G. Wranglen, "An Introduction to Corrosion and Protection of Metals," Chapman and Hall, 1985, pp. 109-112.

3.6 A.J. McEvily, Jr., ed., "Atlas of Stress Corrosion and Corrosion Fatigue Curves," ASM Int'l, 1995, p. 185.

3.7 TN West Document No. 31-B9604.97-003, dated December 19, 1997; Addendum to TN West Document No. 31-B9604.0102, Rev. 2, "An Assessment of Chemical, Galvanic and Other Reactions in NUHOMS® Spent Fuel Storage and Transportation Casks."

3.8 Baratta, et al. "Evaluation of Dimensional Stability and Corrosion Resistance of Borated Aluminum," Final Report submitted to Eagle-Pitcher Industries, Inc. by the Nuclear Engineering Department, Pennsylvania State University.

3.9 "Hydrogen Generation Analysis Report for TN-68 Cask Materials," Test Report No. 61123-99N, Rev. 0, Oct 23, 1998, National Technical Systems.

3.10 R.J. Roark and W.C. Young, "Formulas for Stress and Strain," Fifth Edition, McGraw-Hill, New York, N.Y., 1975

3.11 ANSYS Engineering Analysis System, Users Manual for ANSYS Rev. 5.6, Swanson Analysis Systems, Inc., Houston, PA, 1998.

3.12 U.S. Nuclear Regulatory Commission (U.S. NRC), "Standard Format and Content for the Safety Analysis Report for an Independent Spent Fuel Storage Installation (Dry Storage)," Regulatory Guide 3.48 (Task FP-029-4), (October 1981).

3.13 Not Used.

3.14 American National Standard, "Design Criteria for an Independent Spent Fuel Storage Installation (Dry Storage Type)," ANSI/ANS 57.9-1984, American Nuclear Society, La Grange Park, Illinois (1984).

3.15 U.S. Atomic Energy Commission, "Damping Values for Seismic Design of Nuclear Power Plants," Regulatory Guide 1.61, (October 1973).

3.16 R. D. Blevins, "Formulas for Natural Frequency and Mode Shape," Van Nostrand Reinhold Co., New York, N.Y., (1979).

M.4 Thermal Evaluation

M.4.1 Discussion

The NUHOMS®-32PT system is designed to passively reject decay heat during storage and transfer for normal, off-normal and accident conditions while maintaining temperatures and pressures within specified regulatory limits. Objectives of the thermal analyses performed for this evaluation include: (1) determination of maximum and minimum temperatures with respect to material limits to ensure components perform their intended safety functions, (2) determination of temperature distributions for the NUHOMS®-32PT DSC components to support the calculation of thermal stresses for the structural components, (3) determination of maximum internal NUHOMS®-32PT DSC pressures for the normal, off-normal and accident conditions, (4) determination of the maximum fuel cladding temperature, and (5) confirmation that this temperature will remain sufficiently low to prevent unacceptable degradation of the fuel during storage.

The NUHOMS®-32PT DSC falls under the jurisdiction of 10CFR Part 72 when used as a component of an ISFSI. To establish the heat removal capability, several thermal design criteria are established for the basket. These are as discussed below:

- Maximum temperatures of the confinement structural components must not adversely affect the confinement function.
- The maximum initial fuel cladding temperature during storage (long term) is determined as a function of the initial fuel age using accepted guidelines provided by PNL-6189 [4.1]. In addition, maximum fuel cladding temperature limits are defined for short term conditions like loading, unloading, transfer and accident conditions using PNL-4835 [4.2]. The temperature threshold accounts for the effects of cladding temperature, decay time, burnup and fission gas build-up at burnups of 45 GWd/MTU. For normal conditions of storage, a long term fuel temperature limit based on time after discharge has been established and is shown in Table M.4-1. During short term conditions, the fuel temperature limit is 570°C (1,058°F).
- The maximum DSC cavity internal pressures during normal, off-normal and accident conditions must be below the design pressures of 15 psig, 20 psig and 105 psig, respectively.
- The maximum total heat load per DSC is 24kW with a maximum per assembly heat load of 1.2kW when zoning is used for heat load. Figure M.4-1, Figure M.4-2, and Figure M.4-3 show the heat load zoning configurations used in the NUHOMS®-32PT DSC design.

The analyses consider the effect of the decay heat flux varying axially along a fuel assembly. The axial heat flux profile for a PWR fuel assembly is shown in Figure M.4-4 and is based on [4.3].

A description of the detailed analyses performed for normal storage and transfer conditions is provided in Section M.4.4, off-normal conditions in Section M.4.5, accident conditions in Section M.4.6, and loading/unloading conditions in Section M.4.7. The thermal evaluation concludes that with a design basis heat load of up to 24 kW per DSC, all design criteria are satisfied.

M.4.2 Summary of Thermal Properties of Materials

1. PWR Fuel with Helium Backfill

The effective thermal conductivity is the lowest calculated value for the various PWR fuel assembly types that may be stored in this DSC and corresponds to the B&W 15x15 PWR assembly.

Fuel in Helium, transverse			
Temperature (°F)	**K (Btu/min-in-°F)**	**ρ (lb_m/in^3)**	**C_p (Btu/lb_m-°F)**
205	3.991e-4	0.120	0.0618
286	4.605e-4		0.0642
387	5.442e-4		0.0665
493	6.472e-4		0.0682
595	7.724e-4		0.0696
695	8.868e-4		0.0707
796	1.041e-3		0.0716

Fuel in Helium, Axial			
Temperature (°F)	**K (Btu/min-in-°F)**	**ρ (lb_m/in^3)**	**C_p (Btu/lb_m-°F)**
200	1.029e-3	0.120	0.0617
300	1.089e-3		0.0645
400	1.149e-3		0.0657
500	1.202e-3		0.0683
600	1.255e-3		0.0697
800	1.368e-3		0.0716

2. PWR Fuel in Vacuum

Temperature (°F)	**K (Btu/min-in-°F)**	**ρ (lb_m/in^3)**	**C_p (Btu/lb_m-°F)**
269	1.274E-04	0.120	0.0638
333	1.629E-04		0.0654
420	2.177E-04		0.0671
515	2.956E-04		0.0686
611	3.862E-04		0.0698
706	4.887E-04		0.0708
804	6.140E-04		0.0717

3. SA-240, Type 304 Stainless Steel [4.4]

Temperature (°F)	K (Btu/min-in-°F)	ρ (lbm/in^3)	C_p (Btu/lb$_m$-°F)
70	0.0119	0.284	0.116
100	0.0121		0.117
150	0.0125		0.119
200	0.0129		0.121
250	0.0133		0.124
300	0.0136		0.125
350	0.0140		0.127
400	0.0144		0.128
500	0.0151		-
600	0.0157		-
700	0.0164		-
800	0.0169		-

4. SA-240 Type XM-19 (22Cr-13Ni-5Mn) [4.4]

Temperature (°F)	K (Btu/min-in-°F)	ρ (lb$_m$/in^3)	C_p (Btu/lb$_m$-°F)
70	8.89e-3	0.284	0.113
100	9.17e-3		0.116
150	9.58e-3		0.119
200	9.86e-3		0.120
300	0.0107		0.125
400	0.0114		0.127
500	0.0122		0.130
600	0.0129		0.133
700	0.0138		0.135
800	0.0144		0.137
900	0.0150		0.137

5. Aluminum, Type 1100 [4.4]

Temperature (°F)	K (Btu/min-in-°F)	ρ (lb$_m$/in^3)	C_p (Btu/lb$_m$-°F)
70	0.185	0.098	0.214
100	0.183		0.216
150	0.181		0.219
200	0.178		0.222
250	0.177		0.224
300	0.175		0.227
350	0.174		0.229
400	0.173		0.232

6. Aluminum, Type 6061 [4.4]

Temperature (°F)	K (Btu/min-in-°F)	ρ (lb_m/in^3)	C_p (Btu/lb_m-°F)
70	0.133	0.098	0.213
100	0.135		0.215
150	0.136		0.218
200	0.138		0.221
250	0.139		0.223
300	0.140		0.226
350	0.141		0.228
400	0.142		0.230

7. Aluminum Based Neutron Poison (from Section M.4.3)

Temperature (°F)	K (Btu/min-in-°F)	ρ (lb_m/in^3)	C_p (Btu/lb_m-°F)
68	0.0963	0.098	0.214
212	0.116		0.222
482	0.120		0.232
571	0.120		0.232

8. Air [4.5]

Temperature (°F)	K (Btu/min-in-°F)	ρ (lb_m/in^3)	C_p (Btu/lb_m-°F)
71	2.075E-5	N/A	N/A
107	2.199E-5		
206	2.528E-5		
314	2.869E-5		
404	3.139E-5		
512	3.447E-5		
602	3.693E-5		
692	3.929E-5		
764	4.114E-5		
800	4.203E-5		

9. Helium [4.6]

Temperature (°F)	K (Btu/min-in-°F)	ρ (lb_m/in^3)	C_p (Btu/lb_m-°F)
200	1.361E-4	N/A	N/A
300	1.493E-4		
400	1.635E-4		
500	1.793E-4		
600	1.949E-4		
700	2.094E-4		
800	2.232E-4		

The analyses use interpolated values when appropriate for intermediate temperatures. The interpolation assumes a linear relationship between the reported values.

Thermal radiation effects on the interior surfaces of the basket rails are considered. The emissivity of stainless steel is 0.587 [4.7]. For additional conservatism an emissivity of 0.46 for stainless steel is used for the basket steel plates in the analysis.

M.4.3 Specifications for Components

The thermal conductivity of the neutron poison plates must be verified by testing. The neutron poison plates must have the following minimum thermal conductivity [4.8]:

Temperature (°F)	Thermal Conductivity (Btu/hr-in-°F)
68	5.78
212	6.98
482	7.22
571	7.22
600	7.22
650	7.22

M.4.4 Thermal Evaluation for Normal Conditions of Storage (NCS) and Transfer (NCT)

M.4.4.1 NUHOMS®-32PT DSC Thermal Models

The NUHOMS®-32PT DSC finite element models are developed using the ANSYS computer code [4.9]. ANSYS is a comprehensive thermal, structural and fluid flow analysis package. It is a finite element analysis code capable of solving steady state and transient thermal analysis problems in one, two or three dimensions. Heat transfer via a combination of conduction, radiation and convection can be modeled by ANSYS. Solid entities are modeled by SOLID70 Elements for 3-D models and PLANE55 elements for 2-D models. Heat transfer across small gaps was modeled by LINK32 1-D conduction elements.

M.4.4.1.1 NUHOMS®-32PT DSC Basket and Payload Model

The three-dimensional model (Figure M.4-5) represents the NUHOMS®-32PT DSC with a steel/aluminum composite transition rail, and includes the geometry and material properties of the basket components, the basket rails, and DSC. The model simulates the effective thermal properties of the fuel with a homogenized material occupying the volume within the basket where the 141.8 inch active length of the fuel is used. Within the models, heat is transferred via conduction through fuel regions, the poison plates, steel of the basket and the gas gaps between the poison plate and steel members. Generally, good surface contact is expected between adjacent components within the basket structure. However to bound the heat conductance uncertainty between adjacent components, conservative gaps between the adjacent components have been included in the model. All heat transfer across the gaps is by gaseous conduction. Other modes of heat transfer are conservatively neglected. Heat is transferred through the basket support rails via conduction.

For the vacuum drying and blocked vent transients, axial heat transfer was neglected and a two-dimensional model was used which corresponds to the cross-section shown in Figure M.4-6.

The steel/aluminum transition rails were modeled as being 0.675 in. thick and include the 0.4 in. aluminum plates. The effective conductivity of the rails is adjusted to account for the presence of the aluminum plates. The elements representing the XM-19 grid structure include an adjustment to the conductivity to account for gaps between the basket components. The steel/aluminum rail configuration provides the bounding temperatures for all cases, since the solid aluminum rail configuration has a significantly higher effective conductivity and cross-sectional area, yielding lower temperatures for all cases.

The 3-D model was extended to approximately half the length of the DSC cavity, or 83.5 in. to model the bottom half of the canister. A symmetry boundary was applied on the axial top of the model. The heat generations were applied over the active fuel, starting from 8.625 in. from the bottom of the fuel regions and extending all the way to the top of the model. The placement of the active fuel and the model size results in slight overprediction of temperatures since the symmetry boundary at (167/2-8.625)=74.875 in. from the beginning of active fuel is located well beyond half of the active fuel, or 141.8/2=70.9 in., where peak temperatures would be expected. Longer DSC cavity configurations (32PT-L100 and 32PT-L125) provide larger radial surface areas for heat

dissipation and are therefore bounded by the shorter cavity (32PT-S100 and 32PT-S125) DSC configurations.

M.4.4.1.2 Heat Generation

Heat generation is calculated based on the dimensions of the fuel and basket. The heat is assumed to be distributed evenly radially through the 8.7 in. square nominal fuel cell opening. Axial variations are accounted for in ANSYS by using the peaking factors in Figure M.4-4 along the active length of the PWR fuel assembly. Heat generation rates with the corresponding peaking factors are applied according to the decay heat load zoning configurations 1 through 3 given in Figure M.4-1, Figure M.4-2, and Figure M.4-3.

The normal conditions of storage are used for the determination of the maximum fuel cladding temperature, basket component temperatures, NUHOMS®-32PT DSC internal pressure and thermal stresses. The 10CFR Part 71.71(c) insolation averaged over a 24-hour period is used as steady state boundary condition.

M.4.4.1.3 Thermal Model of DSC in Horizontal Storage Module

To determine the temperature distribution on the surface of the DSC, a two-dimensional ANSYS model of the cross section of the HSM with loaded DSC is used to represent the NUHOMS®-32PT system during storage (Figure M.4-7). Solid entities are modeled in ANSYS by PLANE55 two-dimensional thermal elements. Radiation within the HSM is modeled in ANSYS by MATRIX50 super elements.

The methodology given in Section 8.1.3 is used to calculate bulk air temperatures within the HSM. The decay heat from the payload is modeled as a uniform heat flux on the inner surface of the DSC shell. Heat from the DSC surface dissipates via natural convection to the air within the HSM and via radiation to the HSM heat shield and walls. Heat dissipates from the HSM heat shield via radiation to walls and then via conduction through the walls of the HSM, via convection to the HSM air and via convection and radiation from the HSM outer surfaces to the ambient environment.

M.4.4.1.4 TC Thermal Model

To determine the temperature distribution on the surface of the DSC during transfer operations, a two-dimensional model of the cross section of the TC with loaded DSC (Figure M.4-8). Solid entities were modeled in ANSYS by PLANE55 two-dimensional thermal elements. Radiation within the cask cavity was modeled in ANSYS by MATRIX50 super elements.

The decay heat from the payload is modeled as a uniform heat flux on the inner surface of the DSC shell. The decay heat from the DSC surface dissipates via conduction and radiation to the inner surface of the TC. Heat transferred through the cask via conduction and dissipates to the environment from the outer cask surfaces from the outer cask surfaces by a combination of natural convection and radiation.

M.4.4.1.5 Boundary Conditions, Storage

Normal Conditions of Storage analyses of the NUHOMS®-32PT DSC within the HSM are carried out for the following ambient conditions:

- Maximum normal ambient temperature of 100°F with insolation,
- Minimum normal ambient temperature of 0°F without insolation, and
- Long term average maximum ambient temperature of 70°F, with insolation.

The HSM and TC thermal models described above provide the surface temperatures of the DSC shell that are applied as boundary conditions to the DSC shell in the basket and payload models which calculate the temperature distribution in the basket components and fuel.

M.4.4.1.6 Boundary Conditions, Transfer

In accordance with Section 8.1, analyses of the NUHOMS®-32PT DSC within the TC were performed for the following ambient conditions:

- Maximum normal ambient temperature of 100°F with insolation, and
- Minimum normal extreme ambient temperature of 0°F without insolation.

The maximum calculated DSC temperatures are conservatively applied to the entire exterior surface of the DSC in the DSC/Basket/Payload finite element model.

M.4.4.2 Maximum Temperatures

M.4.4.2.1 Fuel Cladding

M.4.4.2.1.1 Long Term Storage Temperatures

The maximum fuel cladding temperature for long term storage with 70°F ambient condition is evaluated for each of the three decay heat load zoning configurations. Maximum fuel cladding temperatures for each of these five specific decay heat conditions are evaluated and compared with the corresponding fuel cladding temperature limit for long term storage in Table M.4-1.

M.4.4.2.1.2 Short Term Event Temperatures

The short term events are defined in Section M.4.1 for storage and transfer. The results are reported for heat load zoning configuration 1 and 3 which yield the highest fuel cladding temperatures. The maximum fuel cladding temperatures for short term normal conditions of storage and transfer are given in Table M.4-2.

M.4.4.2.1.3 DSC Basket Material Temperatures

The maximum temperatures of the basket assembly for normal conditions of storage and transfer for heat load zoning configurations 1, 2 and 3 are listed in Table M.4-3, Table M.4-4, and Table M.4-5, respectively. The minimum component temperatures reported in these tables represent the minimum temperature for those components at the hottest radial cross section, not the minimum absolute component temperature in the entire basket. The maximum basket temperature distributions for configuration 1 during normal conditions of storage and transfer are presented in Figure M.4-9 and Figure M.4-10, respectively.

M.4.4.3 Minimum Temperatures

Under the minimum temperature condition of 0°F ambient, the resulting DSC component temperatures will approach 0°F if no credit is taken for the decay heat load. Since the DSC materials, including confinement structures, continue to function at this temperature, the minimum temperature condition has no adverse effect on the performance of the NUHOMS®-32PT DSC.

M.4.4.4 Maximum Internal Pressures

M.4.4.4.1 Pressure Calculation

This section describes the pressure calculations used to determine maximum internal pressures during storage and transfer within the NUHOMS®-32PT DSC and basket when loaded with a payload of worst case B&W 15x15 fuel assemblies with a maximum burnup of 45 GWd/MTU.

The calculations include the DSC free volume, the quantities of DSC backfill gas, fuel rod fill gas, and fission products and the average DSC cavity gas temperature. The 32PT-S100, 32PT-S125, 32PT-L100 and 32PT-L125 canister configurations are considered. The calculations include the stainless steel/aluminum and solid aluminum transition rail options. The 32PT-L100 and 32PT-L125 DSC internal pressure evaluations also include the contribution due to BPRAs.

M.4.4.4.2 Free Volume

M.4.4.4.2.1 DSC Cavity

The DSC Cavity free volumes are shown below:

Canister Type	32PT-S100	32PT-S100	32PT-S125	32PT-S125	32PT-L100	32PT-L100	32PT-L125	32PT-L125
Rail Type	Steel/ Aluminum	Solid Aluminum	Steel/ Aluminum	Solid Aluminum	Steel/ Aluminum	Solid Aluminum	Steel/ Aluminum	Solid Aluminum
Cavity Volume (in^3)	585,129	585,129	576,526	576,526	605,774	605,774	597,172	597,172
Basket Volume (in^3)	107,513	163,508	105,859	161,105	111,484	169,353	109,829	166,951
Fuel Volume (in^3)	177,619	177,619	177,619	177,619	189,760	189,760	189,760	189,760
Free Volume (in^3)	299,997	244,002	293,048	237,802	304,530	246,661	297,583	240,461

M.4.4.4.3 Quantity of Helium Fill Gas in DSC

The DSC free volume is assumed to be filled with 3.5 psig (18.2 psia) of helium. The maximum temperatures from the 70°F ambient storage case are used to estimate the number of moles of helium backfill. The Long Cavity (L100 and L125) DSC results are bounded by the Short (S100 and S125) DSC Cavity, and hence, it is conservative to use the Short Cavity DSC results.

The average long term helium fill temperature for the worst case payload is 449°F (909°R). Using the ideal gas law, the quantity of helium in the DSC is calculated and the results are presented in Table M.4-6.

M.4.4.4.4 Quantity of Fill Gas in Fuel Rod

The volume of the helium fill gas in a B&W 15x15 fuel pin at cold, unirradiated conditions is 1.6 in^3, and there are 208 fueled pins in an assembly. The maximum fill pressure is 415 psig (429.7 psia) and the fill temperature is assumed to be room temperature (70°F or 530°R). The quantity of fuel rod fill gas in 32 fuel assemblies is:

$$n_{he} = \frac{(429.7\,psia)(6894.8\,Pa/psi)(32 \cdot 208 \cdot 1.6in^3)(1.6387x10^{-5}\,m^3/in^3)}{(8.314\,J/mol \cdot K)(530°R)(5/9\,K/°R)}$$

$$n_{he} = 211.2\,g-moles$$

Based on NUREG 1536 [4.10], the maximum fraction of the fuel pins that are assumed to rupture and release their fill and fission gas for normal, off-normal and accident events is 1, 10 and 100%, respectively. 100% of the fill gas in each ruptured rod is assumed to be released. The amount of helium fill gas released for each of these conditions is summarized below.

Case	Percentage of Rods Ruptured	Moles of Helium Fill Gas Released
Normal	1	2.11
Off-Normal	10	21.12
Accident	100	211.2

M.4.4.4.5 Quantity of Fission Product Gases in Fuel Rod

The B&W 15x15 fuel assembly used in the pressure calculations is assumed to be burned to 45,000 MWd/MTU, which is the highest burnup proposed for the NUHOMS®-32PT configuration. The maximum burnup creates a bounding case for the amount of fission gases produced in the fuel rod during reactor operation. The amounts of tritium, krypton-85 and xenon-131m at STP for each assembly are summarized below.

Isotope	Volume (liters/assy)	Volume (in^3/assy)
Tritium (H^3)	0.26	16
Kr^{85}	60.4	3,686
Xe^{131m}	547	33,380
Total	607.7	37,081

The total fission gas volume for a DSC is equal to 607.7 liters (37,081 in^3). The total amount of fission gas products produced is calculated using 32°F as:

$$n_{fg} = \frac{(32)(14.7)(6894.8\,Pa/psi)(37{,}081 in^3)(1.6387x10^{-5}\,m^3/in^3)}{(8.314\,J/mol\cdot K)(460°R+32°F)(5/9\,K/°R)}$$

$$n_{fg} = 867\,g-moles$$

The amount of fission gas released into the DSC cavity for normal, off-normal and accident condition cases assuming a 30% gas release from the fuel pellets and a 1%, 10%, and 100% rod rupture percentage, respectively, is summarized below.

Case	Percentage of Rods Ruptured	Moles of Fission Gas Released
Normal	1	2.6
Off-Normal	10	26.0
Accident	100	260

M.4.4.4.6 Quantity of Gas in Control Components (BPRAs)

The 32PT-L100 and 32PT-L125 DSC configurations may include BPRAs. For the controlling B&W 15x15 assembly, up to 16 BPRAs may be present. These BPRAs have an initial helium fill of 14.7 psia, and if 100% of the boron is consumed, and 30% released into the DSC, a total of 53.8 gmoles of gas could be released to the DSC assuming 100% cladding rupture.

The percentage of BPRA rods ruptured during normal, off-normal and accident conditions is assumed to be 1%, 10% and 100%, respectively, similar to the assumptions for the fuel rod rupturing. The maximum amount of gas released to the DSC cavity from the BPRAs for normal, off-normal and accident conditions is given below.

Case	Percentage of Rods Ruptured	Moles of Fission Gas Released per DSC from BPRAs
Normal	1	0.538
Off-Normal	10	5.38
Accident	100	53.8

The maximum average helium temperature for normal conditions of storage and transfer occurs when the 32PT DSC is in the TC with an ambient temperature of 100°F and maximum insolation. This case bounds the 100°F ambient case in the HSM. In addition the maximum pressure will occur with the 45,000 MWd/MTU burnup fuel so that lesser burnups will be enveloped by this calculation. The average helium temperature is 578°F (1,038°R). The maximum normal operating condition pressures are summarized in Table M.4-7.

M.4.4.5 Maximum Thermal Stresses

The maximum thermal stresses during normal conditions of storage and transfer are calculated in Section M.3.

M.4.4.6 Evaluation of Cask Performance for Normal Conditions

The NUHOMS®-32PT DSC shell and basket are evaluated for the calculated temperatures and pressures in Section M.3. The maximum fuel cladding temperatures are well below the allowable long term fuel temperature limits and the short term limit of 1,058°F (570°C). The maximum DSC internal pressure remains below 15.0 psig during normal conditions of storage and transfer. Based on the thermal analysis, it is concluded that the NUHOMS®-32PT DSC design meets all applicable normal condition thermal requirements.

M.4.5 Thermal Evaluation for Off-Normal Conditions

The NUHOMS®-32PT system components are evaluated for the extreme ambient temperatures of -40°F (winter) and 117°F (summer). Should these extreme temperatures ever occur, they would be expected to last for a very short duration of time. Nevertheless, these ambient temperatures are conservatively assumed to occur for a significant duration to result in a steady-state temperature distribution in the NUHOMS®-32PT system components.

M.4.5.1 Off-Normal Maximum/Minimum Temperatures during Storage

The thermal performance of the NUHOMS®-32PT DSC within the HSM under the extreme minimum ambient temperatures of -40°F with no insolation and 117°F with maximum insolation are evaluated with heat load zoning configurations 1, 2 and 3.

M.4.5.1.1 Boundary Conditions, Storage

Off-normal conditions of storage analyses of the NUHOMS®-32PT DSC within the HSM includes:

- Maximum off-normal ambient temperature of 117°F with insolation, and
- Minimum off-normal ambient temperature of -40° F without insolation.

The HSM and TC thermal models described above provide the surface temperatures that are applied to the DSC, basket and payload model.

M.4.5.2 Off-Normal Maximum/Minimum Temperatures during Transfer

The thermal performance of the NUHOMS®-32PT DSC during transfer under the extreme minimum ambient temperatures of -40°F with no insolation and 117°F with maximum insolation, and decay heat load configurations 1, 2 and 3 are examined. For transfer operations when ambient temperatures exceed 100°F up to 117°F, a solar shield is used.

M.4.5.2.1 Boundary Conditions, Transfer

In accordance with Section 8.1, analyses of a 24 kW DSC within the TC are performed for the following ambient conditions:

- Maximum normal ambient temperature of 117°F with solar shield in place, and
- Minimum off-normal extreme ambient temperature of -40°F without insolation.

These analyses, which use a total decay heat load of 24.0 kW per DSC, determine maximum DSC surface temperatures. The maximum calculated DSC temperatures are conservatively applied to the entire exterior surface of the DSC in the DSC/basket/payload finite element model. In the case of the maximum off-normal ambient temperature, the presence of the solar shield makes the maximum normal case temperature results bound the off-normal case.

M.4.5.3 Off-Normal Maximum and Minimum Temperatures During Storage/Transfer

Since the thermal performance of the DSC without sunshade at an ambient temperature of 100°F is limiting, the results presented in Section M.4.4 for the 100°F ambient case bound the maximum off-normal 117°F case.

M.4.5.3.1 Fuel Cladding

The results are reported in Table M.4-8 for heat load zoning configurations 1 and 3 which yield the highest fuel cladding temperatures.

M.4.5.3.2 DSC Basket Materials

The maximum temperatures of the basket assembly for normal conditions of storage and transfer for heat load zoning configurations 1, 2 and 3 are listed in Table M.4-9, Table M.4-10, and Table M.4-11, respectively. The minimum temperatures reported for each component are not the minimum absolute component temperature in the entire basket. The minimums reported in the tables below represent the minimum temperature for those components at the hottest radial cross section. The bounding basket temperature distributions for heat load zoning configuration 1 off-normal conditions of storage and transfer are presented in Figure M.4-11 and Figure M.4-12, respectively.

M.4.5.4 Off-Normal Maximum Internal Pressure During Storage/Transfer

The off-normal condition maximum pressure calculation also considers the DSC in the TC at 100°F ambient. This case bounds the case in which the DSC is in the HSM with 117°F ambient and the 117°F TC case with the sunshade in place. Per NUREG 1536, the percentage of fuel rods ruptured for off-normal cases is 10%.

A summary of the maximum off-normal operating pressures for the various 32PT DSC configurations are presented in Table M.4-12.

M.4.5.5 Maximum Thermal Stresses

The maximum thermal stresses during off-normal conditions of storage and transfer for the NUHOMS®-32PT DSC are calculated in Section M.3.

M.4.5.6 Evaluation of Cask Performance for Off-Normal Conditions

The NUHOMS®-32PT DSC shell and basket are evaluated for calculated temperatures and pressures in Section M.3. The maximum fuel cladding temperatures are well below the allowable fuel temperature limit of 1,058°F (570°C). The maximum DSC internal pressures remain below 20.0 psig during off-normal conditions of storage and transfer. The pressures and temperatures associated with off-normal conditions in the NUHOMS®-32PT DSC design meet all applicable off-normal thermal requirements.

M.4.6 Thermal Evaluation for Accident Conditions

Since the NUHOMS® HSMs are located outdoors, there is a remote possibility that the ventilation air inlet and outlet openings could become blocked by debris from such unlikely events as floods and tornadoes. The NUHOMS® HSM system design features such as the perimeter security fence and redundant protected location of the air inlet and outlet openings reduces the probability of occurrence of such an accident. Nevertheless, for this conservative generic analysis, such an accident is postulated to occur and is analyzed.

During transfer under maximum ambient temperature and insolation, the loss of the sun shield and the liquid neutron shield in the TC represents the controlling transfer case. Although the temperatures for this case are bounded by the blocked vent case, it is included here to provide a bounding condition for maximum internal pressure.

It is determined in Section 3.3.6, that the HSM and DSC contain no flammable material and the concrete and steel used for their fabrication can withstand any credible fire accident condition. Fire parameters are dependent on the amount and type of fuel within the transporter and the fire accident condition shall be addressed within site-specific applications. Licensees are required to verify that loadings resulting from potential fires and explosions are acceptable in accordance with 10CFR72.212(b)(2). The hypothetical fire evaluation for the NUHOMS®-32PT system is included in Section M.4.6.3.

M.4.6.1 Blocked Vent Accident Evaluation

For the postulated blocked vent accident condition, the HSM ventilation inlet and outlet openings are assumed to be completely blocked for a 40 hour period concurrent with the extreme off-normal ambient condition of 117°F with insolation.

For conservatism, a transient thermal analysis is performed using the 2-D model developed in Section M.4.4.1, for heat load zoning configuration 1, which envelopes the temperature results for heat load zoning configurations 2 and 3. When the inlet and outlet vents are blocked, the air surrounding the DSC in the HSM cavity is contained (trapped) in the HSM cavity. The temperature difference between the hot DSC surface and the surrounding cooler heat shield and concrete surfaces in the HSM cavity will result in closed cavity convection. This closed cavity convection in the HSM cavity is accounted for by calculating an effective conductivity of air. The HSM cavity is modeled as a combination of few separate enclosures as described below:

Enclosure 1 includes the HSM cavity within 0° to 90° sector limited by DSC shell surface, vertical and top horizontal heat shield surfaces. Enclosure 2 includes the HSM cavity within -90° to 0° sector limited by DSC shell, vertical heat shield and space under the bottom line of DSC shell surfaces. Enclosure 3 includes bottom of Enclosure 2 and inside surfaces of HSM side wall and floor. Enclosure 4 includes horizontal space limited by concrete roof surface and top horizontal heat shield surface. Enclosure 5 is vertical space limited by inside surface of concrete side wall and vertical heat shield. To be conservative, the closed cavity convection in Enclosure 3 is neglected and Enclosure 2 was assumed to be the average of Enclosure 1 and 3 $(9.09 + 1)/2 = 5.045$.

For zones of closed cavity convection to adjust a thermal conductivity of air k_{air} to account convection an empirical generalized formula was applied [4.12]:

$$\frac{k_{eff\ air}}{k_{air}} = C \cdot Ra^n \cdot \left(\frac{L}{\delta}\right)^m$$

where Ra - Raleigh number, L, δ- length and width of an enclosure, C, n, m - constants, to be defined by flow circumstances (Ra) and geometry (L/δ).

Iterative process is used to determine the mean temperatures used in air property calculations. The results are given below:

Enclosure in HSM Cavity	δ, in	L, in	$\overline{T}_{hot}$, °F	$\overline{T}_{cold}$, °F	Gr_δ	Pr	C	n	m	$k_{eff\ air}/k_{air}$
1	9.95	63	561	428	8.91e+6	0.68	0.4	0.2	0	9.09
4	2	40	432	319	1.55e+5	0.683	0.11	0.29	0	3.149
5	3	72	393	271	7.15e+5	0.685	0.197	0.25	-0.111	3.662

These effective conductivities are used in the ANSYS model to determine the transient DSC shell temperatures during blocked vent accident. These DSC shell temperatures are then used as boundary conditions to calculate the basket and fuel cladding temperatures during blocked vent transient.

The calculated temperature distribution within the hottest cross section is shown in Figure M.4-13. Summaries of the calculated NUHOMS®-32PT DSC cladding and component temperatures are listed in Table M.4-13 and Table M.4-14, respectively.

M.4.6.2 Transfer Accident Evaluation

The postulated transfer accident event consists of transfer in the TC in a 117°F ambient environment with loss of the solar shield and the liquid neutron shielding. Only heat load zoning configuration 1 was evaluated, since it envelopes all other configurations for the normal and off-normal conditions of transfer. Since the temperature of the blocked vent case bound the transfer accident condition, this case is only evaluated to determine the maximum average gas temperature for the accident DSC internal pressure evaluation.

M.4.6.2.1 Fuel Cladding and Basket Materials

The short term events are defined in Section M.4.1 for storage and transfer conditions. The blocked vent results are reported for 40 hours. The results are reported for heat load zoning configuration 1 in Table M.4-13. The maximum temperatures of the basket assembly after 40 hours are listed in Table M.4-14. The minimum temperatures reported for each component are not the minimum absolute component temperature in the entire basket. The minimums reported in the Tables below represent the minimum temperature for those components at the hottest radial cross section.

M.4.6.3 Hypothetical Fire Accident Evaluation

For the postulated worst case fire accident, a 300 gallon diesel fire is simulated for a NUHOMS®-32PT DSC with a decay heat load of 24 kW during transfer in the TC. This bounds fire scenarios associated with loading operations and storage within the HSM due to the large thermal mass of the HSM and the HSM vent configuration which provides protection for the DSC and payload.

Steady-state, off-normal conditions are assumed prior to the fire, which consist of a 117°F ambient condition with solar shield in place on the TC. The fire has a temperature of 1,475°F, and an emittance of 0.9 and a duration of 15 minutes based on the 300 gallon diesel fuel source and complete engulfment of the TC for the duration of the fire. Subsequent to the fire, the TC is subjected to 117°F ambient conditions with maximum solar load. Note that these hypothetical fire parameters are very conservative.

The calculated temperature response of selected components in the TC and DSC during the first 2,000 minutes of the fire accident is shown in Figure M.4-14. A summary of the calculated maximum fire transient temperatures for these components is listed in Table M.4-16. The calculated maximum fire transient DSC surface temperature is 499°F, which is less than the blocked vent case maximum DSC temperature of 581°F. Therefore, the NUHOMS®-32PT DSC temperatures and pressures calculated for the blocked vent case bound the hypothetical fire accident case.

M.4.6.4 Maximum Internal Pressures

The maximum accident pressure condition for the DSC occurs during the transfer accident case with the loss of the sun shield and liquid neutron shielding in the TC under extreme ambient temperature conditions of 117°F and maximum insolation. Higher average gas temperatures are achieved during the blocked vent case, but since no DSC drop events can occur in conjunction with a blocked vent event, the maximum fraction of fuel pins that can be ruptured is limited. For this transfer accident condition, the average helium temperature is 664°F (1,124°R). In accordance with NUREG 1536, 100% of the fuel pins are assumed to rupture during this event.

A summary of the maximum accident operating pressures for the various 32PT DSC configurations are presented in Table M.4-15.

M.4.6.5 Evaluation of Cask Performance During Accident Conditions

The temperatures in the NUHOMS® HSM and TC are bounded by the existing analyses because of the same heat load for the NUHOMS®-24P DSC design. The NUHOMS®-32PT DSC shell and basket are evaluated for calculated pressures and temperatures in Section M.3.

The maximum fuel cladding temperature of less than 800°F is below the short-term limit of 1058°F (570°C). The accident pressure in the NUHOMS®-32PT DSC of 103 psig remains below the accident design pressure of 105 psig. It is concluded that the NUHOMS®-32PT system maintains confinement during the postulated accident condition.

M.4.7 Thermal Evaluation for Loading/Unloading Conditions

All fuel transfer operations occur when the NUHOMS®-32PT DSC and TC are in the spent fuel pool. The fuel is always submerged in free-flowing pool water permitting heat dissipation. After fuel loading is complete, the cask and DSC are removed from the pool and the DSC is drained, dried, backfilled with helium and sealed.

The bounding loading condition evaluated for the NUHOMS®-32PT DSC is the heatup of the DSC before its cavity is backfilled with helium. This typically occurs during the performance of the vacuum drying operation of the DSC cavity. A transient thermal analysis is performed to predict the heatup time history for the NUHOMS®-32PT DSC components assuming air is in the DSC cavity.

M.4.7.1 Vacuum Drying Analysis

Heatup of the DSC prior to being backfilled with helium typically occurs as DSC operations are being performed to drain and dry the DSC. The vacuum drying of the DSC generally does not reduce the pressure sufficiently to reduce the thermal conductivity of the air in the DSC cavity. However, a hard vacuum is conservatively assumed. Analyses are performed to determine the transient heat-up during the vacuum drying condition.

M.4.7.1.1 Vacuum Drying Evaluation

A transient thermal analysis is performed using two-dimensional model developed in Section M.4.4.1, decay heat loads for zoning configuration 1, and a maximum DSC temperature of 215°F. The initial temperature of the DSC, basket and fuel is assumed to be 215°F, based on the boiling temperature of the fill water. Table M.4-17 and Table M.4-18 provide the maximum temperatures for the fuel cladding and basket components, respectively.

M.4.7.1.2 Reflooding Evaluation

For unloading operations, the DSC will be filled with the spent fuel pool water through the siphon port. During this filling operation, the DSC vent port is maintained open with effluents routed to the plant's off-gas monitoring system. The NUHOMS®-32PT DSC operating procedures recommend that the DSC cavity atmosphere be sampled first before introducing any reflood water in the DSC cavity.

When the pool water is added to a DSC cavity containing hot fuel and basket components, some of the water will flash to steam causing internal cavity pressure to rise. This steam pressure is released through the vent port. The procedures also specify that the flow rate of the reflood water be controlled such that the internal pressure in the DSC cavity does not exceed 20 psig. This is assured by monitoring the maximum internal pressure in the DSC cavity during the reflood event. The reflood for the DSC is considered as a service level D event and the design pressure of the DSC is 105 psig. Therefore, there is sufficient margin in the DSC internal pressure during the reflooding event to assure that the DSC will not be over pressurized.

The maximum fuel cladding temperature during reflooding event will be significantly less than the vacuum drying condition due to the presence of water/steam in the DSC cavity. The analysis presented in Section M.4.7.1.1 shows that the maximum cladding temperature during vacuum drying after 55 hours is 810°F. Since the reflooding procedure requires significantly less than 55 hours, the peak cladding temperature during the reflooding operation will be less than 810°F. Therefore, no cladding damage is expected due to the reflood event. This is also substantiated by the operating experience gained with the loading and unloading of transportation packages like IF-300 [4.11] which show that fuel cladding integrity is maintained during these operations and fuel handling and retrieval is not impacted.

M.4.8 References

4.1 Levy, Chin, Simonen, Beyer, Gilbert and Johnson, *Recommended Temperature Limits for Dry Storage of Spent Light Water Reactor Zircalloy-Clad Fuel Rods in Inert Gas,* May 1987, Pacific Northwest Laboratory, PNL Document PNL-6189.

4.2 Johnson, A. B. and E. R. Gilbert, *Technical Basis for Storage of Zircalloy-Clad Spent Fuel in Inert Gas,* September 1983, Pacific Northwest Laboratory, PNL Document PNL-4835.

4.3 Report, "Topical Report on Actinide-Only Burnup Credit for PWR Spent Nuclear Fuel Packages," Office of Civilian Radioactive Waste Management, DOE/RW-0472, Revision 2, September, 1998.

4.4 ASME Boiler and Pressure Vessel Code, Section II, Part D, Properties, 1998, including 1999 addenda.

4.5 Roshenow, W. M., J. P. Hartnett, and Y. I. Cho, *Handbook of Heat Transfer*, 3rd Edition, 1998.

4.6 Bolz, R. E., G. L. Tuve, *CRC Handbook of Tables for Applied Engineering Science*, 2nd Edition, 1973. Transfer, McGraw Hill, 1989.

4.7 Bucholz, J. A., *Scoping Design Analysis for Optimized Shipping Casks Containing 1-, 2-, 3-, 5-, 7-, or 10-Year old PWR Spent Fuel*, Oak Ridge National Laboratory, January, 1983, ORNL/CSD/TM-149.

4.8 Report, *TN-68 Dry Storage Cask Final Safety Analysis Report*, NRC Docket No. 72-1027.

4.9 ANSYS, Inc., ANSYS Engineering Analysis System User's Manual for ANSYS Revision 5.6, Houston, PA.

4.10 NRC NUREG-1536, *Standard Review Plan for Dry Cask Storage Systems,* January 1997.

4.11 Consolidated Safety Analysis Report for IF-300 Shipping Cask, CoC 9001.

4.12 J.P. Holman, Heat Transfer, McGraw Hill, 1989.

Table M.4-1
Fuel Cladding Long Term Storage Temperatures

Assembly Decay Heat (kW)	Maximum Temperature (°F)	Limit (°F)
0.63	613	615
0.87	530	635
0.60	603	613
1.20	503	681
0.70	618	621

Table M.4-2
Fuel Cladding Short Term Normal Condition Maximum Temperatures

Operating Condition	Configuration 1 (°F)	Configuration 3 (°F)	Limit (°F)
0°F Storage	565	566	1,058
100°F Storage	639	640	1,058
0°F Transfer	675	670	1,058
100°F Transfer	735	730	1,058

Table M.4-3
DSC Basket Assembly Maximum Normal Operating Component Temperatures; Configuration 1

Configuration	$T_{grid,max}$ (°F)	$T_{grid,min}$ (°F)	$T_{rail,max}$ (°F)	$T_{rail,min}$ (°F)	$T_{Al,max}$ (°F)[1]	$T_{DSC\ shell}$ (°F)
DSC in HSM, 0°F	547	236	329	224	547	277
DSC in HSM, 100°F	624	319	420	306	624	374
DSC horizontal in cask, 0°F	660	363	460	349	660	406
DSC horizontal in cask, 100°F	723	437	530	423	722	482

[1] Includes aluminum and poison plates.

Table M.4-4
DSC Basket Assembly Maximum Normal Operating Component Temperatures; Configuration 2

Configuration	$T_{grid,max}$ (°F)	$T_{grid,min}$ (°F)	$T_{rail,max}$ (°F)	$T_{rail,min}$ (°F)	$T_{Al,max}$ (°F)[1]	$T_{DSC\ shell}$ (°F)
DSC in HSM, 0°F	533	236	332	223	533	277
DSC in HSM, 100°F	610	319	422	305	610	374
DSC horizontal in cask, 0°F	647	363	462	348	647	406
DSC horizontal in cask, 100°F	710	437	532	422	709	482

[1] Includes aluminum and poison plates.

Table M.4-5
DSC Basket Assembly Maximum Normal Operating Component Temperatures; Configuration 3

Configuration	$T_{grid,max}$ (°F)	$T_{grid,min}$ (°F)	$T_{rail,max}$ (°F)	$T_{rail,min}$ (°F)	$T_{Al,max}$ (°F)[1]	$T_{DSC\ shell}$ (°F)
DSC in HSM, 0°F	546	223	314	213	546	277
DSC in HSM, 100°F	623	307	405	295	622	374
DSC horizontal in cask, 0°F	654	344	439	331	654	406
DSC horizontal in cask, 100°F	716	418	511	405	716	482

[1] Includes aluminum and poison plates.

Table M.4-6
32PT DSC Initial Helium Fill Molar Quantities

DSC Configuration	Helium Fill (g-moles)
S100, Steel/Aluminum Rails	146.9
S100, Solid Aluminum Rails	119.5
S125, Steel/Aluminum Rails	143.5
S125, Solid Aluminum Rails	116.5
L100, Steel/Aluminum Rails	149.1
L100, Solid Aluminum Rails	120.8
L125, Steel/Aluminum Rails	145.7
L125, Solid Aluminum Rails	117.8

Table M.4-7
32PT DSC Maximum Normal Operating Condition Pressures

	DSC Cavity Volume (in^3)	Helium Fill (g-moles)	Plenum Helium (g-moles)	BPRA Gas (g-moles)	Fission Products (g-moles)	Total Gas (g-moles)	Pressure (psig)	DSC Design Pressure (psig)
S100, Steel/ Aluminum Rails	299,997	146.9	2.1	0.00	2.6	151.6	6.7	15
S100, Solid Aluminum Rails	244,002	119.5	2.1	0.00	2.6	124.2	6.9	15
S125, Steel/ Aluminum Rails	293,048	143.5	2.1	0.00	2.6	148.2	6.8	15
S125, Solid Aluminum Rails	237,802	116.5	2.1	0.00	2.6	121.2	6.9	15
L100, Steel/ Aluminum Rails	304,530	149.1	2.1	0.54	2.6	154.4	6.8	15
L100, Solid Aluminum Rails	246,661	120.8	2.1	0.54	2.6	126.1	7.0	15
L125, Steel/ Aluminum Rails	297,583	145.7	2.1	0.54	2.6	151.0	6.8	15
L125, Solid Aluminum Rails	240,461	117.8	2.1	0.54	2.6	123.0	7.0	15

Table M.4-8
Off-Normal Event Fuel Cladding Maximum Temperatures

Operating Condition	Configuration 1 (°F)	Configuration 3 (°F)	Limit (°F)
-40°F Storage	536	537	1,058
117°F Storage	645	645	1,058
-40°F Transfer	659	653	1,058
117°F Transfer	724	719	1,058

Table M.4-9
Off-Normal Event DSC Basket Assembly Maximum Component Temperatures; Configuration 1

Configuration	$T_{grid,max}$ (°F)	$T_{grid,min}$ (°F)	$T_{rail,max}$ (°F)	$T_{rail,min}$ (°F)	$T_{Al,max}$ (°F)[1]	$T_{DSC\ shell}$ (°F)
DSC in HSM, -40°F	517	202	292	192	516	237
DSC in HSM, 117°F	629	325	427	312	629	382
DSC horizontal in cask, -40°F	644	339	443	324	644	390
DSC horizontal in cask with shade, 117°F	711	432	513	419	711	459

[1]Includes aluminum and poison plates.

Table M.4-10
Off-Normal Event DSC Basket Assembly Maximum Component Temperatures; Configuration 2

Configuration	$T_{grid,max}$ (°F)	$T_{grid,min}$ (°F)	$T_{rail,max}$ (°F)	$T_{rail,min}$ (°F)	$T_{Al,max}$ (°F)[1]	$T_{DSC\ shell}$ (°F)
DSC in HSM, -40°F	502	203	295	191	501	237
DSC in HSM, 117°F	615	325	429	311	615	382
DSC horizontal in cask, -40°F	630	339	445	323	630	390
DSC horizontal in cask with shade, 117°F	698	432	515	419	698	459

[1] Includes aluminum and poison plates.

Table M.4-11
Off-Normal Event DSC Basket Assembly Maximum Component Temperatures; Configuration 3

Configuration	$T_{grid,max}$ (°F)	$T_{grid,min}$ (°F)	$T_{rail,max}$ (°F)	$T_{rail,min}$ (°F)	$T_{Al,max}$ (°F)[1]	$T_{DSC\ shell}$ (°F)
DSC in HSM, -40°F	516	190	277	180	515	237
DSC in HSM, 117°F	628	313	412	301	628	382
DSC horizontal in cask, -40°F	636	319	421	305	636	390
DSC horizontal in cask with shade, 117°F	705	413	494	401	705	459

[1] Includes aluminum and poison plates.

Table M.4-12
32PT DSC Maximum Off-Normal Operating Condition Pressures

	DSC Cavity Volume (in3)	Helium Fill (g-moles)	Plenum Helium (g-moles)	BPRA Gas (g-moles)	Fission Products (g-moles)	Total Gas (g-moles)	Pressure (psig)	DSC Design Pressure (psig)
S100, Steel/ Aluminum Rails	299,997	146.9	21.1	0.00	26.0	194.1	12.7	20
S100, Solid Aluminum Rails	244,002	119.5	21.1	0.00	26.0	166.6	14.2	20
S125, Steel/ Aluminum Rails	293,048	143.5	21.1	0.00	26.0	190.7	12.8	20
S125, Solid Aluminum Rails	237,802	116.5	21.1	0.00	26.0	163.6	14.4	20
L100, Steel/ Aluminum Rails	304,530	149.1	21.1	5.38	26.0	201.7	13.3	20
L100, Solid Aluminum Rails	246,661	120.8	21.1	5.38	26.0	173.3	15.0	20
L125, Steel/ Aluminum Rails	297,583	145.7	21.1	5.38	26.0	198.3	13.5	20
L125, Solid Aluminum Rails	240,461	117.8	21.1	5.38	26.0	170.3	15.2	20

Table M.4-13
Accident Fuel Cladding Maximum Temperatures

Operating Condition	Configuration 1 (°F)	Limit (°F)
Blocked Vent, 40 hours	806	1,058

Table M.4-14
DSC Basket Assembly Maximum Accident Condition Component Temperatures; Heat Load Zoning Configuration 1

Configuration	$T_{grid,max}$ (°F)	$T_{grid,min}$ (°F)	$T_{rail,max}$ (°F)	$T_{rail,min}$ (°F)	$T_{Al,max}$ (°F)[1]	$T_{DSC\ shell}$ (°F)
DSC in HSM blocked vent, 117°F	797	485	603	469	797	574

(1) Includes aluminum and poison plates.

Table M.4-15
32PT DSC Maximum Accident Condition Pressures

	DSC Cavity Volume (in3)	Helium Fill (g-moles)	Plenum Helium (g-moles)	BPRA Gas (g-moles)	Fission Products (g-moles)	Total Gas (g-moles)	Pressure (psig)	DSC Design Presure (psig)
S100, Steel/ Aluminum Rails	299,997	146.9	211.2	0.00	260.1	618.2	76.7	105
S100, Solid Aluminum Rails	244,002	119.5	211.2	0.00	260.1	590.8	91.9	105
S125, Steel/ Aluminum Rails	293,048	143.5	211.2	0.00	260.1	614.8	78.3	105
S125, Solid Aluminum Rails	237,802	116.5	211.2	0.00	260.1	587.8	94.0	105
L100, Steel/ Aluminum Rails	304,530	149.1	211.2	53.80	260.1	674.3	83.6	105
L100, Solid Aluminum Rails	246,661	120.8	211.2	53.80	260.1	645.9	100.6	105
L125, Steel/ Aluminum Rails	297,583	145.7	211.2	53.80	260.1	670.9	85.3	105
L125, Solid Aluminum Rails	240,461	117.8	211.2	53.80	260.1	642.9	102.9	105

Table M.4-16
Maximum Component Temperatures for the Hypothetical Fire Accident Case for the NUHOMS®-32PT DSC in the TC

Component	Maximum Temperature (°F)	Allowable Range (°F)
DSC Shell	499	**
Cask Structural Shell	1,420	**
Cask Lead Shielding	369	621
Inside of Cask Lid	331	**
Cask Neutron Shield	688	*

* Cask neutron shield is assumed to be lost during fire event. Effects of loss of shielding are evaluated in Section M.11.2.5.

** The components perform their intended safety function within the operating range.

Table M.4-17
Vacuum Drying Fuel Cladding Maximum Temperatures

Operating Condition	Configuration 1 (°F)	Limit (°F)
Vacuum Drying, 55 hours	810	1,058

Table M.4-18
DSC Basket Assembly Maximum Component Temperatures During Vacuum Drying After 55 hours; Configuration 1

Configuration	$T_{grid,max}$ (°F)	$T_{grid,min}$ (°F)	$T_{rail,max}$ (°F)	$T_{rail,min}$ (°F)	$T_{Al,max}$ (°F)[1]
Vacuum Drying	791	534	591	527	791

[1] Includes aluminum and poison plates.

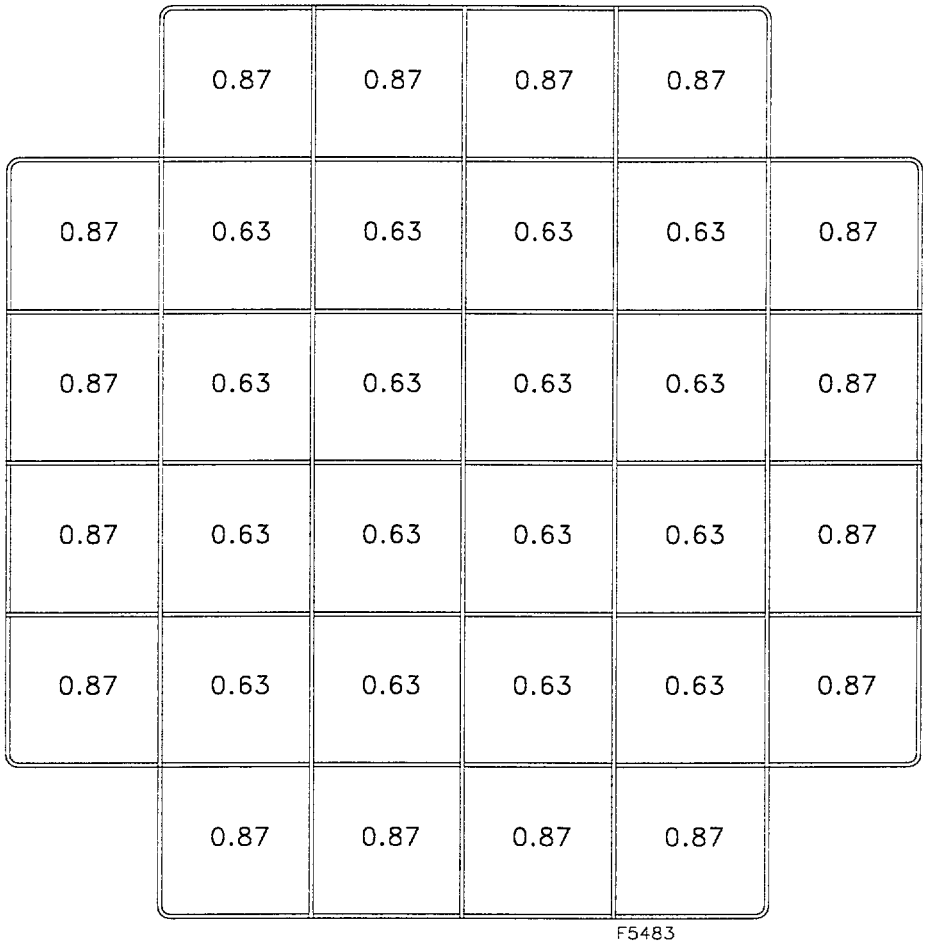

Figure M.4-1
Heat Load Zoning Configuration 1, Maximum Decay Heat for Various Assemblies

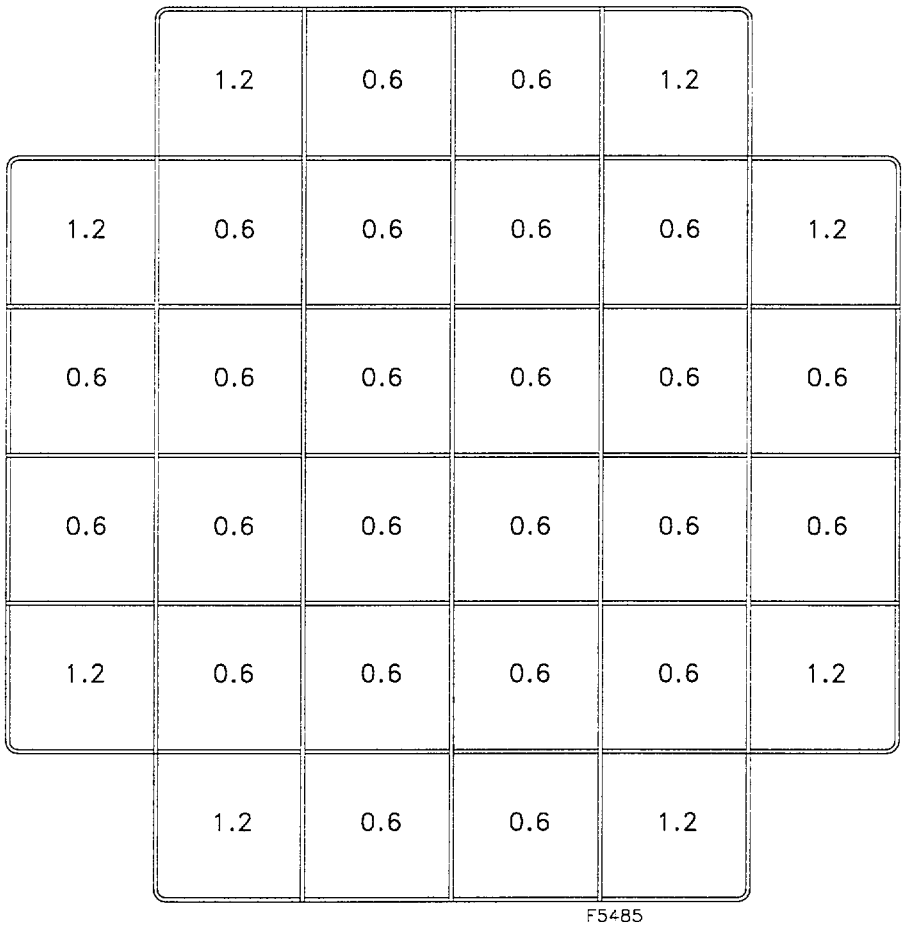

Figure M.4-2
Heat Load Zoning Configuration 2, Maximum Decay Heat for Various Assemblies

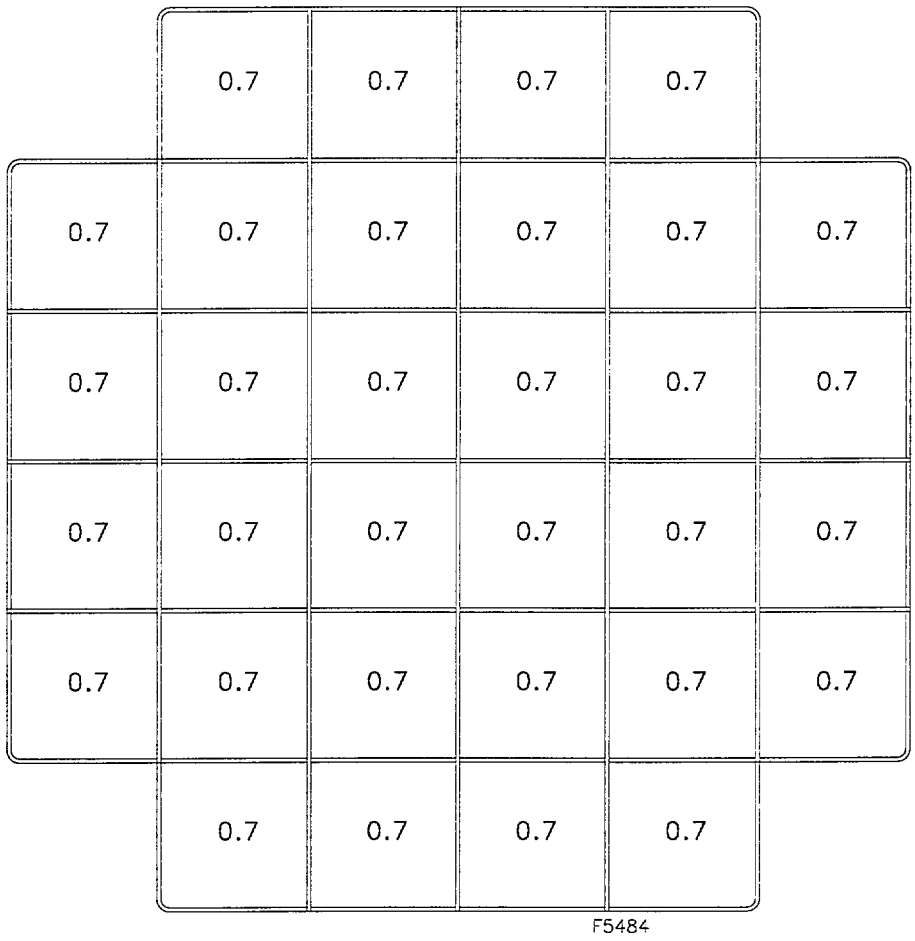

Figure M.4-3
Heat Load Zoning Configuration 3, Maximum Decay Heat for Various Assemblies

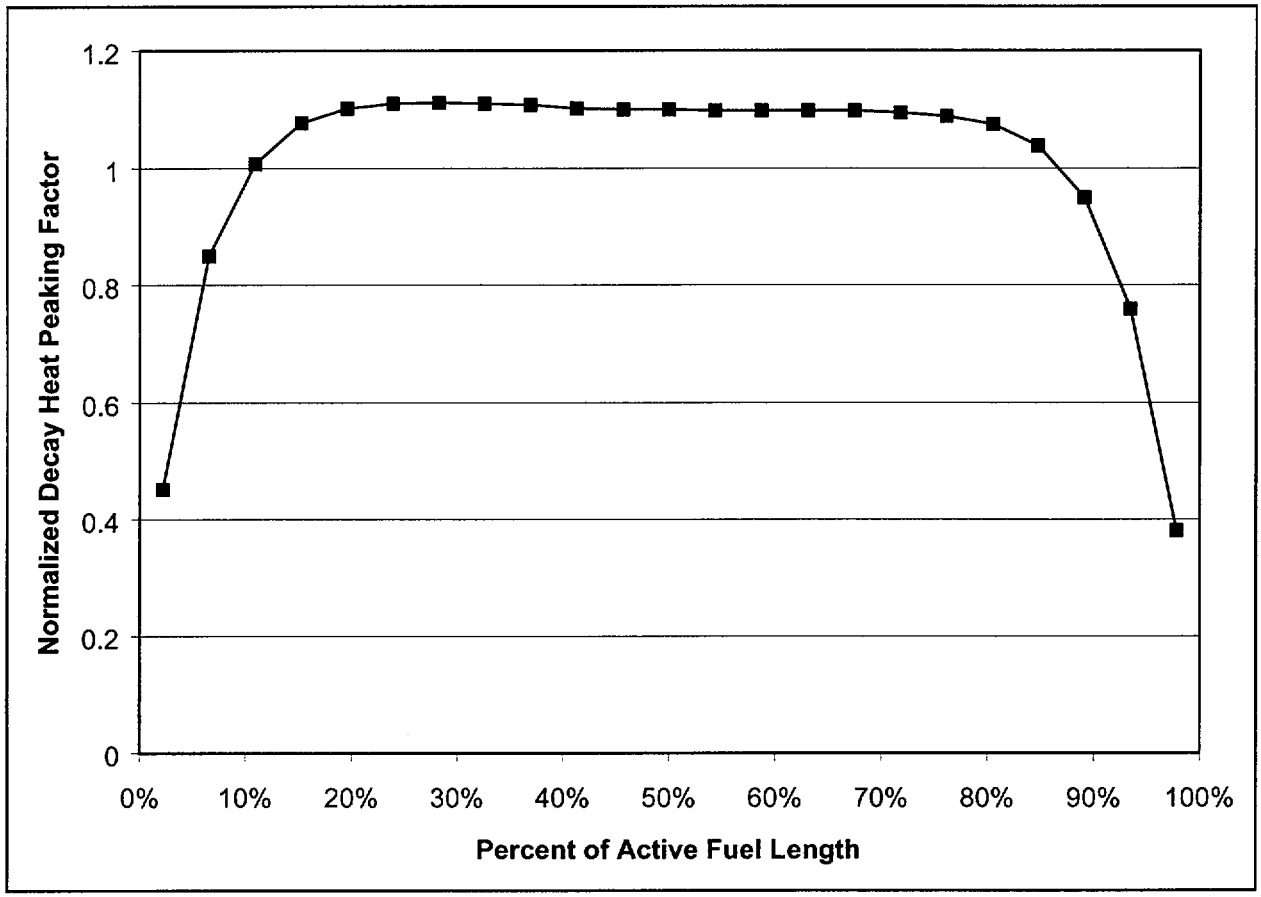

Figure M.4-4
Axial Heat Profile for PWR Fuel

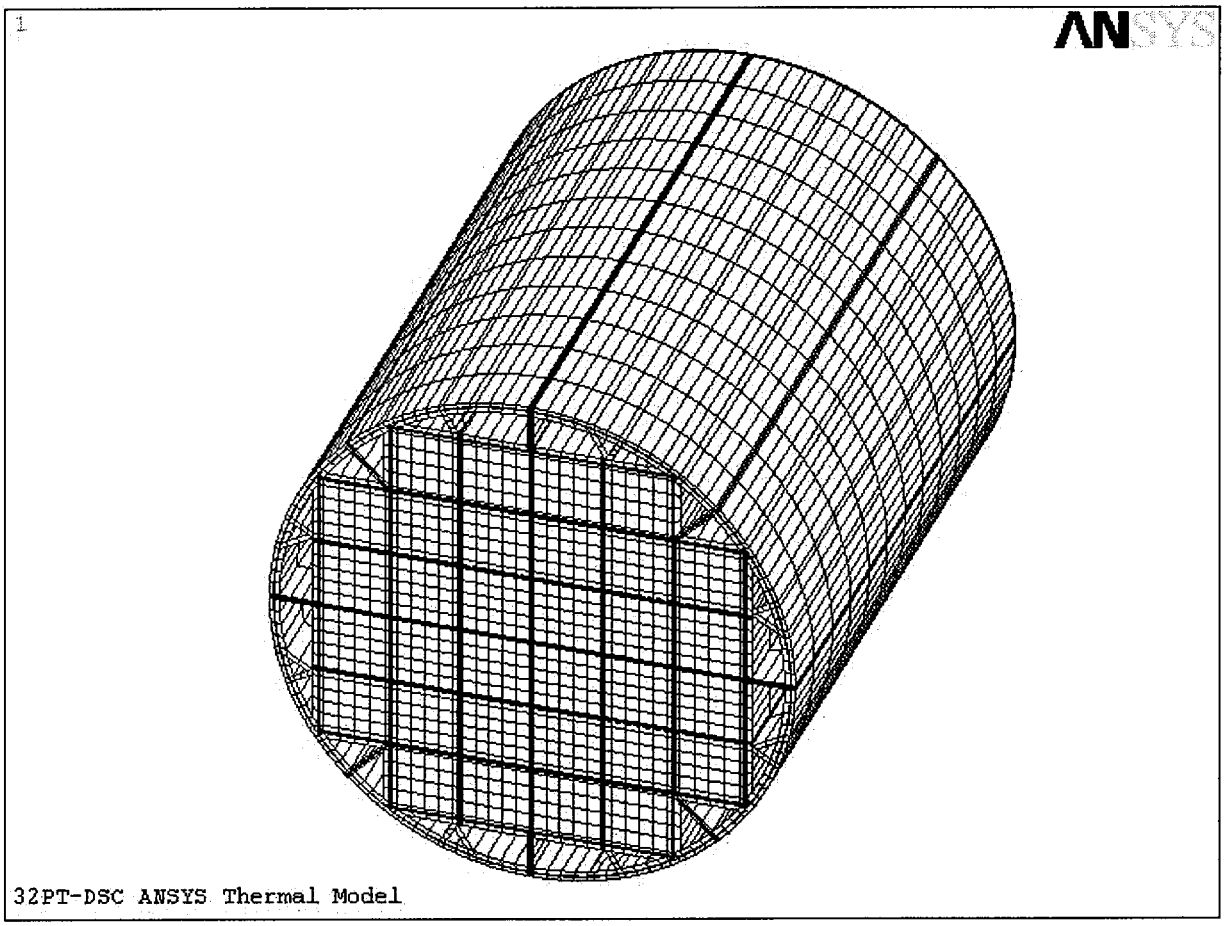

Figure M.4-5
32PT-DSC Thermal ANSYS Model, Isometric View

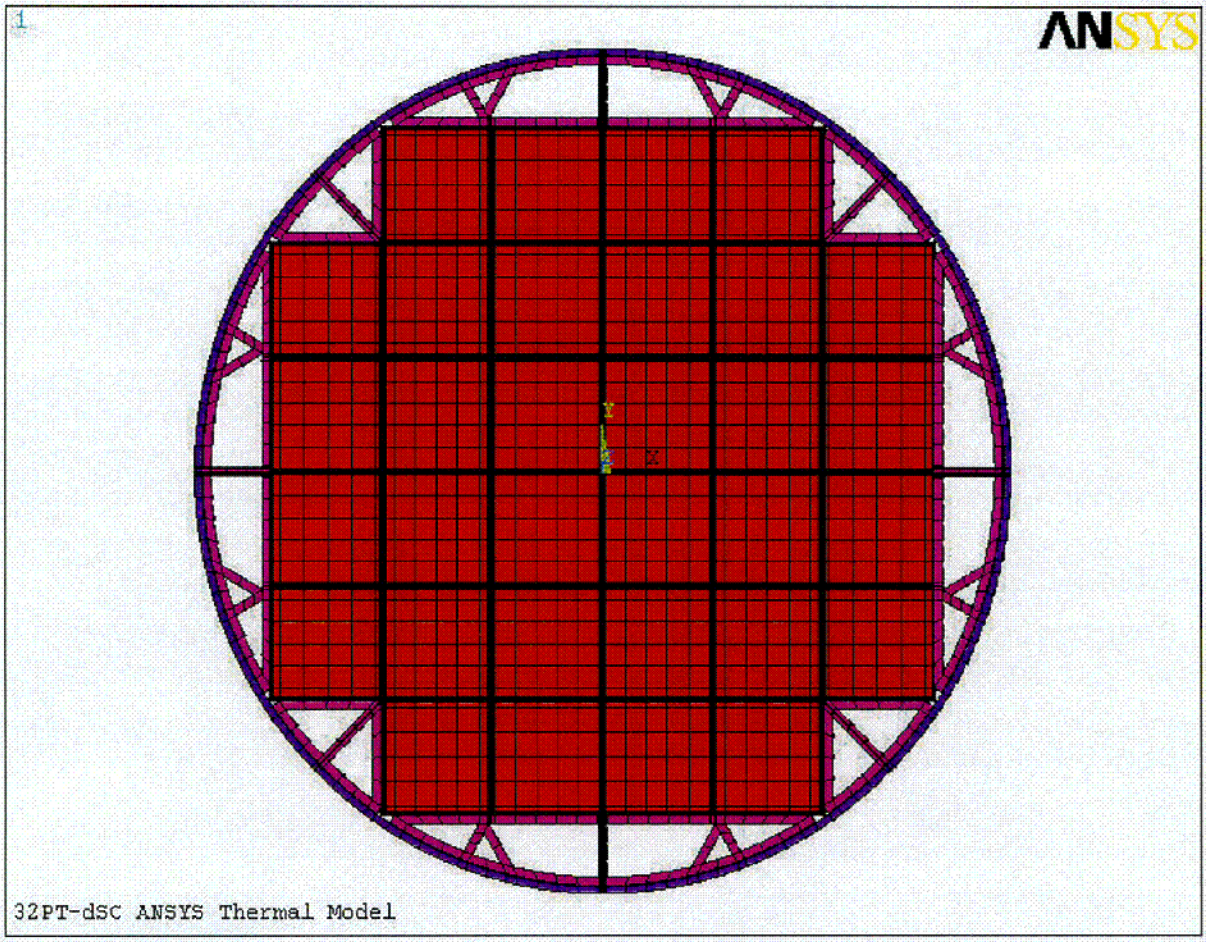

Figure M.4-6
32PT-DSC Thermal ANSYS Model, Cross Section View

C01

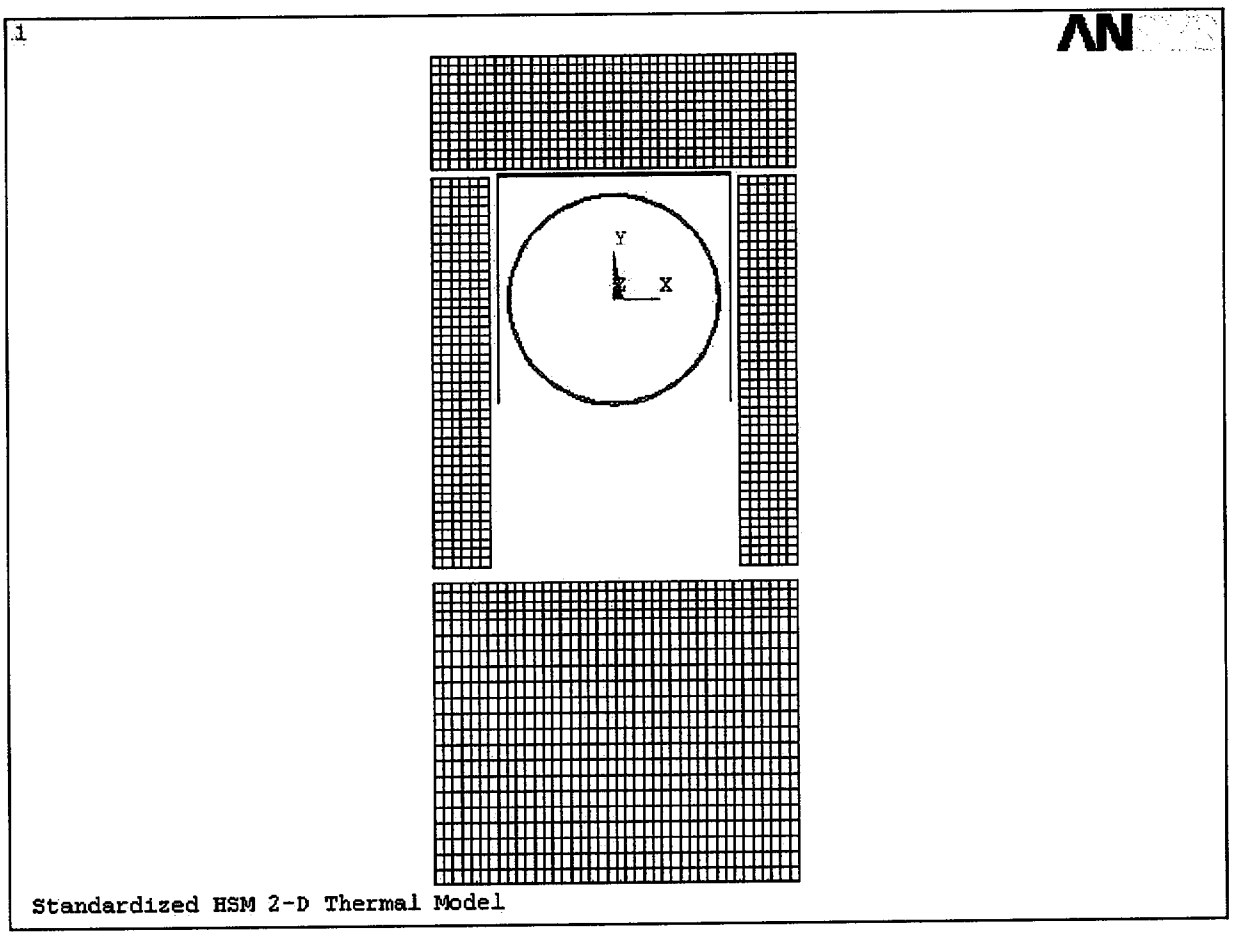

Figure M.4-7
Thermal Model of DSC in HSM

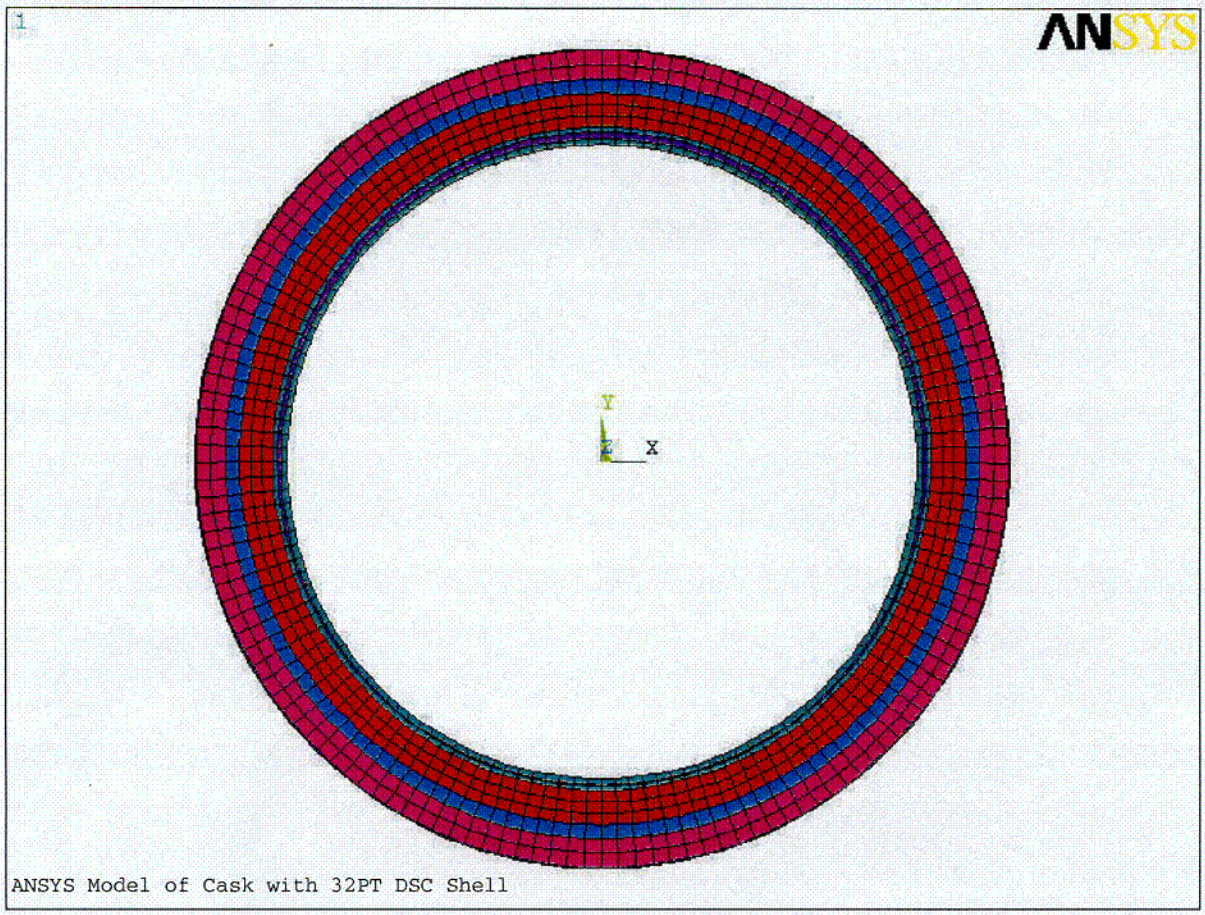

Figure M.4-8
Thermal Model of TC

C02

Heat Load: 0.63 kW/assy Inner 16 cells, 0.87 kW/assy outer 16 cells
Environment Condition: 100°F ambient
Operating Condition: Storage in HSM

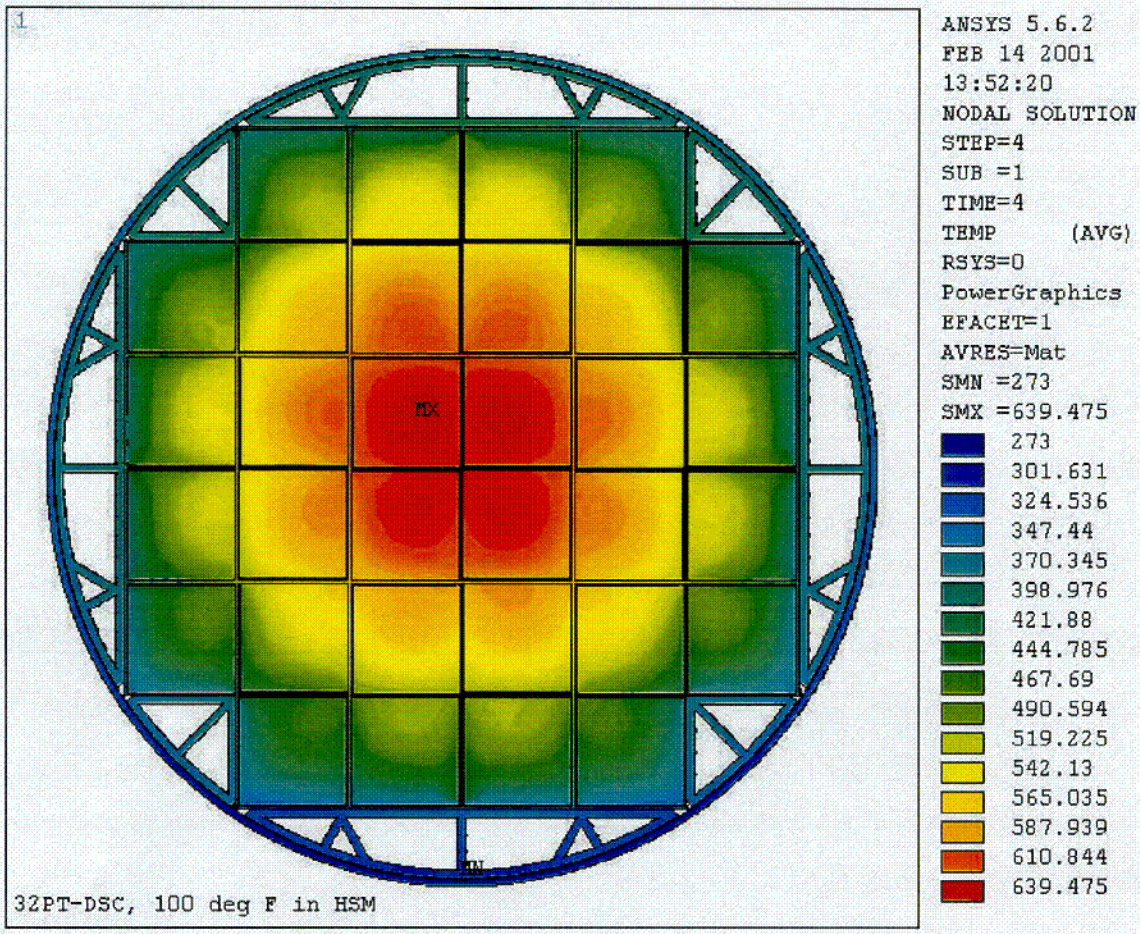

Figure M.4-9
Results for 100°F Storage Case With Heat Load Zoning Configuration 1 C03

Heat Load: 0.63 kW/assy Inner 16 cells, 0.87 kW/assy outer 16 cells
Environment Condition: 100°F ambient
Operating Condition: Transfer in cask

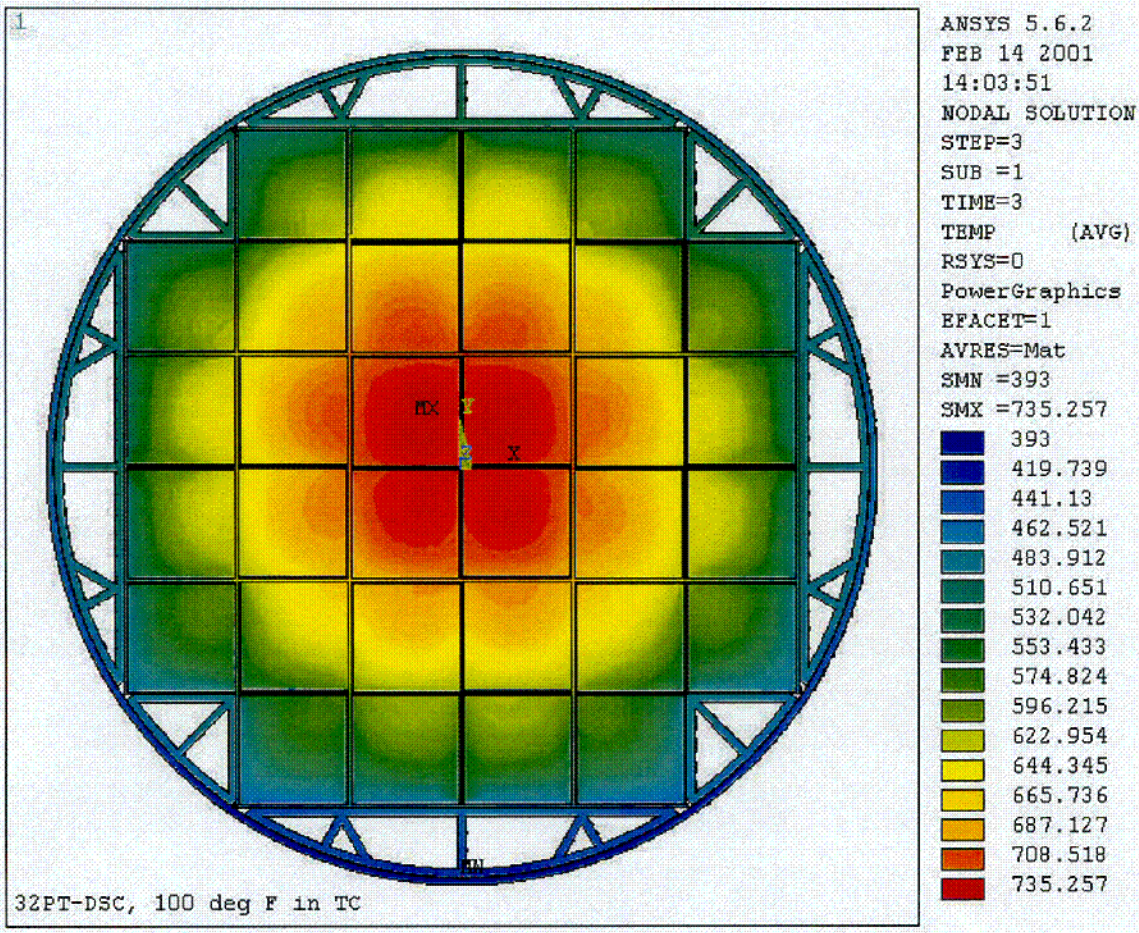

Figure M.4-10
Results for 100°F Transfer Case With Heat Load Zoning Configuration 1

C04

Heat Load: 0.63 kW/assy Inner 16 cells, 0.87 kW/assy outer 16 cells
Environment Condition: 117°F ambient
Operating Condition: Storage in HSM

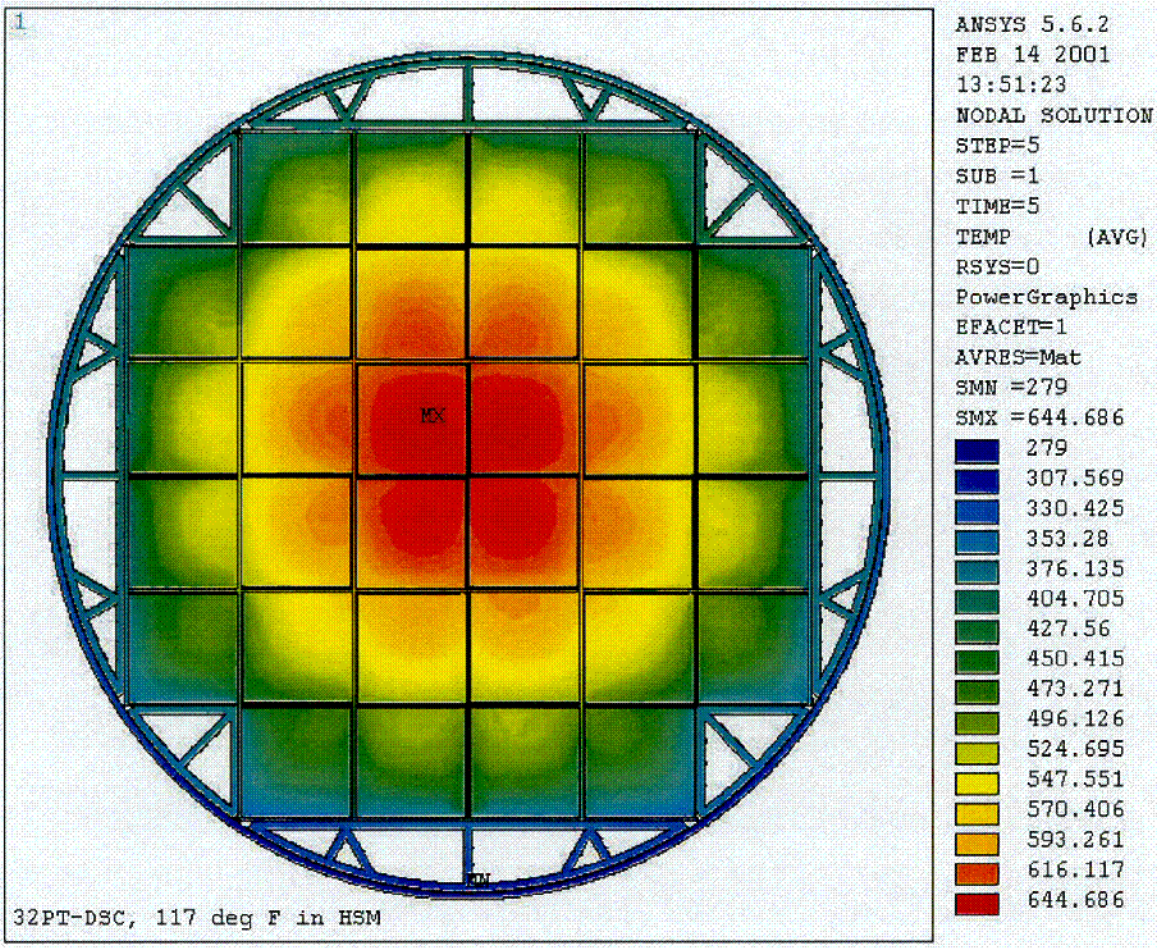

Figure M.4-11
Results for 117°F Storage Case With Heat Load Zoning Configuration 1

COS

Heat Load: 0.63 kW/assy Inner 16 cells, 0.87 kW/assy outer 16 cells
Environment Condition: 117°F ambient
Operating Condition: Transfer in cask

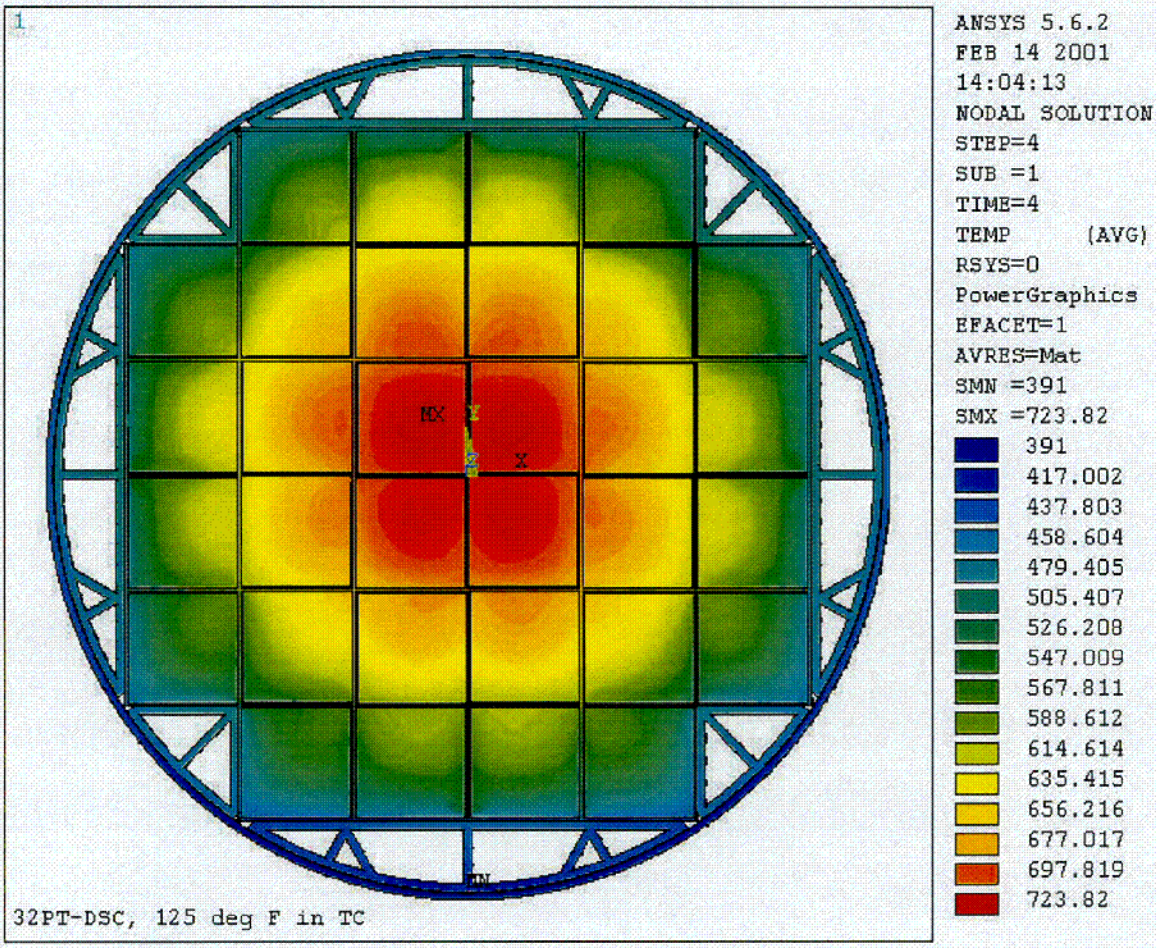

Figure M.4-12
Results for 117°F Transfer Case With Heat Load Zoning Configuration 1

C06

Heat Load: 0.63 kW/assy Inner 16 cells, 0.87 kW/assy outer 16 cells
Environment Condition: 117°F in HSM.
Operating Condition: Blocked Vent Accident, 40 hours

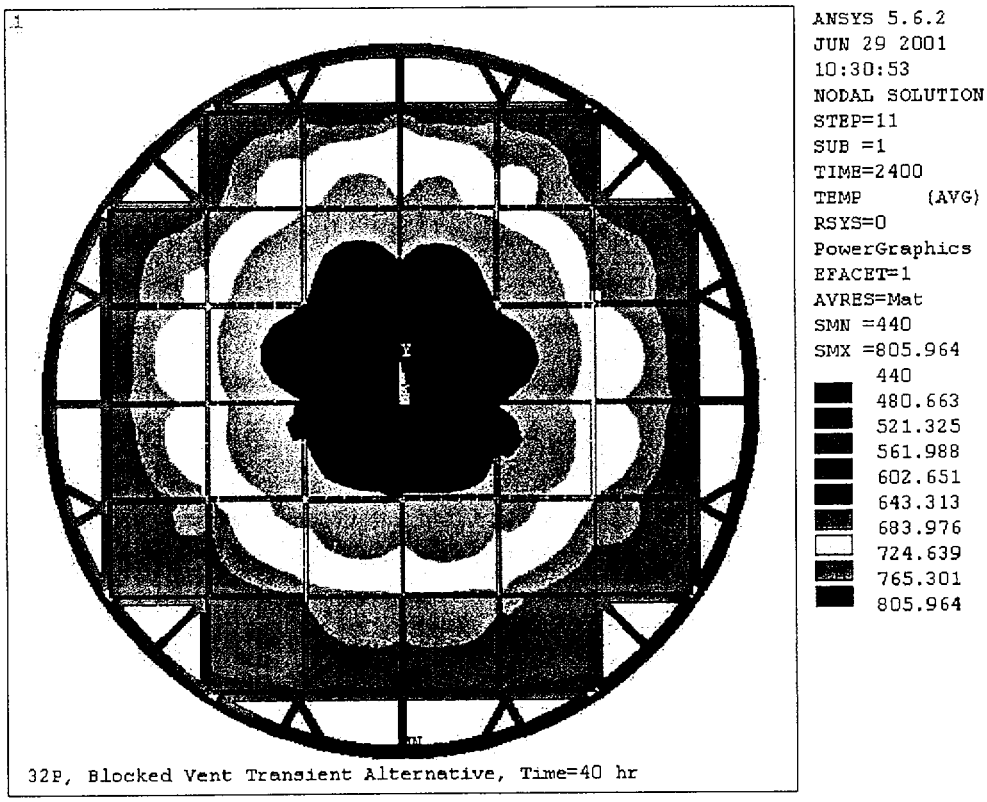

Figure M.4-13
Results for Blocked Vent Case With Heat Load Zoning Configuration 1 at 40 Hours

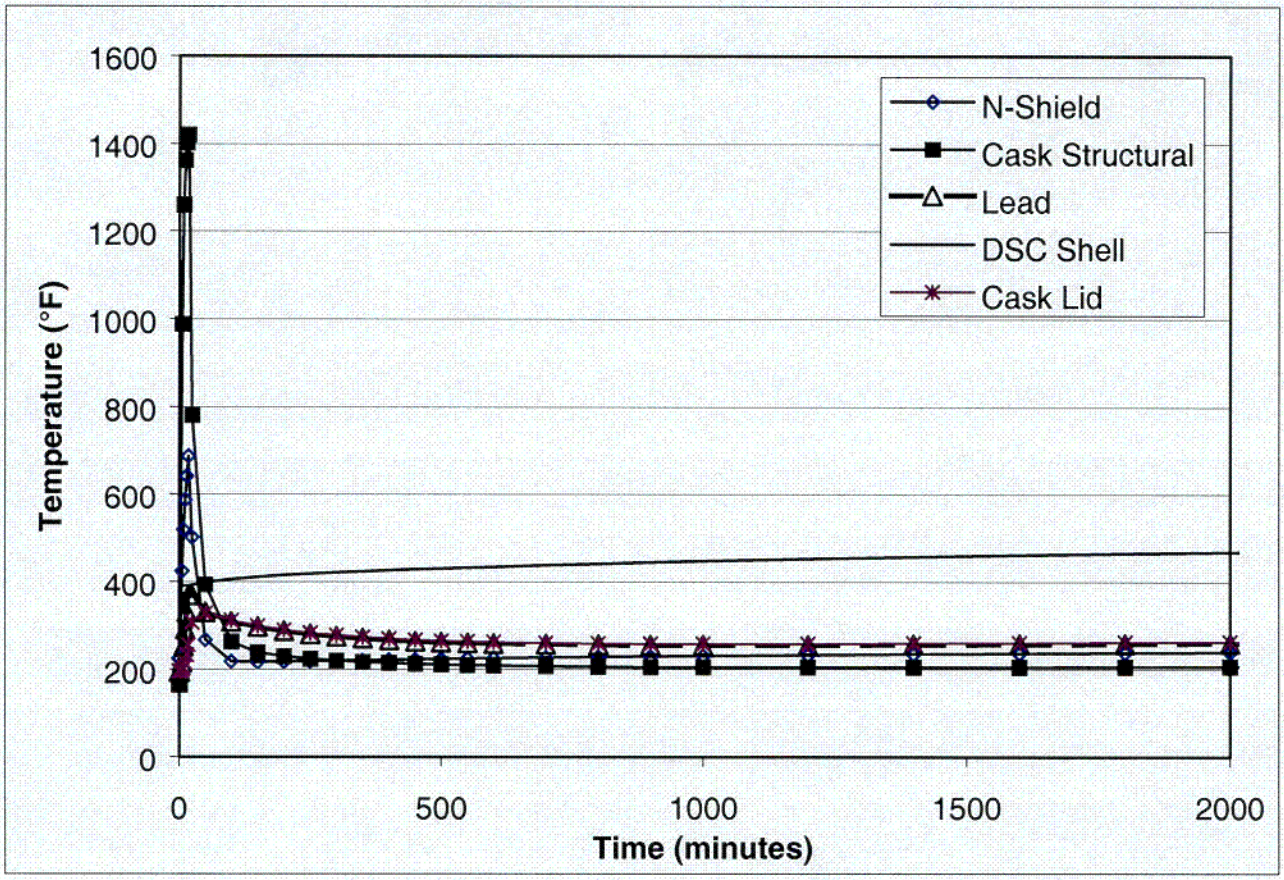

Figure M.4-14
NUHOMS®-32PT DSC and TC Temperature Response to
15 Minute Fire Accident Conditions

C07